UNIVERSIDAD DE CONCEPCIÓN

FACULTAD DE FARMACIA

TITULO DE LA TESIS

EFECTO BENÉFICO DEL FRUTO DE CALAFATE SOBRE FACTORES DE RIESGO ASOCIADOS A ENFERMEDAD CARDIOVASCULAR, MEDIANTE UN ENSAYO DE INTERVENCIÓN NUTRICIONAL Y UNA ESTRATEGIA METABOLÓMICA BASADA EN UHPLC-QTOF/MS

TESIS PRESENTADA A LA FACULTAD DE FARMACIA PARA OPTAR AL GRADO ACADÉMICO DE DOCTOR EN CIENCIAS Y TECNOLOGÍA ANALÍTICA

POR: LIA PAZ OLIVARES CARO

PROFESORA GUÍA: CLAUDIA ALEJANDRA MARDONES PEÑA

PROFESORA CO-GUÍA: CLAUDIA PAMELA RADOJKOVIC NAVARRO

CONCEPCION, CHILE, 2022

En memoria del Dr. Daniel Durán

quien estará por siempre

en nuestros corazones.

AGRADECIMIENTOS

Quisiera dar las gracias a todas las personas que me apoyaron en esta etapa de mi vida en primer lugar a mis padres Paz Alejandra Caro Ramos y Manuel German Olivares Jofré, que siempre han sido un pilar de apoyo y me han dado fuerzas para seguir adelante, siempre con perseverancia. Mi mama Miriam del Carmen Jofré Carrillo que siempre ha estado presente para entregarme una palabra de aliento, a mi marido Jose Miguel Salazar Cartes quien apoyó cada una de mis decisiones con amor, y a mis abuelos, tios, primos, vecinos, compañeros y amigos quienes siempre han estado presentes en cada uno de los momentos importantes de mi vida.

Agradecer a Dios, por los desafíos que ha puesto en mi vida, y por guiar cada día mis pasos.

Dar gracias a la institución y a todos los profesores del Doctorado en Ciencias y Tecnología Analítica por la formación entregada. Agradecer en particular a mi profesora Guía la Dra. Claudia Mardones, quién confió en mí y me permitió trabajar junto a ella, ayudándome a desarrollar el pensamiento crítico necesario para desarrollar investigación y a superar los cambios que hubo que enfrentar producto de la pandemia, motivándome cada día. A la Dra. Claudia Radojkovic quién actuó como co-Guía de esta tesis doctoral, quién me enseñó acerca del trabajo con células y el cómo aprender a tolerar la frustración, lo que fue muy difícil en un comienzo. Gracias a cada una por su incondicional apoyo.

Agradecer a ANID por mi beca Doctorado Nacional 21170812 y por los gastos de operación entregados, al proyecto FONDECYT 1191276 por los recursos otorgados y FONDEQUIP EQM 170023 con el cuál se adquirió UHPLC-DAD-QTOF sin el cual esta tesis no hubiese sido posible.

Finalmente, como me dijo mi padre alguna vez “El que quiere puede” y por sobre todo “La Fe mueve montañas”.

TABLA DE CONTENIDO

TABLA DE CONTENIDOS ..... **iv**

Índice de tablas ix

Índice de figuras x

Resumen xii

Abstract xiii

CAPITULO 1: Introducción **1**

1.1 Enfermedad cardiovascular y estrés oxidativo 1

1.2 Metodologías *in vitro* en la evaluación de marcadores biológicos de estrés oxidativo 6

1.3 Polifenoles y protección vascular 8

1.4 Fuentes alimentarias de polifenoles 16

1.5 Metabolismo de polifenoles 20

1.6 Polifenoles en *Berberis microphylla* 23

1.7 Metabolómica 26

CAPITULO 2: Hipótesis y objetivos **34**

2.1 Hipótesis 34

2.2 Objetivo 35

2.3 Objetivos específicos 35

CAPITULO 3: Estrategia analítica

Estrategia analítica 37

Referencias 44

CAPITULO 4: Resultados

4.1 El extracto del fruto de *Berberis microphylla* G. Forst (calafate) reduce el estrés oxidative y la peroxidación lipídica de LDL humana.

Berberis microphylla G. Forst (calafate) berry extract reduces oxidative stress and lipid peroxidation of human LDL 56

4.1.1. Introduction 59

4.1.2. Materials and Methods 63

4.1.2.1. Reagents and vegetable material 63

4.1.2.2. Instrumentation 64

4.1.2.3 Full chemical characterization of calafate 66

4.1.2.3.1 Extraction protocols 66

4.1.2.3.2 Identification and quantitation of anthocyanins 68

4.1.2.3.3 Hydroxycinnamic acid derivatives (HCAD) analysis by LC-MS 69

4.1.2.3.4 Metal profile analysis 70

4.1.2.3.5 Analysis of fatty acid profile 70

4.1.2.4. *In vitro* assays 72

4.1.2.4.1 Antioxidant capacity and total phenolic compounds 72

4.1.2.4.2 Cell culture 73

4.1.2.4.2.1 Viability assay 73

4.1.2.4.2.2 ROS measurement 74

4.1.2.4.3 LDL isolation 75

4.1.2.4.3.1 LDL oxidation 75

4.1.2.4.3.2 MDA assay 76

4.1.2.5 Statistical Analysis 76

4.1.3. Results and discussion 77

4.1.3.1 Phenolic profile in calafate fruit by UHPLC-DAD-ESI-QTOF-MS/MS 77

4.1.3.2 Fatty acid profile of calafate berry by GC-MS 85
4.1.3.3 Metal contents in calafate berry by TXRF 87
4.1.3.4 Concentration of main compounds in the extracts 90
4.1.3.5 Antioxidant capacity of calafate extracts 91
4.1.3.6 Calafate extracts reduced ROS production caused by H_2O_2 in HUVECs 92
4.1.3.7 Calafate extract reduced lipidic peroxidation caused by $CuSO_4$ in human LDL 96
4.1.4. Conclusions 101

4.2 La ingesta de *Berberis microphylla* G. Forst reduce el impacto de una dieta alta en grasas sobre factores de riesgo plasmáticos relacionados con la patología cardiovascular

Berberis microphylla G. Forst intake reduces the impact of a high-fat diet on plasma cardiovascular disease factors 111
4.2.1 Introduction. 114
4.2.2. Materials and Methods 118
4.2.2.1. Reagents and vegetable material 118
4.2.2.2. Instrumentation 118
4.2.2.3.1 Calafate extract 120
4.2.2.3.2 *In vivo* assay 120
4.2.2.3.3 Biochemical analyses and protein quantification 122
4.2.2.3.4 Metabolite extraction from plasma samples. 123
4.2.2.3.5 UHPLC-DAD-ESI-QTOF-MS/MS metabolomics analysis 124
4.2.2.3.6 Data Processing and Data Analysis 126
4.2.3 Results and Discussion 129
4.2.3.1 Calafate berry extract composition 129
4.2.3.2 Animal characteristics 130

4.2.3.3 Biochemical analysis. 130
4.2.3.3.1 Clinical Biochemistry 130
4.2.3.3.2 Inflammation and cardiovascular risk markers..... 131
4.2.3.4 Metabolomics..... 135
4.2.3.4.1 Metabolite annotation and observational changes..... 138
4.2.3.5 Biological interpretation 148
4.2.4 Conclusion. 151
4.2.5 Acknowledgment 152
4.2.6 Conflict of interest 153
4.2.7. CRediT author statement. 153
4.2.8 References..... 154

4.3 Cambios en el metaboloma de tejido cardiaco de raton son asociados al consumo de calafate y reducción de riesgo cardiovascular

Changes in the metabolome of heart tissue of mice associated to calafate intake and reduction of cardiovascular risk. 163
4.3.1 Introduction..... 166
4.3.2. Materials and Methods..... 169
4.3.2.1. Reagents and vegetable material..... 169
4.3.2.2. Instrumentation 170
4.3.2.3.1 Calafate extract 171
4.3.2.3.2 *In vivo* assay..... 171
4.3.2.3.3 Tissue sample treatment..... 173
4.3.2.3.4 UHPLC-DAD-ESI-QTOF-MS/MS analyses..... 174
4.3.2.3.5 Data Processing and Data Analysis 176
4.3.3 Results and discussion 179
4.3.3.1Multivariate analysis of the data..... 181

4.3.3.2 Significant features and biological interpretation 184
4.3.4 Conclusion 197
4.3.5 Acknowledgment 197
4.3.6 Conflict of interest 197
4.3.7 CRediT author statement 197
4.3.8 References 198

CAPITULO 5: Conclusión general

Conclusión 206

PRODUCTIVIDAD:

1. Publicaciones científicas 209
2. Participación en otras publicaciones. 210
3. Participación en congresos. 210
4. Participación en proyectos de investigación. 214
5. Becas y distinciones. 216

ANEXOS:

1. SUPPLEMENTARY MATERIAL: *Berberis microphylla* (calafate) berry extract reduces oxidative stress and lipid peroxidation of human LDL in *in vitro* models 218
2. Evaluación de las diferencias existentes entre los extractos metánólico y etanólico, utilizando análisis multivariado. 226
3. SUPPLEMENTARY MATERIAL: *Berberis microphylla* G. Forst intake reduces the impact of high-fat diet on plasma cardiovascular disease factors. 232

ÍNDICE DE TABLAS

Tabla 1.1: Contenido de Antocianinas en alimentos de origen vegetal ... 19

Table 4.1.1: Metabolic profile of calafate obtained by UHPLC-DAD-ESI-QTOF-MS/MS in positive and negative ionization modes 78

Table 4.1.2: Fatty acids profile of calafate fruit (GC-MS) 87

Table 4.1.3: Estimated concentration of metals in calafate berry by TXRF 89

Table 4.1.4: Total polyphenol concentration and antioxidant capacity in calafate extracts. 91

Tabla 4.2.1: Significant metabolites identified by UHPLC-DAD-QTOF which are related with CVD (positive and negative ionization modes). 138

Tabla 4.3.1: Parameters of Metaboscape software 178

Tabla 4.3.2: Significant metabolites identified by UHPLC-DAD-QTOF which are related with CVD (positive and negative ionization modes). 185

ÍNDICE DE FIGURAS

Figura 1.1: Estructura básica de un flavonoide..... 11

Figura 1.2: Acciones cardiovasculares de los flavonoides 16

Figura 1.3: Flujo de trabajo de un análisis metabolómico..... 32

Figura 3.1: Estrategia analítica utilizada para cumplir con los objetivos planteados 42

Figure 4.1. 1: Protective effect of calafate extract on ROS production upon H_2O_2 stimulation 94

Figure 4.1.2: Effect of calafate extract on lipidic peroxidation of LDL .. 97

Figure 4.2.1: Box-plot proteins markers in endothelial dysfunction and adipokines related with metabolic risk factors. 133

Figure 4.2.2: Principal component analysis (PCA). a) Score plot in negative mode and b) Score plot in positive mode for method 1, method 2 and method 3..... 137

Figure 4.2.3: Box plot features significative ($p<0.05$) identified.. 141

Figure 4.2.4: Heatmap of significant metabolites..... 147

Figure 4.2.5: Proposal of the systemic effect caused by *Berberis microphylla* (calafate) berries 151

Figura 4.3.1: Base peak chromatogram (BPC) in negative polarity for different chromatographic method. 180

Figura 4.3.2 : Base peak chromatogram (BPC) in positive polarity for different chromatographic method 180

Figura 4.3.3 : Principal component analysis (PCA) Score plot negative mode a) method 1, b) method 2 and c) method 3. Score plot positive mode d)method 1, e) method 2 and f) method 3..... 182

Figura 4.3.4: Principal component analysis H vs Hcal 183

Figura 4.3.5: Principal component analysis H vs N 184

Figura 4.3.6: Significant metabolites found by ANOVA in negative and positive mode present in table 4.3.2. 187
Figura 4.3.7: Biological effect of calafate on cardiac tissue 196

RESUMEN

La enfermedad cardiovascular corresponde a una de las primeras causas de muerte en Chile y en el mundo, siendo un problema de salud pública.

Se ha descrito que los polifenoles podrían participar en la prevención de las enfermedades crónicas a través de una disminución del estrés oxidativo.

En esta tesis, desarrollando un estudio metabolómico basado en UHPLC-QTOF-MS complementado con ensayos *in vitro* e *in vivo* y la determinación de marcadores proteicos de estrés oxidativo e inflamación, se construyó una plataforma para el estudio holístico del efecto del consumo de calafate, en el contexto de la patología cardiovascular, siendo este fruto rico en polifenoles.

Como resultado hemos demostrado que el extracto de calafate es capaz de disminuir el estrés oxidativo en un modelo de células endoteliales y en LDL humana, así como también provocar un cambio en el metaboloma de ratones alimentados con una dieta alta en grasa, cambios que son asociados al efecto protector de la ingesta de calafate frente a factores de riesgo de la patología cardiovascular. El estudio metabolómico incluyó el análisis de muestras de plasma y de tejido cardiaco, encontrando que el efecto es a nivel de parámetros asociados a estrés oxidativo, disfunción endotelial y peroxidación lipídica, activando el ciclo de Krebs y la oxidación de ácidos grasos.

ABSTRACT

Cardiovascular disease corresponds to one of the main causes of death in Chile and in the world, becoming a relevant public health problem.

It has been described that polyphenols, hydroxylated aromatic compounds with antioxidant properties, participate in the prevention of chronic diseases through the reduction of oxidative stress.

In this thesis, a metabolomic study based on UHPLC-QTOF-MS complemented with *in vitro* and *in vivo* assays and determination of protein markers of oxidative stress and inflammation was carried out through a platform built for the holistic study of the effect of calafate consumption in the context of cardiovascular pathology, fruit rich in polyphenol compounds.

Our results showed that the calafate extract reduced oxidative stress in an cells endothelial model and in human LDL, as well as it caused a change in the metabolome of mice fed a high-fat diet. These changes are associated with the protective effect of calafate intake against risk factors of cardiovascular pathology. The metabolomic study included the analysis of plasma samples and cardiac tissue, where the calafate affected parameters associated with oxidative stress, endothelial dysfunction and lipid peroxidation, activating the Krebs cycle and fatty acid oxidation.

CAPITULO 1: INTRODUCCIÓN GENERAL

1.1 Enfermedad cardiovascular y estrés oxidativo

La enfermedad cardiovascular (ECV) corresponde a una de las primeras causas de muerte en Chile y en el mundo, convirtiéndose en un problema de salud pública *(MINSAL, 2021).* Esta patología y sus factores de riesgo: hipertensión, dislipidemias, diabetes mellitus, y síndrome metabólico, entre otros, tienen como común denominador la disfunción endotelial, la cual se define como una disminución de la capacidad funcional de las células endoteliales, que determina un desbalance en la síntesis y biodisponibilidad de moléculas bioactivas derivadas del endotelio, que causa un aumento en la vasoconstricción, inflamación y permeabilidad vascular (Andriantsitohaina et al., 2012). Dentro de las moléculas bioactivas más importantes en la regulación del tono vascular, se encuentra el óxido nítrico (NO), el cual es generado en el endotelio por la enzima óxido nítrico sintasa (eNOS) desde L-arginina. Este factor activa a la enzima guanilato ciclasa en las células musculares lisas, lo que genera un aumento en los niveles de 3',5'-guanosina monofosfato cíclico (GMPc), que induce un cambio en la concentración intracelular de ion calcio, generando la dilatación de los vasos sanguíneos.

Además, el NO previene la adhesión de plaquetas y monocitos, la expresión de factores trombóticos y la oxidación de lipoproteínas de alta densidad (LDL), elementos que juegan un rol central en el desarrollo y complicaciones de la aterosclerosis (Cai & Harrison, 2000).

La disfunción endotelial es asociada frecuentemente con el estrés oxidativo, el cual corresponde a un estado en que aumenta la producción o concentración de especies reactivas de oxígeno (ROS), no siendo capaces los antioxidantes endógenos de controlar este desequilibrio (Andriantsitohaina et al., 2012). El estrés oxidativo puede ser causado por un aumento de la expresión o actividad de la enzima NADPH oxidasa, una de las responsables de la producción del radical superóxido (O_2^-). Este radical es capaz de generar otros radicales (radical hidroxilo, etc.), como consecuencia de la acción de enzimas antioxidantes (superóxido dismutasa) y de reaccionar con el NO y generar peroxinitrito ($ONOO^-$), reduciendo la biodisponibilidad del NO y, en consecuencia, sus efectos protectores a nivel cardiovascular (Andriantsitohaina et al., 2012).

La producción controlada de ROS se considera un mecanismo de defensa en condiciones fisiopatológicas y ha sido implicado en la oxidación de macromoléculas, como lípidos, proteínas y ácidos nucleicos. El peroxinitrito

promueve la nitración de proteínas también contribuyendo a la disfunción y muerte de células endoteliales. En los lípidos, los ROS generan una reacción en cadena de radicales libres; en el caso de los ácidos grasos poli-insaturados (PUFA), se producen distintos radicales lipídicos que finalmente se acumulan en las membranas plasmáticas, generando su disfunción, así como la de receptores unidos a membrana. Los productos finales de la peroxidación lipídica incluyen aldehídos insaturados y otros metabolitos, que poseen actividad mutagénica y citotóxica (Cai & Harrison, 2000). La disfunción endotelial causada por el aumento en la producción de ROS genera un aumento en los niveles de expresión de moléculas de adhesión, tales como, VCAM-1 (del inglés, *vascular cell adhesion molecule-1*), ICAM-1 (del inglés, *intercellular adhesion molecule-1*) y E-selectina, y como consecuencia transmigración de leucocitos (Incalza et al., 2018). Los neutrófilos son las primeras células en llegar al lugar de la inflamación, respondiendo a citoquinas proinflamatorias (IL-1β y tumor necrosis factor-alpha (TNF-α)), se unen a E-Selectina e ICAM-1 favoreciendo la unión a células endoteliales y la transmigración. La expresión de moléculas de adhesión responde a factores de transcripción tales como nuclear factor (NF)-κB. Por otra parte, las células del músculo liso juegan un papel fundamental

al responder a citoquinas proinflamatorias aumentando la producción de ROS via angiotensina II, la expresión de moléculas de adhesión y la señalización del complejo CD40/CD40L, donde este último es uno de los principales mediadores inflamatorios en la formación y desarrollo de la placa atherosclerótica (Incalza et al., 2018; Libby, 2000). Este complejo en el macrófago activado por el aumento en LDL oxidada, aumenta las complicaciones de la lesión aterosclerótica (Libby, 2000). Es importante destacar que la patología cardiovascular es un proceso que comienza en la infancia y avanza a lo largo de la vida (Olson et al., 2017).

La Organización Mundial de la Salud (OMS) estima que el 80% de las ECV podrían prevenirse a través del control de sus principales factores de riesgo. Un factor de riesgo se define como "cualquier rasgo, característica o exposición de un individuo que aumente su probabilidad de sufrir una enfermedad o lesión" (MINSAL, 2014). Entre los factores de riesgo de ECV se encuentran la alimentación no saludable (alta ingesta de grasas saturadas, grasas trans, azúcar y sal), la obesidad, el tabaquismo, sedentarismo y consumo excesivo de alcohol, dado la asociación que existe entre estos factores con presión arterial elevada, hiperglicemia e hipercolesterolemia. Los factores de riesgo actúan de forma combinada y multiplicativa,

promoviendo la progresión de la lesión aterosclerótica, principal causa de la ECV (Paccot, 2014).

La obesidad es una condición caracterizada por una excesiva acumulación de grasa, lo que conduce a un estado alterado del metabolismo y de la fisiología corporal (Curtasu et al., 2019). Una dieta alta en grasas (HFD, del inglés high-fat diet), en asociación con un estilo de vida sedentario incrementa la probabilidad de desarrollar un estado de obesidad (Kesherwani et al., 2015). Por otro lado, una dieta alta en grasas calórica ha sido relacionada con un incremento en el estrés oxidativo y la inflamación, ya que se asocia a un aumento de la expresión de p^{47}phox (subunidad clave de la enzima nicotinamida adenina dinucleotido fosfato oxidasa), de las ROS y el factor de transcripción NF-κB (nuclear factor-κB) con una subsecuente elevación de la citoquina proinflamatoria TNF-α (Biobaku et al., 2019). A su vez se ha propuesto, que la obesidad causa una excesiva generación de ROS, debido a la acumulación de ATP, conducente a una disminución en velocidad del flujo de electrones a través de la cadena transportadora de electrones, promoviendo la generación de intermediarios reactivos y la generación de anión superóxido (Incalza et al., 2018).

Para evaluar marcadores biológicos de estrés oxidativo y cómo fuentes

exógenas son capaces de disminuirlos es que actualmente se utilizan diversas metodologías *in vitro*, las cuales son presentadas en la sección 1.2.

1.2 Metodologías *in vitro* en la evaluación de marcadores biológicos de estrés oxidativo.

La determinación de la capacidad antioxidante de frutos o sus extractos es relevante, puesto que su consumo se asocia con una disminución del estrés oxidativo y, en consecuencia, a un beneficio en la salud cardiovascular. Por lo general, esta aproximación se realiza mediante ensayos químicos, los cuales corresponden a métodos de *screening*, basados en la comparación del efecto reductor de un patrón de capacidad antioxidante conocida con el compuesto o extracto a evaluar. Esta metodología, si bien es rápida y fácil de realizar, no representa necesariamente el efecto que un extracto podría tener a nivel biológico, debido a que los radicales utilizados en estas metodologías no se encuentran normalmente en nuestro organismo (Manach et al., 2005). Es por ello que el estudio de la capacidad antioxidante debe ser complementado con métodos biológicos, los cuales permiten definir la eficacia en relación con la disminución del estrés oxidativo, la viabilidad celular y la posible implicancia en diversas patologías. Estos antecedentes

son centrales para el diseño de ensayos en animales y humanos que validan el efecto antioxidante *in vivo*.

Para la determinación de la capacidad antioxidante de un extracto, molécula o compuesto mediante métodos biológicos *in vitro* se requieren cultivos celulares, en los cuales se miden productos de oxidación. Entre los métodos biológicos se encuentran: la determinación de ROS mediante la sonda fluorescente 2,7-diclorodihidrofluoresceínadiacetato (H_2DCF-DA) (Keyse, 2000)*;* la determinación de productos generados por estrés oxidativo tales como: malondialdehído (MDA) y 4- hidroxinonenal (4-HNE), ambos generados por la peroxidación de ácidos grasos insaturados (Rossi et al., 2016)*;* activación de factores de transcripción inflamatorios, tales como el NF-kB; determinación de los niveles de cGMP que media la vasodilatación dependiente de endotelio (Profumo et al., 2016), entre otros. Sin embargo, la primera aproximación que se debe realizar es la evaluación de viabilidad celular en presencia de los extractos o compuestos polifenólicos que se quieran evaluar, debido al posible efecto citotóxico de dichas moléculas o de los solventes en los cuales son solubilizadas (Lin et al., 2012).

Los cultivos celulares utilizados para la determinación de la capacidad antioxidante son variados e incluyen células tumorales, como las células de

cáncer de hígado (HepG2) (Macias-Barragan et al., 2014), cardiomiocitos (H9C2) (Zhang et al., 2018), células mononucleares de sangre periférica, células estelares hepáticas (Macias-Barragan et al., 2014), entre otras. Para evaluar el efecto de moléculas o extractos con capacidad antioxidante en el desarrollo de la ECV, con frecuencia se utilizan modelos de células endoteliales, ya sea obtenidas desde cultivos primarios, como ocurre con las células endoteliales de vena umbilical humana (HUVEC) (Jaffe et al., 1973), o de líneas celulares, como las EA hy926 (Karbach et al., 2012). El uso de estos modelos es de gran utilidad, debido a que las células endoteliales son las responsables de la mantención de homeostasis vascular, por lo que cualquier alteración en su función puede desencadenar la disfunción endotelial y el desarrollo del proceso ateromatoso.

1.3 Polifenoles y protección vascular

Los polifenoles corresponden a un grupo de compuestos fitoquímicos distribuidos como metabolitos secundarios en el reino vegetal, contribuyendo en el crecimiento y morfología de los vegetales. Algunos de estos metabolitos son responsables de otorgar el gusto y color a vegetales (Soares et al., 2018), además de participar en su sistema de defensa, siendo capaces

de responder a estrés por radiación ultravioleta, patógenos o daño físico (Apak et al., 2007). El proceso de síntesis de los polifenoles se realiza mediante la vía del ácido shikímico, desde el fosfoenolpiruvato a fenilalanina, posteriormente a cinamato y 4-cumarato, formándose chalcona, flavonona, dihidroflavonol y las antocianinas (Apak et al., 2007). Dentro de estos compuestos se encuentran los flavonoides, ácidos hidroxicinámicos y sus derivados, los cuales presentan altas concentraciones en *Berberis microphylla* (calafate), fruto objeto de estudio durante esta tesis doctoral.

1)Flavonoides: corresponden al grupo mayoritario de los compuestos fenólicos. Actualmente se conocen aproximadamente 5.000 flavonoides, presentes en frutas, verduras y sus derivados, tales como vino, jugos y cerveza. La estructura básica de los flavonoides consta de 15 átomos de carbono, distribuidos en 2 anillos fenilo (anillos A y B), unidos por un esqueleto de 3 carbonos (Figura 1.1). Entre los flavonoides se encuentran los flavonoles y las antocianidinas.

a) Antocianidinas: por lo general no se encuentran libres en la naturaleza, debido a su baja estabilidad, pero sí es posible detectarlos en su forma glicosilada, formando los antocianos, los cuales pueden estar hidroxilados en las posiciones 3, 5 y 7 y metoxilados en diferentes

posiciones (Prior & Wu, 2006). Los hidroxilos y azúcares a los cuales están unidos les otorgan polaridad, siendo solubles en agua, metanol y etanol. Los azúcares que se unen a antocianidinas son glucosa, galactosa, ramnosa, arabinosa, xilosa y fructosa. Entre las antocianidinas, las más comúnmente encontradas en alimentos son: pelargonidina, cianidina, peonidina, delfinidina, petunidina y malvidina (Crozier et al., 2009). Además, se ha demostrado que las antocianinas se reorganizan estructuralmente, de acuerdo al pH: pH 1-3 se encuentran como catión flavilio, y sobre pH 4 como carbinol y chalcona, esta última es susceptible a la degradación hacia ácidos fenólicos (Fang, 2014). Se han descrito más de 500 antocianinas distintas en literatura (de Pascual-Teresa et al., 2010).

b) Flavonoles: se encuentran representados principalmente por quercetina, kaempferol y miricetina entre otros. Se caracterizan por presentar una insaturación entre los carbonos C2 y C3 del anillo C y se diferencian entre ellos por los sustituyentes del anillo B (Hollman & Arts, 2000). En su mayoría están glicosilados en la posición 3 del anillo C, pero también pueden aparecer en las posiciones 5, 7, 4´, 3´ y 5´.

Estos compuestos están presentes en baja concentración en el reino vegetal (15-30 mg/kg de peso fresco de fruto) (Hollman & Arts, 2000).

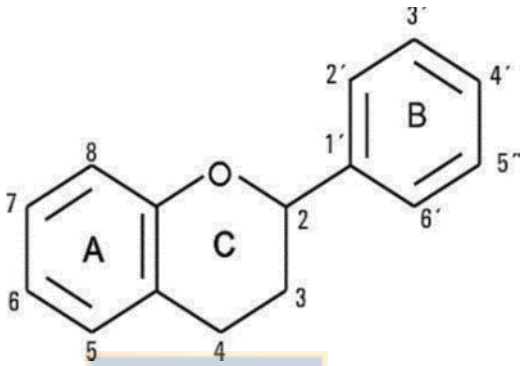

Figura 1.1: Estructura básica de un flavonoide (Hidalgo.2013).

2) Ácidos fenólicos: se encuentran conformados sólo por un anillo aromático con uno o más grupos hidroxilos. En su mayoría se encuentran conjugados con azúcares. Se dividen en los derivados del ácido benzoico y derivados del ácido cinámico. Los ácidos hidroxicinámicos son más abundantes que los derivados benzoicos, encontrándolos en legumbres, cereales, cacao, el aceite de hierbas, en nueces, el café, y en las frutas. Los principales son los ácidos p-cumárico, cafeico y ferúlico (Alam et al., 2016). Se ha reportado que los compuestos polifenólicos poseen propiedades antibióticas, antitumorales, antioxidantes y antivirales, y que participan en la

prevención de enfermedades crónicas, tales como, patologías neurodegenerativas, cáncer y enfermedades cardiovasculares, todas estas asociadas entre otros factoresal estrés oxidativo (Andriantsitohaina et al., 2012).

Los polifenoles, especialmente los flavonoides, donan fácilmente sus hidrógenos y ceden electrones, por lo que poseen una gran capacidad antioxidante, que depende del número de grupos hidroxilos, la posición en que se encuentran estos sustituyentes, y su conjugación (Kuskoski et al., 2004). Además, este tipo de compuestos posee electrones donadores en el anillo estructural, lo que se debe a la capacidad del grupo aromático para soportar el desapareamiento de electrones, esto por desplazamiento del sistema de electrones π, por lo que ellos pueden actuar como reductores de los ROS (Kuskoski et al., 2004).

Se ha demostrado que el consumo de compuestos polifenólicos disminuye el riesgo asociado de desarrollar ECV y síndrome metabólico (Tresserra-Rimbau et al., 2014), esto debido a que reducen la presión sanguínea y la expresión de marcadores de inflamación, como consecuencia de una menor expresión de la enzima NADPH oxidasa y un aumento de la actividad de enzimas antioxidantes, tales como la superóxido dismutasa (SOD) y la

catalasa (Andriantsitohaina et al., 2012; Sarr et al., 2006; Sandoval-Acuña et al., 2014). En relación con los principales polifenoles con acción antioxidante, destaca el resveratrol, el cual aumenta el mRNA y la expresión de Nrf2, y regula positivamente la expresión de sus genes blanco, tales como, la Hemoxigenasa y NADPH quinona oxidorreductasa, enzimas que contribuyen a su acción antioxidante (Haskó & Pacher, 2010).

Los flavonoides producen una amplia gama de efectos protectores de la función cardiovascular (figura 1.2). De hecho, en un estudio realizado en el año 2014, se demostró una asociación inversa entre el consumo de antocianinas, flavonoles y ácidos hidroxicinámicos y el desarrollo de la ECV (Tresserra-Rimbau et al., 2014). A este respecto, un estudio realizado por Teixeira et al., 2021 demostró que un extracto de purpura grumixama rico en antocianinas y flavonoles (401.81 ± 11.15 y 71.82 ± 2.02 mg/100g peso seco, respectivamente), administrado diariamente (200 mg/kg de peso corporal) durante 8 semanas en ratones C57BL/6J con dieta alta en grasa y azúcares, es capaz de prevenir la ganancia de peso en alrededor de un 10%, mejorar la tolerancia a la glucosa y la sensibilidad a la insulina, evidenciado por una reducción significativa del índice HOMA (Teixeira et al., 2021). Por otra parte, se ha demostrado que la quercetina, un flavonoide del grupo de los

flavonoles, disminuye la concentración de anión superóxido y peroxinitrito, reduciendo el estrés oxidativo (Fuentes et al., 2017; Hanasaki et al., 1994); este efecto es logrado mediante la supresión de la actividad de la enzima xantina oxidasa, responsable del catabolismo de las purinas y producción de ácido úrico, y cuya menor actividad genera enfermedades tales como, gota y cálculos renales. La xantina oxidasa contribuye al estrés oxidativo por la producción del radical superóxido y peróxido de hidrógeno en el proceso de conversión de hipoxantina a ácido úrico (Martínez S. et al., 2001). También se ha encontrado que quercetina es capaz de aumentar la expresión del ARNm de la eNOS y del factor de crecimiento de endotelio vascular (VEGF) en células endoteliales de vena umbilical humana (HUVEC), así como de disminuir la expresión de endotelina-1 (ET-1); todos estos resultados se relacionarían con un efecto vasodilatador (Nicholson et al., 2010). Por otro lado, la delfinidina, un flavonoide perteneciente al grupo de las antocianinas es un potente antioxidante que ha demostrado una gran potencia *in vitro* en cultivo de células HUVEC, contra el anión superóxido y peroxinitrito, a concentraciones de 25 a 200 µM (Chen et al., 2010). Este efecto depende de la capacidad de delfinidina de restaurar la actividad de la enzima SOD manteniendo la función de las células endoteliales y atenuando la

peroxidación lipídica (Chen et al., 2010). También se demostró que delfinidina disminuye la expresión de Bax y aumenta la expresión de Bcl-2 en HUVEC pretratadas con LDLox 100 µg/mL, lo que disminuye la apoptosis celular causada por estrés oxidativo (Chen et al., 2010). Por último, un estudio realizado en ratones C57BL/6J alimentados con dieta alta en grasas (HFD) y HFD suplementada con ácido clorogénico (100 mg/Kg de peso) durante 13 semanas, demostró que su ingesta es capaz de disminuir en un 15% el aumento de peso corporal en comparación con los ratones HFD, esto debido a un aumento del 3% en la termogénesis y catabolismo energético. Estos resultados se correlacionaron con una mayor tolerancia a la glucosa y a una disminución de los niveles de lactato deshidrogenasa (LDH) y nitrógeno ureico en sangre (BUN) (He et al., 2021). Este ácido hidroxicinámico, aumenta los niveles de adiponectina en suero y tejido adiposo. Siendo esta última responsable de un aumento en la expresión y actividad de PPAR-α, lo que favorece la oxidación de ácidos grasos y la actividad del ciclo del ácido tricarboxílico en el hígado, inhibiendo la activación de NF-κB y en consecuencia la expresión de moléculas de adhesión (Shabalala et al., 2020).

En conclusión, diversas fuentes alimenticias enriquecidas en polifenoles, tales como, vino, jugo de uva, maqui o té verde, tienen el potencial de mejorar la salud vascular, debido a que sus metabolitos secundarios hidroxilados estimulan la formación de factores vasodilatadores, tales como, NO y el factor hiperpolarizante derivado de endotelio (EDHF), y disminuyen el stress oxidativo producto del aumento en la actividad de enzimas antioxidantes y el bloqueo del sistema de angiotensina activador de la NADPH oxidasa (Andriantsitohaina, et al; 2012).

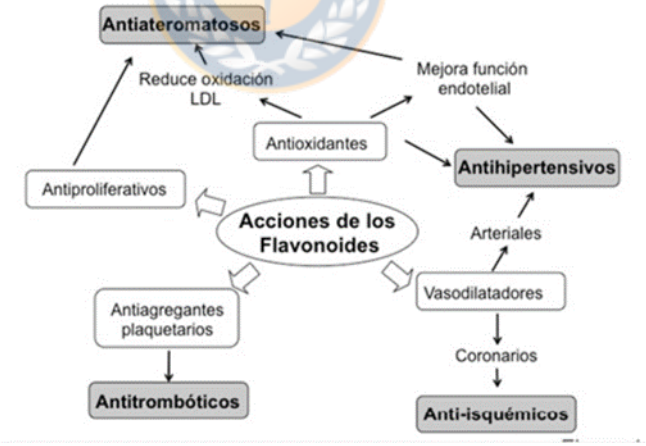

Figura 1.2: Acciones cardiovasculares de los flavonoides (Duarte & Pérez-Vizcaíno, 2015).

1.4 Fuentes alimentarias de polifenoles

Los polifenoles poseen una distribución ubicua en frutas y alimentos, estimándose que al menos 1 gramo de flavonoides se consume en la dieta por día (de Pascual-Teresa et al., 2010; Carnauba et al., 2021). Entre los polifenoles alimentarios se encuentran:

a) Antocianinas: corresponden a antocianidinas glicosiladas. Las antocianidinas son inestables a la luz e insolubles en agua, por lo que su unión a azúcares les provee estabilidad y solubilidad. Las antocianinas están presentes en bayas rojas, azules y moradas, otorgándoles su característico color. Se ha demostrado por métodos químicos una gran capacidad antioxidante de las antocianinas, por lo que se han convertido en uno de los compuestos polifenólicos de mayor interés en investigación (Ruiz et al., 2013). Sus principales fuentes alimentarias son las frutas rojas (Tabla 1.1). Además, este tipo de compuestos corresponden a uno de los pocos polifenoles presentes en su forma nativa en plasma, por lo que su capacidad antioxidante podría relacionarse con la evaluada *in vitro* (de Pascual-Teresa et al., 2010; Matsumoto et al., 2006).

b) Flavonoles: su principal representante en la dieta es la quercetina, presente en manzana, cebolla y otros frutos (Nile et al., 2021; Kumar

et al., 2022). La ingesta de estos compuestos corresponde a un promedio de 20 a 35 mg/día (Manach et al., 2005). En plasma se han encontrado metabolitos derivados de quercetina, tales como: quercetina-3-O-glucuronido, 3'-O-methylquercetina-3-O-glucuronido, quercetina-3'-O-sulfato y sus ácidos fenólicos derivados (Manach et al., 2005; Loke et al., 2009).

c) Ácidos fenólicos: se encuentran en tomates, café, vino tinto, cereales, cerveza, etc., y su concentración varía ampliamente (Carnauba et al., 2021; Lafay & Gil-Izquierdo, 2008). A modo de ejemplo, la ingesta de ácido clorogénico en consumidores de café alcanza valores de alrededor de 800 mg/día, y se ha reportado la presencia de ácido cafeico en el plasma de estos sujetos (Lafay & Gil-Izquierdo, 2008). Además, se ha verificado que el ácido ferúlico, un representante de ácidos hidroxicinámicos presente en tomates y cerveza, se absorbe de manera eficiente, siendo encontrado en plasma (Manach et al., 2005).

Tabla 1.1: Contenido de Antocianinas en alimentos de origen vegetal *(Tabla modificada desde Pascual, et al. 2010).*

Alimento	**Contenido (mg/100 g fruto fresco)**	**Método de cuantificación**
Manzana	0-60	HPLC-DAD
Grosella	2-43,3	Método pH diferencial
Arandano	67-140	Método pH diferencial
Melocotón	4,2	HPLC-DAD
Maíz morado	1642	Método pH diferencial
Ciruela	2-25	HPLC-DAD-ESI-MS/MS
Frambuesa	20-687	HPLC-DAD-ESI-MS/MS
Uva roja	30-750	Beer-Lambert relationship
Rábano rojo	100-154	HPLC-DAD-ESI-MS/MS
Calafate	1683-1879	HPLC-DAD-ESI-MS/MS
Maqui	1673-1903	HPLC-DAD-ESI-MS/MS

En este contexto, se han descrito frutos de alto contenido en polifenoles, entre los cuales los más estudiados son el maqui y el arándano (Speisky et al., 2012). En ellos se ha reportado un contenido total de polifenoles de 113 ± 12

y 17 ± 1 equivalentes de ácido gálico/g f.w (fruto fresco), respectivamente (Ruiz et al., 2010), que se condice con la capacidad antioxidante de estos frutos, evaluada por métodos químicos (100,5 ± 24,5 µmol de Trolox/ g f.w y 14,5 ± 0,59 µmol de Trolox/ g f.w, respectivamente). La mayor capacidad antioxidante del maqui se puede deber a su gran contenido de antocianinas, correspondiente a 20,22 ± 1,30 µmol /g f.w, (Ruiz et al., 2010).

1.5 Metabolismo de polifenoles

Los polifenoles consumidos en la dieta sufren una serie de reacciones metabólicas, las cuales alteran sus estructuras y, en muchas ocasiones, sus propiedades antioxidantes. A continuación, se describen algunos procesos metabólicos que pueden sufrir estos compuestos.

a) Antocianinas: su concentración máxima en plasma se ha reportado entre las 0,5 - 2 horas posteriores al consumo de frutos ricos en antocianinas, alcanzando niveles de 1 a 100 nmol/L en humanos. Además, se ha descrito una absorción rápida de antocianinas a los pocos minutos de su ingesta, lo que sugiere una absorción a nivel estomacal (Passamonti et al., 2003). Este hallazgo fue corroborado en ratas, a las cuales se les realizó una perfusión gástrica con una mezcla

de antocianinas (3,8 μmol en 4 ml de HCl 10 mM / NaCl 0,15 M), encontrándose que éstas aumentaban rápidamente en plasma, tanto en circulación sanguínea como portal (Passamonti et al., 2003). Este tipo de compuestos también son absorbidos en el intestino delgado, principalmente en el yeyuno, encontrándose una absorción del 55,3 ± 7,6% con respecto a la ingesta. Es por estas razones se observan dos peaks de máxima absorción que, para el caso de delfinidina-3-glucósido, se obtienen a los 15 y 30 minutos, y corresponden a la absorción gástrica e intestinal, respectivamente (Fang, 2014).

En un estudio en humanos se administró vía oral cianidina-3-glucósido marcada con ^{13}C, y se siguió la aparición de metabolitos en circulación sanguínea, en la orina y heces. Se detectó como principales metabolitos aquellos metilados y glucoronidados en orina, y ácidos derivados en plasma, orina y heces (Fang, 2014). Así también se ha reportado que pelargonidina-3-glucósido es metabolizada a ácido 4-hidroxibenzoico. El hígado juega un rol fundamental en su metabolismo, encontrándose pelargonidina-3-glucurónido (Pg-3-GlcA) y pelargonidina-3-glucosido-glucuronido (Pg-3-glc-glcA) como principales metabolitos (Fang, 2014).

Por otro lado, delfinidina-3-glucósido, petunidina-3-glucósido y malvinidina-3-glucósido, así como sus respectivos metabolitos glucoronidados, fueron encontradas en plasma y orina luego de la administración de jugo de uva a humanos (Fang, 2014).

b) Ácidos hidroxicinámicos: muy pocos estudios se han centrado en evaluar la ingesta diaria de ácidos hidroxicinámicos; sin embargo, se piensa que ésta puede llegar a ser elevada, principalmente en consumidores de vino y café.

   Se ha demostrado en ratas que la esterificación de ácido cafeico a ácido clorogénico reduce significativamente su absorción, por lo que la absorción de ácido clorogénico principalmente se produce debido a esterasas encontradas en el microbiota intestinal (Lafay & Gil-Izquierdo, 2008). Nardini et al., 2002 han encontrado sólo ácido cafeico luego de la absorción de café, reportando presencia de ácido clorogénico. Algunos metabolitos de este ácido, además del cafeico son: ácido ferúlico, ácido isoferúlico, ácido dihidroferúlico, ácido vanilico, ácido 3,4-dihidroxifenilpropionico, ácido 3-hidroxihipurico y ácido hipúrico.

1.6 Polifenoles en *Berberis microphylla*

Muchos de los polifenoles de la dieta han sido encontrados en el fruto de *Berberis microphylla* (calafate), un arbusto endémico de la Patagonia Chilena y Argentina. El contenido polifenólico del fruto de calafate ha sido caracterizado y cuantificado en el Departamento de Análisis Instrumental de la Facultad de Farmacia en la Universidad de Concepción, destacándose la presencia de: antocianinas (22,91 ± 0,04 – 35,99 ± 0,05 µmol / g f.w), siendo las mayoritarias delfinidina-3-glucósido, petunidina-3-glucósido y malvidina-3-glucósido (Ruiz, Hermosín-Gutiérrez, et al., 2013); flavonoles (1,33 ± 0,54 µmol / g f.w), con quercetina como principal representante (Ruiz et al., 2014); y ácidos hidroxicinámicos (0,60 ± 0,14 – 7,47 ± 0,15 µmol / g f.w), cuyo mayor constituyente corresponde al ácido 3-cafeoilquínico (Ruiz, et al., 2013). Además, se ha determinado la capacidad antioxidante del extracto crudo obtenido desde el fruto del calafate mediante métodos químicos, como ORAC, ABTS y CUPRAC, demostrando similar actividad antioxidante que *Aristotelia chilensis* (Maqui) (Ruiz et al., 2010), fruto al cual se le han atribuido propiedades tales como: alta capacidad antioxidante, efecto cardioprotector (Céspedes et al., 2008), antidiabético (Rojo et al., 2012), entre otros.

Mariangel et al., 2013 demostró similares resultados a los obtenidos por Ruiz et al., 2014, en calafate obtenido desde diferentes localidades de la novena región de Chile, reportándose que *Berberis microphylla* presenta un alto contenido de polifenoles (antocianinas, ácidos fenólicos y flavonoles), lo cual es influenciado por la ubicación geográfica al igual que la capacidad antioxidante; esto sugiere que las condiciones climáticas presentes en cada zona causan una variación en la concentración de estos compuestos (Mariangel et al., 2013; Ruiz et al., 2014). De igual forma, Ramirez et al., 2015 reportó similares resultados en bayas, como arándano azul (*Vaccinium corymbosum*) y calafate, lo que se correlacionó con su capacidad antioxidante determinada por métodos químicos y biológicos. En este estudio se reportó que extractos de estos frutos inhibían en más del 90% la peroxidación lipídica causada en eritrocitos por la incubación durante 15 minutos a 37°C con ter-butilhidroxiperóxido (1mM) (Ramirez et al., 2015). Cabe señalar que la peroxidación lipídica es crucial en la inducción y propagación de enfermedades relacionadas con estrés oxidativo, de particular importancia en la ECV (Shao et al., 2018).

Similares resultados han sido presentados por Reyes-Farias et al., 2016, quienes reportaron un gran contenido de antocianinas en dos frutos

endógenos de Chile: *Aristotelia chilensis* (maqui) y *Berberis microphylla* (calafate), gracias al análisis por cromatografía de líquido acoplada a espectrometría de masas (LC-MS). También *in vitro*, por análisis de co-cultivo de adipocitos y monocitos diferenciados obtenidos desde ratones, este grupo demostró que dichos frutos reducen la inflamación, el estrés oxidativo y la resistencia a la insulina, resultados que se correlacionaron con un aumento en la razón entre glutatión reducido y oxidado (GSH/GSSG) y la disminución del estrés oxidativo, la inhibición de la inducción de la caspasa-3 y de la apoptosis de los adipocitos (Reyes-Farias et al., 2016). Otro estudio reportó la inhibición en la expresión del gen del factor de necrosis tumoral alfa (TNF-α) en macrófagos murinos estimulados con liposacáridos, en presencia de extracto de calafate (Reyes-farias et al., 2015). Además, Calfío & Huidobro-Toro, 2019 describieron un efecto vasodilatador de un extracto de calafate hidroalcohólico, el que fue inhibido en un 89.6% por N-Nitro-L-Arginina (L-NNA) (150 µM), un inhibidor de la eNOS (Calfío & Huidobro-Toro, 2019). Finalmente, Bustamante et al., 2018 llevó a cabo una intervención nutricional aguda en gerbos con calafate, siguiendo las recomendaciones de la Organización Mundial de la Salud (OMS) para la prevención de enfermedades crónicas (300g fruto por día), con el fin de

estudiar la metabolización de sus principales compuestos fenólicos. El estudio reportó el análisis farmacocinético de los compuestos fenólicos y la concentración plasmática de 16 ácidos fenólicos derivados (0,1-1µM). Este estudio definió las concentraciones plasmáticas que pueden ser estudiadas en nuevos ensayos *in-vitro*, para demostrar el efecto de este fruto (Bustamante et al., 2018). Así también confirmó el aumento de metabolitos derivados de compuestos fenólicos en plasma, los cuales podrían tener un efecto benéfico *in-vivo* (Bustamante et al., 2018).

Estos antecedentes permiten considerar que el calafate puede otorgar grandes beneficios para la salud humana, por lo que se hace imprescindible identificar los cambios metabólicos asociados a su consumo. Para este objetivo, actualmente se utiliza la metabolómica, estrategia analítica que permite identificar metabolitos presentes en fluidos biológicos posterior al consumo de algún fruto o su extracto, así como también detectar cambios en biomarcadores asociados, por ejemplo, al estrés oxidativo, como consecuencia del consumo de polifenoles y los efectos de éstos en el metaboloma.

1.7 Metabolómica

La metabolómica (*Metabolomics*) relaciona directamente una respuesta química medible con un evento biológico, vinculando el genotipo y el fenotipo de un organismo (Marshall & Powers, 2017;McGarrah et al., 2018). Su principal objetivo corresponde al análisis exhaustivo de matrices amplias de metabolitos en muestras biológicas (Dettmer et al., 2007).

El metaboloma representa un gran número de componentes que pertenecen a una amplia variedad de clases de compuestos, como aminoácidos, lípidos, ácidos orgánicos, nucleótidos, etc. Estos compuestos son muy diversos en sus propiedades físicas y químicas y se encuentran en un amplio rango de concentración (Dettmer et al., 2007) que puede ser modificado producto de la exposición a factores externos. En la actualidad existen dos enfoques complementarios para los estudios metabolómicos: "*targeted metabolomics*" y "*untargeted metabolomic*". Los resultados de "*targeted metabolomics*" son cuantitativos y permiten crear bases de datos que se pueden integrar con mapas de rutas metabólicas u otros datos "ómicos". El segundo enfoque hacia la metabolómica es la "*untargeted metabolomic*", cuya intención no es identificar cada metabolito observado, sino comparar patrones o "huellas digitales" de metabolitos que cambian en respuesta a estímulos, patologías,

exposición a toxinas, alteraciones ambientales o genéticas (Dettmer et al., 2007).

La metabolómica basada en espectrometría de masas (MS) ofrece análisis con alta selectividad y sensibilidad y el potencial de identificar los metabolitos detectados (Marshall & Powers, 2017), para lo cual es importante contar con un adecuado control de calidad (Evans et al., 2020). La combinación de MS con una técnica de separación como la cromatografía, reduce la complejidad de los espectros de masas y además entrega información adicional sobre las propiedades fisicoquímicas de los metabolitos, lo que contribuye en su posterior identificación. A pesar de ello, las técnicas basadas en MS necesitan una preparación previa de muestra, lo que puede causar pérdidas de metabolitos (Marshall & Powers, 2017) (Dettmer et al., 2007).

Los resultados obtenidos en estudios metabolómicos por MS son analizados mediante métodos estadísticos multivariantes, con el objetivo de simplificar y acelerar el análisis de datos. Si bien estas técnicas agilizan regularmente este proceso, si se usan de manera incorrecta o carecen de una validación

adecuada, conducen a una proliferación de datos erróneos (Worley & Powers, 2016).

Las técnicas estadísticas multivariadas más utilizadas son el Análisis de Componentes Principales (PCA) y el análisis de cuadrados mínimos parciales ortogonales (OPLS-DA), que permiten determinar si los metabolomas difieren y, si lo hacen, identificar las características espectrales que definen la separación grupal, es decir, los metabolitos responsables de dicha separación (Worley & Powers, 2016; Bujak et al., 2014). Un resultado típico de un modelo de PCA u OPLS es un gráfico de "s*cores*" o "puntuaciones", donde cada espectro de MS se ha reducido a un solo punto en el espacio de PC (Componente Principal), observándose en el sí existe separación o no entre dos grupos. De manera similar, se genera un gráfico de "*loadings"* o "cargas", donde la intensidad relativa y la dirección de los picos espectrales indican la contribución y la correlación del pico a la separación de grupo (Marshall & Powers, 2017). Lo correcto para estos análisis es realizar en una primera instancia un PCA, para observar si existe separación espontánea de grupos, y verificar la presencia de *outliers*, y posteriormente realizar un OPLS-DA, ya que un modelo PLS / OPLS puede producir la apariencia de

una separación de grupo clara incluso para ruido o datos completamente aleatorios (Worley & Powers, 2016).

Para la selección de *features* o características significativas también es posible llevar a cabo análisis univariados, tales como un test-t de Student o un ANOVA, estos de igual forma permiten establecer diferencias entre grupos de estudio; sin embargo, no consideran la interacción entre diferentes metabolitos (Alonso et al., 2015).

Un aspecto relevante en un ensayo metabolómico es el control de calidad, que abarca tanto procedimientos generales como específicos. Los procedimientos generales que garantizan la calidad corresponden al chequeo del sistema LC-MS previo al análisis y las acciones realizadas para mantener las condiciones ambientales y las muestras. Por ejemplo, el uso de aire acondicionado, almacenamiento de muestras a -80°C con un sistema registrador de temperatura, mantención de muestras durante la extracción a 4°C, etc (Evans et al., 2020).

Con respecto a los procedimientos específicos en un análisis metabolómico por LC-MS, la calidad de los análisis es validada mediante el uso de muestras de control de calidad, las que incluyen: 1) Muestras blanco (blanco de análisis

sin inyección, blanco de solvente de reconstitución, blanco de extracción), que permiten evaluar posibles contaminaciones del sistema y la limpieza de la columna previo al análisis; 2) muestras de control de calidad (QCs), que corresponden a una mezcla de igual proporción de las muestras y son analizadas durante la adquisición de la data. Permiten evaluar la reproducibilidad instrumental y el método de extracción, en el caso de muestras de plasma (Curtasu et al., 2019; Evans et al., 2020).

Por otra parte, la calidad de la identificación de los compuestos significativos es de gran importancia y para ello es necesario contar con información de MS y MS/MS con el objetivo de realizar identificaciones de acuerdo con los estándares metabolómicos reportados en "*Mass spectrometry-based metabolomics: a guide for annotation, quantification and best reporting practices*" (Alseekh et al., 2021). En este sentido, el nivel de anotación es relevante, ya que da sustento al análisis y favorece la interpretación biológica de los datos.

En resumen, el *workflow* ó flujo de trabajo metabolómico incluye (Figura 1.3): 1) Diseño experimental y preparación de muestra (población muestral, variabilidad de la población, evaluación del método de extracción, etc); 2)

adquisición de la data por UHPLC-MS/MS en modalidad de ionización positiva y negativa; 3) Procesamiento de la data y obtención de la *bucket table* caracterizada por ser una tabla de intensidades que relaciona las muestras que se encuentran en columnas y los *features* (m/z, t_R) (metabolitos) ubicados en las filas; 4) análisis de datos e identificación de metabolitos; 5) Interpretación biológica (Alonso et al., 2015).

Mediante las estrategias metodológicas y estadísticas descritas previamente, se desea evaluar el efecto del consumo crónico de fruto de *Berberis microphylla* sobre el metaboloma de ratones expuestos a una dieta alta en grasas, con el objeto de detectar biomarcadores asociados a posibles efectos cardioprotectores.

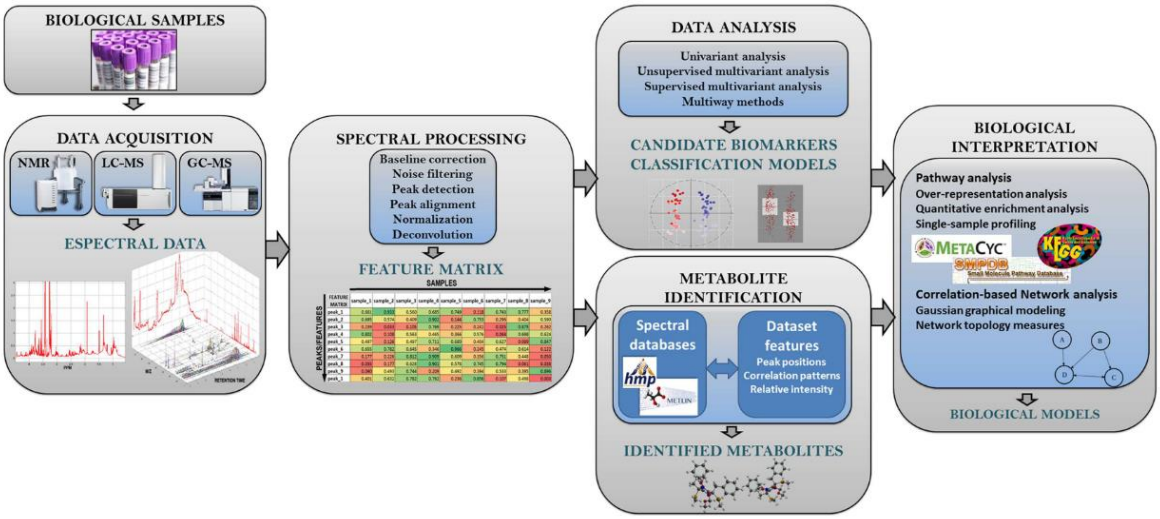

Figura 1.3: Flujo de trabajo de un análisis metabolómico (Alonso et al., 2015).

CAPITULO 2: HIPÓTESIS Y OBJETIVOS

2.1 Hipótesis

Un extracto del fruto de *Berberis microphylla* G. Forst (Calafate) reduce ciertos biomarcadores y/o parámetros biológicos asociados al desarrollo de enfermedades cardiovasculares.

La implementación secuencial de ensayos *in vitro* y de modelos *in vivo*, asociados a tecnología instrumental avanzada, permiten constituir una plataforma de estudios bioanalíticos para el análisis holístico del efecto del consumo de calafate.

2.2 Objetivo general

Evaluar el efecto cardioprotector del fruto de calafate mediante la implementación de una plataforma de bioanálisis basada en ensayos *in vitro* e *in vivo*, asociados a instrumentación analítica avanzada, para una interpretación integral de resultados.

2.3 Objetivos específicos

- Evaluar el efecto protector de extractos del fruto de calafate frente a estrés oxidativo en cultivos primarios de células endoteliales de vena umbilical humana y en la lipoperoxidación de lipoproteínas de alta densidad (LDL) humanas.
- Desarrollar una estrategia analítica que incluya tratamiento de muestras biológicas obtenidas de un modelo murino de dieta alta en grasa tratados con calafate y análisis metabolómico basado en UHPLC-QTOF/MS, con el fin de detectar metabolitos con significancia biológica.
- Identificar biomarcadores asociados a protección cardiovascular, a partir de los metabolitos con significancia biológica obtenidos por análisis metabolómico desde el estudio con un modelo murino,

- Cuantificar citoquinas en el plasma de ratones alimentados con dieta alta en grasas, mediante tecnología Milliplex, y determinar su significancia biológica en relación con los diferentes grupos de estudio.

CAPITULO 3: ESTRATEGIA ANALÍTICA

Previo a toda investigación en el área clínica, se deben realizar ensayos previos para determinar la pertinencia de las etapas posteriores en animales y humanos. Esto está establecido en la declaración de Helsinki "La investigación médica en seres humanos debe conformarse con los principios científicos generalmente aceptados, y debe apoyarse en un profundo conocimiento de la bibliografía científica, en otras fuentes de información pertinentes, así como en experimentos de laboratorio correctamente realizados y en animales, cuando sea oportuno". Esta tesis doctoral tiene por objetivo sentar las bases para en un futuro desarrollar un estudio con seres humanos, por lo que requiere establecer el efecto de extracto de calafate en modelos biológicos *in vitro* y en un modelo murino, *in vivo*.

Durante el de desarrollo de esta tesis doctoral se evaluó el efecto protector de un extracto de calafate en un modelo de cultivo primario humano de células HUVEC y de LDL obtenidas desde plama humano. Para ello, fue necesario caracterizar extractos metanólicos y etanólicos de calafate, lo cual fue realizado mediante HPLC-DAD-QTOF, TXRF (Medina et al., 2019) y GC-

MS (Pino Ramos et al., 2019), para la determinación de compuestos fenólicos, metales y ácidos grasos, respectivamente. Además, se determinó la capacidad antioxidante de estos extractos, utilizando los métodos de ORAC, CUPRAC y ABTS, y determinación de polifenoles totales por Folin-Ciocalteu (Ruiz et al., 2010; Ruiz, Hermosín-Gutiérrez, et al., 2013;Ou et al., 2013).

A continuación, se evaluó el efecto sobre la viabilidad celular de estos extractos mediante el método absorciométrico del MTT, basado en la actividad mitocondrial (Mosmann, 1983), y se estableció su efecto protector frente a la producción de ROS en células HUVEC estimuladas con H_2O_2, utilizando un método semicuantitativo con la sonda H_2DCF-DA (dihidrodiclorofluoresceina-diacetato)(Keyse, 2000). Finalmente, con el objeto de determinar el efecto de extractos de calafate sobre la peroxidación lipídica en LDL humana (Havel et al., 1955), se siguió la formación de dienos conjugados por absorbancia a 232nm (Campos et al., 2014) y se cuantificó malondialdehído (MDA), producto final de la lipoperoxidación, mediante el método cuantitativo de las especies reactivas del ácido tiobarbitúrico (Richard et al., 1992).

Finalmente, se llevó a cabo un estudio metabolómico en un modelo murino de dieta alta en grasa tratados con calafate, con el fin de detectar metabolitos con significancia biológica relacionados con un efecto protector del fruto. Para ello se consideraron dos grupos de ratones: uno que consumía una dieta normal y el otro una dieta alta en grasa; además, en cada grupo se consideró 2 subgrupos: uno de ellos recibió el extracto de calafate en su dieta. Se obtuvieron muestras biológicas, tales como, sangre y corazón. Posteriormente se realizó la purificación de los metabolitos, basados en el principio del mínimo tratamiento de muestra, siendo posteriormente analizados mediante cromatografía acoplada a espectrometría de masas, UHPLC-QTOF/MS (Marshall & Powers, 2017; Bujak et al., 2014)..

Los resultados obtenidos fueron analizados utilizando el programa MetaboScape de Bruker (www.bruker.com), el cual permitió realizar la extracción de "*features*" (algoritmo T-ReX), caracterizados por el tiempo de retención, m/z e intensidad (*bucket table*). Las *bucket tables* obtenidas fueron procesadas en el programa de libre acceso MetaboAnalyst (Curtasu et al., 2019). Con ello se realizó el pretratamiento de datos (alineación, agrupamiento, normalización y preprocesamiento), análisis de componentes principales (PCA) como análisis exploratorio y el análisis posterior mediante

ANOVA para determinar los *features* significativos (Bujak et al., 2014). La identificación se realizó mediante bases de datos disponibles públicamente, por comparación de los tiempos de retención y masas precisas obtenidas por UHPLC-QTOF/MS.

Finalmente, en el plasma de los ratones se cuantificaron citoquinas y proteínas inflamatorias relacionadas con la patología cardiovascular, utilizando diferentes paneles inmunológicos (MILLIPLEX MAP KIT).

La estrategia analítica general de esta tesis doctoral se puede visualizar en la Figura 3.1.

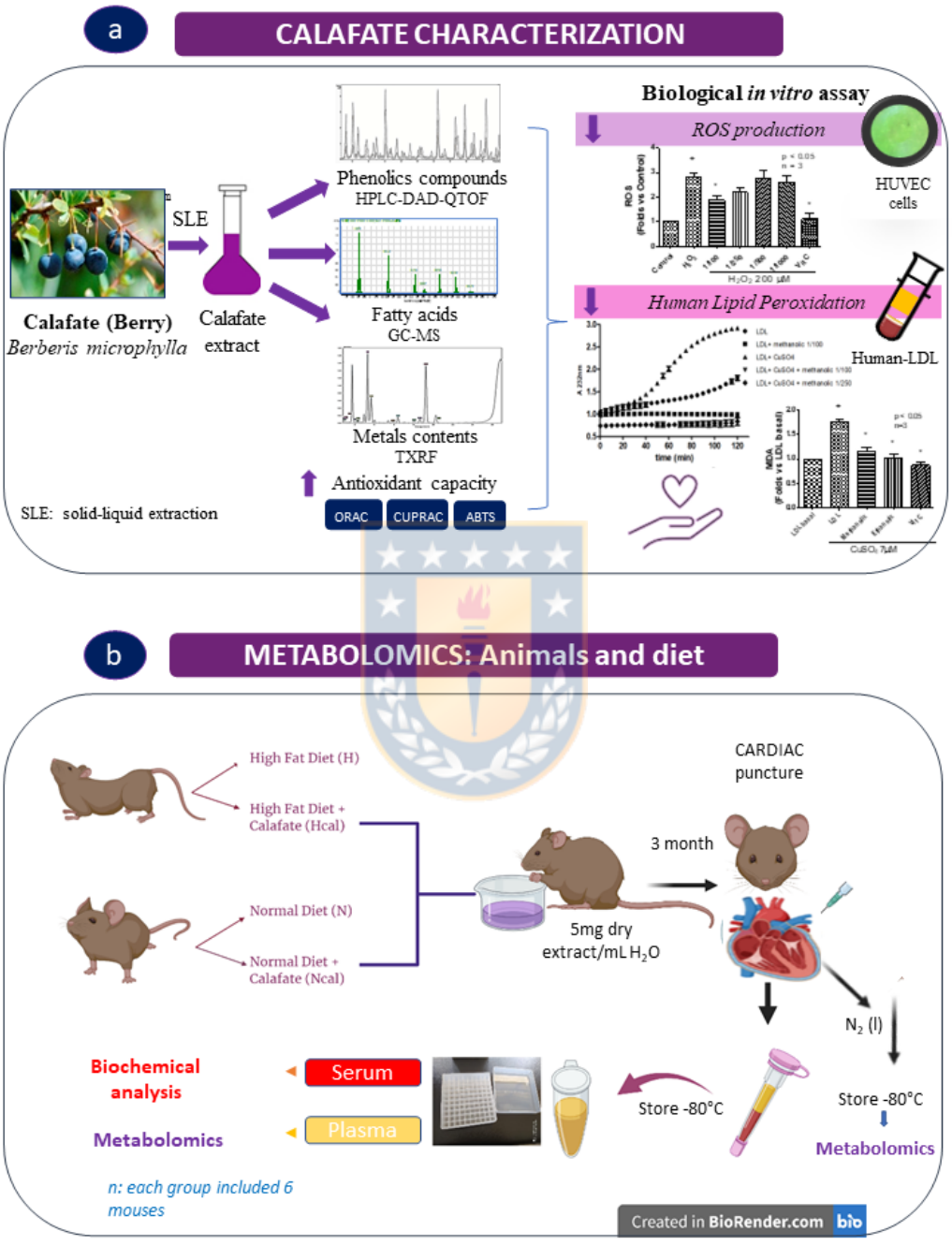
a
CALAFATE CHARACTERIZATION
Biological in vitro assay
ROS production
HUVEC cells
Human Lipid Peroxidation
Human-LDL
SLE
Calafate (Berry)
Berberis microphylla
Calafate extract
Phenolics compounds
HPLC-DAD-QTOF
Fatty acids
GC-MS
Metals contents
TXRF
Antioxidant capacity
ORAC
CUPRAC
ABTS
SLE: solid-liquid extraction
b
METABOLOMICS: Animals and diet
High Fat Diet (H)
High Fat Diet + Calafate (Hcal)
Normal Diet (N)
Normal Diet + Calafate (Ncal)
5mg dry extract/mL H2O
3 month
CARDIAC puncture
N2 (l)
Store -80°C
Metabolomics
Biochemical analysis
Serum
Plasma
Store -80°C
n: each group included 6 mouses
Created in BioRender.com

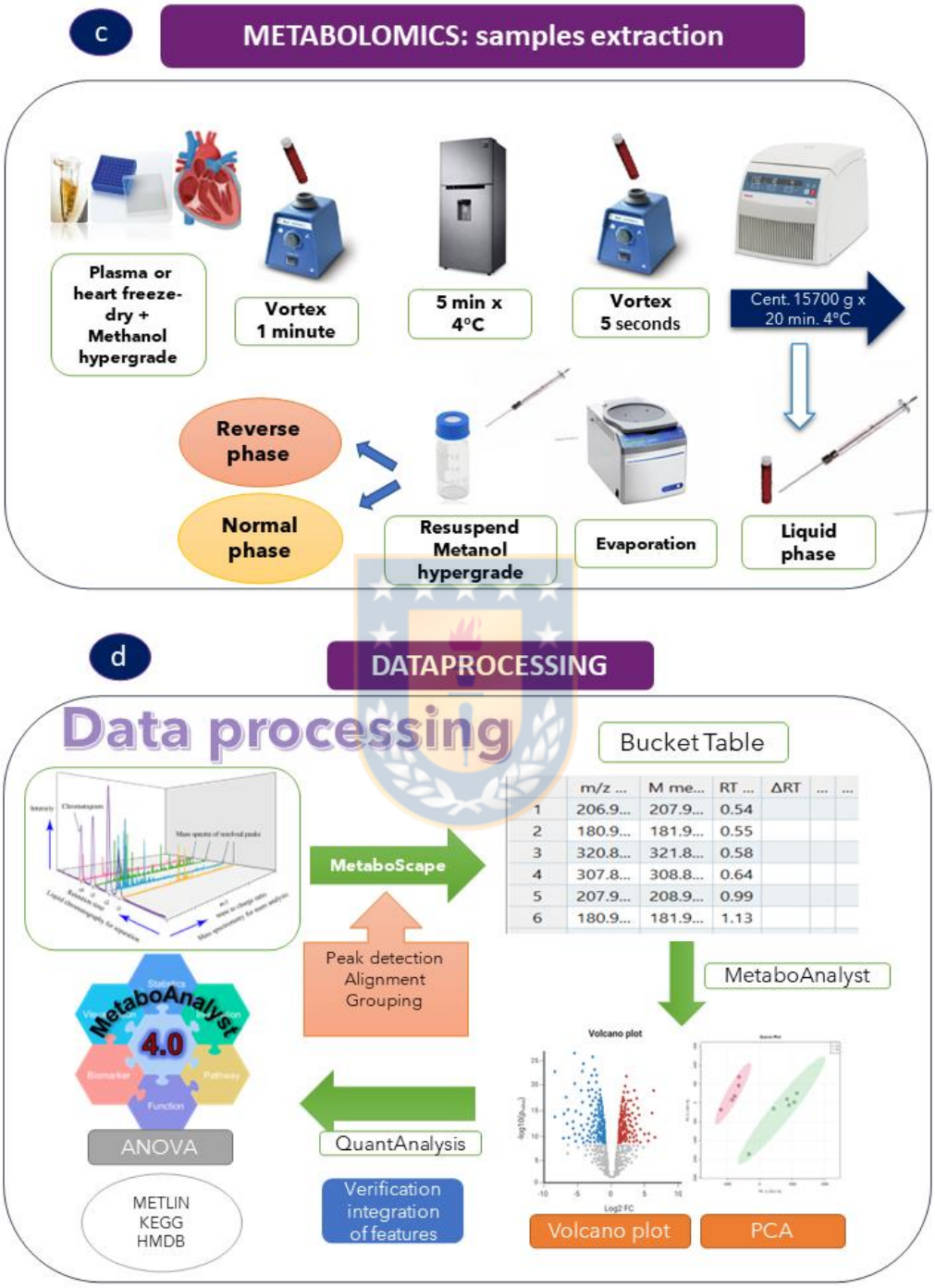
c
METABOLOMICS: samples extraction
Plasma or heart freeze-dry + Methanol hypergrade
Vortex 1 minute
5 min x 4°C
Vortex 5 seconds
Cent. 15700 g x 20 min. 4°C
Reverse phase
Normal phase
Resuspend Metanol hypergrade
Evaporation
Liquid phase
d
DATAPROCESSING
Data processing
Bucket Table
m/z ... M me... RT ... ΔRT
1 206.9... 207.9... 0.54
2 180.9... 181.9... 0.55
3 320.8... 321.8... 0.58
4 307.8... 308.8... 0.64
5 207.9... 208.9... 0.99
6 180.9... 181.9... 1.13
MetaboScape
Peak detection
Alignment
Grouping
MetaboAnalyst
MetaboAnalyst 4.0
ANOVA
METLIN
KEGG
HMDB
QuantAnalysis
Verification integration of features
Volcano plot
Volcano plot
PCA

Figura 3.1: Estrategia analítica utilizada para cumplir con los objetivos planteados. a) Caracterización y determinación la de capacidad antioxidante de calafate utilizando aproximaciones químicas y biológicas *in-vitro*. b) Modelo de estudio murino de dieta alta en grasas utilizado para evaluar el cambio en el metaboloma producto del consumo de calafate. c) Estrategia de extracción utilizada en muestras de plasma y corazón. d) Procesamiento de data utilizado para determinar *features* y biomarcadores significativos asociados con un posible efecto benéfico de calafate frente a la patología cardiovascular.

Referencias

Alam, M. A., Subhan, N., Hossain, H., Hossain, M., Reza, H. M., Rahman, M. M., & Ullah, M. O. (2016). Hydroxycinnamic acid derivatives: A potential class of natural compounds for the management of lipid metabolism and obesity. Nutrition and Metabolism, 13(1), 1–13. https://doi.org/10.1186/s12986-016-0080-3

Alonso, A., Marsal, S., & Julià, A. (2015). Analytical methods in untargeted metabolomics: State of the art in 2015. Frontiers in Bioengineering and Biotechnology, 3(MAR), 1–20. https://doi.org/10.3389/fbioe.2015.00023

Alseekh, S., Aharoni, A., Brotman, Y., Contrepois, K., D'Auria, J., Ewald, J., C. Ewald, J., Fraser, P. D., Giavalisco, P., Hall, R. D., Heinemann, M., Link, H., Luo, J., Neumann, S., Nielsen, J., Perez de Souza, L., Saito, K., Sauer, U., Schroeder, F. C., … Fernie, A. R. (2021). Mass spectrometry-based metabolomics: a guide for annotation, quantification and best reporting practices. Nature Methods, 18(7), 747–756. https://doi.org/10.1038/s41592-021-01197-1

Andriantsitohaina, R., Auger, C., Chataigneau, T., Étienne-Selloum, N., Li, H., Martínez, M. C., Schini-Kerth, V. B., & Laher, I. (2012). Molecular mechanisms of the cardiovascular protective effects of polyphenols. British Journal of Nutrition, 108(9), 1532–1549. https://doi.org/10.1017/S0007114512003406

Apak, R., Güçlü, K., Demirata, B., Özyürek, M., Çelik, S. E., Bektaşoğlu, B., Berker, K. I., & Özyurt, D. (2007). Comparative evaluation of various total antioxidant capacity assays applied to phenolic compounds with the CUPRAC assay. Molecules, 12(7), 1496–1547. https://doi.org/10.3390/12071496

Biobaku, F., Ghanim, H., Batra, M., & Dandona, P. (2019). Macronutrient-Mediated Inflammation and Oxidative Stress: Relevance to Insulin Resistance, Obesity, and Atherogenesis. Journal of Clinical Endocrinology

and Metabolism, 104(12), 6118–6128. https://doi.org/10.1210/jc.2018-01833

Bujak, R., García-Álvarez, A., Rupérez, F. J., Nuño-Ayala, M., García, A., Ruiz-Cabello, J., Fuster, V., Ibáñez, B., & Barbas, C. (2014). Metabolomics reveals metabolite changes in acute pulmonary embolism. Journal of Proteome Research, 13(2), 805–816. https://doi.org/10.1021/pr400872j

Bustamante, L., Pastene, E., Duran-Sandoval, D., Vergara, C., Von Baer, D., & Mardones, C. (2018). Pharmacokinetics of low molecular weight phenolic compounds in gerbil plasma after the consumption of calafate berry (Berberis microphylla) extract. Food Chemistry, 268(February), 347–354. https://doi.org/10.1016/j.foodchem.2018.06.048

Cai, H., & Harrison, D. G. (2000). Endothelial Dysfunction in Cardiovascular Diseases The Role of Oxidant Stress. Circulation Reasearch, 87(10), 840–844. https://doi.org/10.1161/01.res.87.10.840

Calfío, C., & Huidobro-Toro, J. P. (2019). Potent vasodilator and cellular antioxidant activity of endemic patagonian calafate berries (berberis microphylla) with nutraceutical potential. Molecules, 24(15). https://doi.org/10.3390/molecules24152700

Campos, J., Schmeda-Hirschmann, G., Leiva, E., Guzmán, L., Orrego, R., Fernández, P., González, M., Radojkovic, C., Zuñiga, F. A., Lamperti, L., Pastene, E., & Aguayo, C. (2014). Lemon grass (Cymbopogon citratus (D.C) Stapf) polyphenols protect human umbilical vein endothelial cell (HUVECs) from oxidative damage induced by high glucose, hydrogen peroxide and oxidised low-density lipoprotein. Food Chemistry, 151, 175–181. https://doi.org/10.1016/j.foodchem.2013.11.018

Carnauba, R. A., Hassimotto, N. M. A., & Lajolo, F. M. (2021). Estimated dietary polyphenol intake and major food sources of the Brazilian population. British Journal of Nutrition, 126(3), 441–448. https://doi.org/10.1017/S0007114520004237

Céspedes, C. L., El-Hafidi, M., Pavon, N., & Alarcon, J. (2008). Antioxidant and cardioprotective activities of phenolic extracts from fruits of Chilean blackberry Aristotelia chilensis (Elaeocarpaceae), Maqui. Food Chemistry, 107(2), 820–829. https://doi.org/10.1016/j.foodchem.2007.08.092

Chen, C. ye, Yi, L., Jin, X., Mi, M. tian, Zhang, T., Ling, W. hua, & Yu, B. (2010). Delphinidin attenuates stress injury induced by oxidized low-density lipoprotein in human umbilical vein endothelial cells. Chemico-Biological Interactions, 183(1), 105–112. https://doi.org/10.1016/j.cbi.2009.09.024

Crozier, A., Jaganath, I. B., & Clifford, M. N. (2009). Dietary phenolics: Chemistry, bioavailability and effects on health. Natural Product Reports, 26(8), 1001–1043. https://doi.org/10.1039/b802662a

Curtasu, M. V., Knudsen, K. E. B., Callesen, H., Purup, S., Stagsted, J., & Hedemann, M. S. (2019). Obesity Development in a Miniature Yucatan Pig Model: A Multi-compartmental Metabolomics Study on Cloned and Normal Pigs Fed Restricted or Ad Libitum High-Energy Diets. Journal of Proteome Research, 18(1), 30–47. https://doi.org/10.1021/acs.jproteome.8b00264

de Pascual-Teresa, S., Moreno, D. A., & García-Viguera, C. (2010). Flavanols and anthocyanins in cardiovascular health: A review of current evidence. International Journal of Molecular Sciences, 11(4), 1679–1703. https://doi.org/10.3390/ijms11041679

Duarte, J., & Pérez-Vizcaíno, F. (2015). Cardiovascular protection by flavonoids. Pharmacokinetic mystery. Ars Pharmaceutica, 56(4), 193–200.

Evans, A. M., O'Donovan, C., Playdon, M., Beecher, C., Beger, R. D., Bowden, J. A., Broadhurst, D., Clish, C. B., Dasari, S., Dunn, W. B., Griffin, J. L., Hartung, T., Hsu, P. C., Huan, T., Jans, J., Jones, C. M., Kachman, M., Kleensang, A., Lewis, M. R., Monge, M. E., Mosley, J. D., Taylor, E., Tayyari, F., Theodoridis, G., Torta, F., Ubhi, B.K., & Vuckovic, D. (2020). Dissemination and analysis of the quality assurance (QA) and quality control (QC) practices of LC–MS based untargeted metabolomics practitioners. Metabolomics, 16(10), 1–16. https://doi.org/10.1007/s11306-020-01728-5

Fang, J. (2014). Bioavailability of anthocyanins. Drug Metabolism Reviews, 46(4), 508–520. https://doi.org/10.3109/03602532.2014.978080

Fuentes, J., Atala, E., Pastene, E., Carrasco-Pozo, C., & Speisky, H. (2017). Quercetin Oxidation Paradoxically Enhances its Antioxidant and Cytoprotective Properties. Journal of Agricultural and Food Chemistry, 65(50), 11002–11010. https://doi.org/10.1021/acs.jafc.7b05214

Hanasaki, Y., Ogawa, S., & Fukui, S. (1994). The Correlation Between Active Oxygens Scavenging and Antioxidative Effects of Flavonoids. Free Radical Biology & Medicine, 16(6), 845–850.

Haskó, G., & Pacher, P. (2010). Endothelial Nrf2 activation: A new target for resveratrol? American Journal of Physiology - Heart and Circulatory Physiology, 299(1), 10–12. https://doi.org/10.1152/ajpheart.00436.2010

Havel, R. J., Eder, H. A., & Bragdon, J. H. (1955). The distribution and chemical composition of ultracentrifugally separated lipoproteins in human serum. The Journal of Clinical Investigation, 34(9), 1345–1353. https://doi.org/10.1172/JCI103182

He, X., Zheng, S., Sheng, Y., Miao, T., Xu, J., Xu, W., Huang, K., & Zhao, C. (2021). Chlorogenic acid ameliorates obesity by preventing energy balance shift in high-fat diet induced obese mice. Journal of the Science of Food and Agriculture, 101(2), 631–637. https://doi.org/10.1002/jsfa.10675

Hollman, P. C. H., & Arts, I. C. W. (2000). Flavonols, flavones and flavanols - Nature, occurrence and dietary burden. Journal of the Science of Food and Agriculture, 80(7), 1081–1093. https://doi.org/10.1002/(SICI)1097-0010(20000515)80:7<1081::AID-JSFA566>3.0.CO;2-G

Incalza, M. A., D'Oria, R., Natalicchio, A., Perrini, S., Laviola, L., & Giorgino, F. (2018). Oxidative stress and reactive oxygen species in endothelial dysfunction associated with cardiovascular and metabolic diseases. Vascular Pharmacology, 100(April 2017), 1–19. https://doi.org/10.1016/j.vph.2017.05.005

JAFFE, E. A., NACHMAN, R. L., BECKER, C. G., & MIINICK, C. R. (1973). Culture of human endothelial cells from umbilical veins. The Journal of Clinical Investigation, 52, 2745–2756. https://doi.org/10.1172/JCI107470%0ACulture

Karbach, S., Jansen, T., Horke, S., Heeren, T., Scholz, A., Coldewey, M., Karpi, A., Hausding, M., Kröller-Schön, S., Oelze, M., Münzel, T., & Daiber, A. (2012). Hyperglycemia and oxidative stress in cultured endothelial cells - A comparison of primary endothelial cells with an immortalized endothelial cell line. Journal of Diabetes and Its Complications, 26(3), 155–162. https://doi.org/10.1016/j.jdiacomp.2012.03.011

Katja Dettmer, Aronov, P. A., & Hammock, B. D. (2007). MASS SPECTROMETRY-BASED METABOLOMICS Katja. Mass Spectrometry Reviews, 26(1), 51–78.

Kesherwani, V., Chavali, V., Hackfort, B. T., Tyagi, S. C., & Mishra, P. K. (2015). Exercise ameliorates high fat diet induced cardiac dysfunction by increasing interleukin 10. Frontiers in Physiology, 6(APR), 1–7. https://doi.org/10.3389/fphys.2015.00124

Keyse, S. M. (2000). Stress Response: Methods ans Protocols. In Journal of Chemical Information and Modeling (Vol. 99). https://doi.org/10.1017/CBO9781107415324.004

Kumar, M., Barbhai, M. D., Hasan, M., Punia, S., Dhumal, S., Radha, Rais, N., Chandran, D., Pandiselvam, R., Kothakota, A., Tomar, M., Satankar, V., Senapathy, M., Anitha, T., Dey, A., Sayed, A. A. S., Gadallah, F. M., Amarowicz, R., & Mekhemar, M. (2022). Onion (Allium cepa L.) peels: A review on bioactive compounds and biomedical activities. Biomedicine & Pharmacotherapy, 146, 112498. https://doi.org/10.1016/j.biopha.2021.112498

Kuskoski, E. M., Asuero, A. G., García-Parilla, M. C., Troncoso, A. M., & Fett, R. (2004). Actividad antioxidante de pigmentos antociánicos. Ciência e Tecnologia de Alimentos, 24(4), 691–693. https://doi.org/10.1590/s0101-20612004000400036

Lafay, S., & Gil-Izquierdo, A. (2008). Bioavailability of phenolic acids. Phytochemistry Reviews, 7, 301–311. https://doi.org/10.1007/s11101-007-9077-x

Libby, P. (2000). Coronary artery injury and the biology of atherosclerosis: Inflammation, thrombosis, and stabilization. American Journal of Cardiology, 86(8 SUPPL. 2), 3–8. https://doi.org/10.1016/S0002-9149(00)01339-4

Lin, Q., Yu, H., Das, U. N., & Shen, S. (2012). Water caltrop pericarps extracts attenuate H 2O 2-induced human umbilical vein endothelial cell injury. Advanced Materials Research, 554–556, 1757–1761. https://doi.org/10.4028/www.scientific.net/AMR.554-556.1757

Loke, W. M., Jenner, A. M., Proudfoot, J. M., McKinley, A. J., Hodgson, J. M., Halliwell, B., & Croft, K. D. (2009). A metabolite profiling approach to identify biomarkers of flavonoid intake in humans. Journal of Nutrition, 139(12), 2309–2314. https://doi.org/10.3945/jn.109.113613

Macias-Barragan, J., Caligiuri, A., García-Banuelos, J., Parola, M., Massimo Pinzani, M. D., & Armendariz-Borunda, J. (2014). Effects of alpha lipoic acid and pirfenidone on liver cells antioxidant modulation against oxidative damage. Revista Medica de Chile, 142(12), 1553–1564. https://doi.org/10.4067/S0034-98872014001200009

Manach, C., Williamson, G., Morand, C., Scalbert, A., & Rémésy, C. (2005). Bioavailability and bioefficacy of polyphenols in humans. I. Review of 97 bioavailability studies. The American Journal of Clinical Nutrition, 81(1 Suppl), 230S-242S. https://doi.org/10.1093/ajcn/81.1.230s

Mariangel, E., Reyes-Diaz, M., Lobos, W., Bensch, E., Schalchli, H., & Ibarra, P. (2013). The antioxidant properties of calafate (Berberis microphylla) fruits from four different locations in southern Chile. Ciencia e Investigacion Agraria, 40(1), 161–170. https://doi.org/10.4067/S0718-16202013000100014

Marshall, D. D., & Powers, R. (2017). Beyond the Paradigm: Combining Mass Spectrometry and Nuclear Magnetic Resonance for Metabolomics. Progress in Nuclear Magnetic Resonance Spectroscopy, 100, 1–16. https://doi.org/10.1016/j.pnmrs.2017.01.001

Martínez S., A., Pérez C., P., Ossa A., C., Corbalán H., R., Jalil M., J., Castro G., P., & Acevedo B., M. (2001). Hyperuricemia as a marker for anaerobic threshold in chronic cardiac failure. Revista Medica de Chile, 129(5), 503–508. https://doi.org/10.4067/S0034-98872001000500005

Matsumoto, H., Nakamura, Y., Iida, H., Ito, K., & Ohguro, H. (2006). Comparative assessment of distribution of blackcurrant anthocyanins in rabbit and rat ocular tissues. Experimental Eye Research, 83(2), 348–356. https://doi.org/10.1016/j.exer.2005.12.019

McGarrah, R. W., Crown, S. B., Zhang, G., Shah, S. H., & Newgard, C. B. (2018). Cardiovascular Metabolomics. Circulation Reasearch, 122(9), 1238–1258. https://doi.org/10.1161/CIRCRESAHA.117.311002.Cardiovascular

Medina, G., Castillo, R. del P., & Neira, J. Y. (2019). Multivariate calibration for the improvement of the quantification of cadmium in the presence of potassium as interferent by total reflection X - ray fluorescence. X-Ray Spectrometry, 48(6), 700–707. https://doi.org/10.1002/xrs.3113

MINSAL, 2021. INFORME SEMANAL DE DEFUNCIONES POR COVID19 N°30. Departamento de Estadísticas e Información de Salud, DEIS Ministerio de Salud. https://www.minsal.cl/wp-content/uploads/2021/01/Informe-Semanal-del-ene-7-2021.pdf.

MINSAL, 2014. ENFOQUE DE RIESGO PARA LA PREVENCIÓN DE ENFERMEDADES CARDIOVASCULARES. http://www.repositoriodigital.minsal.cl/bitstream/handle/2015/907/Enfoque-de-riesgo-para-la-prevencion-de-enfermedades-cardiovasculares.-MINSAL-Chile-2014-1%20%281%29.pdf?sequence=1&isAllowed=y

Mosmann, T. (1983). Rapid colorimetric assay for cellular growth and survival: Application to proliferation and cytotoxicity assays. Journal of Immunological Methods, 65, 55–63. https://doi.org/10.1016/0022-1759(83)90303-4

Nardini, M., Cirillo, E., Natella, F., & Scaccini, C. (2002). Absorption of phenolic acids in humans after coffee consumption. Journal of Agricultural and Food Chemistry, 50(20), 5735–5741. https://doi.org/10.1021/jf0257547

Nicholson, S. K., Tucker, G. A., & Brameld, J. M. (2010). Physiological concentrations of dietary polyphenols regulate vascular endothelial cell expression of genes important in cardiovascular health. British Journal of Nutrition, 103, 1398–1403. https://doi.org/10.1017/S0007114509993485

Nile, A., Nile, S. H., Shin, J., Park, G., & Oh, J. W. (2021). Quercetin-3-glucoside extracted from apple pomace induces cell cycle arrest and apoptosis by increasing intracellular ROS levels. International Journal of Molecular Sciences, 22(19). https://doi.org/10.3390/ijms221910749

Olson, M., Melissa Chambers, & Shaibi, G. (2017). Pediatric Markers of Adult Cardiovascular Disease Micah. Current Pediatric Review, 13(4), 255–259. https://doi.org/10.2174/1573396314666180117092010.Pediatric

Ou, B., Chang, T., Huang, D., & Prior, R. (2013). Determination of Total Antioxidant Capacity by Oxygen Radical Absorbance Capacity (ORAC) Using Fluorescein as the Fluorescence Probe: First Action 2012.23. Journal of AOAC International, 96(6), 1372–1376. https://doi.org/10.5740/jaoacint.13-175

Paccot, M. (2014). Enfoque de riesgo para la prevención de enfermedades cardiovasculares. Departamento de Enfermedades No Transmisibles., 1–63.

Passamonti, S., Vrhovsek, U., Vanzo, A., & Mattivi, F. (2003). The stomach as a site for anthocyanins absorption from food. FEBS Letters, 544(1–3), 210–213. https://doi.org/10.1016/S0014-5793(03)00504-0

Pino Ramos, L. L., Jiménez-Aspee, F., Theoduloz, C., Burgos-Edwards, A., Domínguez-Perles, R., Oger, C., Durand, T., Gil-Izquierdo, Á., Bustamante, L., Mardones, C., Márquez, K., Contreras, D., & Schmeda-Hirschmann, G. (2019). Phenolic, oxylipin and fatty acid profiles of the Chilean hazelnut (Gevuina avellana): Antioxidant activity and inhibition of pro-inflammatory and metabolic syndrome-associated enzymes. Food Chemistry, 298. https://doi.org/10.1016/j.foodchem.2019.125026

Prior, R. L., & Wu, X. (2006). Anthocyanins: Structural characteristics that result in unique metabolic patterns and biological activities. Free Radical Research, 40(10), 1014–1028. https://doi.org/10.1080/10715760600758522

Profumo, E., Buttari, B., D'Arcangelo, D., Tinaburri, L., Dettori, M. A., Fabbri, D., Delogu, G., & Riganò, R. (2016). The nutraceutical dehydrozingerone and its dimer counteract inflammation- and oxidative stress-induced dysfunction of in vitro cultured human endothelial cells: A novel perspective for the prevention and therapy of atherosclerosis. Oxidative Medicine and Cellular Longevity. https://doi.org/10.1155/2016/1246485

Ramirez, J. E., Zambrano, R., Sepúlveda, B., Kennelly, E. J., & Simirgiotis, M. J. (2015). Anthocyanins and antioxidant capacities of six Chilean berries by HPLC-HR-ESI-ToF-MS. Food Chemistry, 176, 106–114. https://doi.org/10.1016/j.foodchem.2014.12.039

Reyes-Farias, M., Vasquez, K., Fuentes, F., Ovalle-Marin, A., Parra-Ruiz, C., Zamora, O., Pino, M. T., Quitral, V., Jimenez, P., Garcia, L., & Garcia-Diaz, D. F. (2016). Extracts of Chilean native fruits inhibit oxidative stress, inflammation and insulin-resistance linked to the pathogenic interaction between adipocytes and macrophages. Journal of Functional Foods, 27, 69–83. https://doi.org/10.1016/j.jff.2016.08.052

Reyes-farias, M., Vasquez, K., Ovalle-marin, A., Fuentes, F., Parra, C., Quitral, V., Jimenez, P., & Garcia-diaz, D. F. (2015). Chilean Native Fruit Extracts Inhibit Inflammation Linked to the Pathogenic Interaction Between Adipocytes and Macrophages. JOURNAL OF MEDICINAL FOOD, 18(5), 601–608. https://doi.org/10.1089/jmf.2014.0031

Richard, M. J., Portal, B., Meo, J., Coudray, C., Hadjian, A., & Favier, A. (1992). Malondialdehyde kit evaluated for determining plasma and lipoprotein fractions that react with thiobarbituric acid. Clinical Chemistry, 38(5), 704–709.

Rojo, L. E., Ribnicky, D., Logendra, S., Poulev, A., Rojas-Silva, P., Kuhn, P., Dorn, R., Grace, M. H., Lila, M. A., & Raskin, I. (2012). In Vitro and in Vivo Anti-Diabetic Effects of Anthocyanins from Maqui Berry (Aristotelia chilensis). Physiology & Behavior, 131(2), 387–396. https://doi.org/10.1016/j.foodchem.2011.08.066

Rossi, W. M., Garrido, G., & Sellés, A. J. N. (2016). Biomarcadores del estrés oxidativo en la terapia antioxidante. Journal of Pharmacy and Pharmacognosy Research, 4(2), 62–83.

Ruiz, A., Hermosín-Gutiérrez, I., Mardones, C., Vergara, C., Herlitz, E., Vega, M., Dorau, C., Winterhalter, P., & Von Baer, D. (2010). Polyphenols and antioxidant activity of calafate (berberis microphylla) fruits and other native berries from Southern Chile. Journal of Agricultural and Food Chemistry, 58(10), 6081–6089. https://doi.org/10.1021/jf100173x

Ruiz, A., Hermosín-Gutiérrez, I., Vergara, C., von Baer, D., Zapata, M., Hitschfeld, A., Obando, L., & Mardones, C. (2013). Anthocyanin profiles in south Patagonian wild berries by HPLC-DAD-ESI-MS/MS. Food Research International, 51(2), 706–713. https://doi.org/10.1016/j.foodres.2013.01.043

Ruiz, A., Mardones, C., Vergara, C., Hermosín-Gutiérrez, I., von Baer, D., Hinrichsen, P., Rodriguez, R., Arribillaga, D., & Dominguez, E. (2013). Analysis of hydroxycinnamic acids derivatives in calafate (Berberis microphylla G. Forst) berries by liquid chromatography with photodiode array and mass spectrometry detection. Journal of Chromatography A, 1281, 38–45. https://doi.org/10.1016/j.chroma.2013.01.059

Ruiz, A., Zapata, M., Sabando, C., Bustamante, L., Baer, D. Von, Vergara, C., & Mardones, C. (2014). Flavonols, Alkaloids, and Antioxidant Capacity of Edible Wild Berberis Species from Patagonia. Journal of Agricultural and Food Chemistry, 62, 12407–12417.

Sandoval-Acuña, C., Ferreira, J., & Speisky, H. (2014). Polyphenols and mitochondria: An update on their increasingly emerging ROS-scavenging independent actions. Archives of Biochemistry and Biophysics, 559, 75–90. https://doi.org/10.1016/j.abb.2014.05.017

Sarr, M., Chataigneau, M., Martins, S., Schott, C., El Bedoui, J., Oak, M. H., Muller, B., Chataigneau, T., & Schini-Kerth, V. B. (2006). Red wine polyphenols prevent angiotensin II-induced hypertension and endothelial dysfunction in rats: Role of NADPH oxidase. Cardiovascular Research, 71, 794–802. https://doi.org/10.1016/j.cardiores.2006.05.022

Shabalala, S. C., Dludla, P. V., Mabasa, L., Kappo, A. P., Basson, A. K., Pheiffer, C., & Johnson, R. (2020). The effect of adiponectin in the pathogenesis of non-alcoholic fatty liver disease (NAFLD) and the potential role of polyphenols in the modulation of adiponectin signaling. Biomedicine and Pharmacotherapy, 131(May), 110785. https://doi.org/10.1016/j.biopha.2020.110785

Shao, D., Lian, Z., Di, Y., Zhang, L., Rajoka, M. shahid riaz, Zhang, Y., Kong, J., Jiang, C., & Shi, J. (2018). Dietary compounds have potential in controlling atherosclerosis by modulating macrophage cholesterol metabolism and inflammation via miRNA. Npj Science of Food, 2, 13. https://doi.org/10.1038/s41538-018-0022-8

Soares, S., Silva, M. S., García-Estevez, I., Groβmann, P., Brás, N., Brandão, E., Mateus, N., Freitas, V. de, Behrens, M., & Meyerhof, W. (2018). Human Bitter Taste Receptors Are Activated by Di ff erent Classes of Polyphenols. Journal of Agricultural and Food Chemistry, 66, 8814–8823. https://doi.org/10.1021/acs.jafc.8b03569

Speisky, H., López-Alarcón, C., Gómez, M., Fuentes, J., & Sandoval-Acuña, C. (2012). First web-based database on total phenolics and oxygen radical absorbance capacity (ORAC) of fruits produced and consumed within the south andes region of South America. Journal of Agricultural and Food Chemistry, 60(36), 8851–8859. https://doi.org/10.1021/jf205167k

Teixeira, L. D. L., Pilon, G., Coutinho, C. P., Dudonné, S., Dube, P., Houde, V., Desjardins, Y., Lajolo, F. M., Marette, A., & Hassimotto, N. M. A. (2021). Purple grumixama anthocyanins (: Eugenia brasiliensis Lam.) attenuate obesity and insulin resistance in high-fat diet mice. Food and Function, 12(8), 3680–3691. https://doi.org/10.1039/d0fo03245j

Tresserra-Rimbau, A., Rimm, E. B., Medina-Remón, A., Martínez-González, M. A., de la Torre, R., Corella, D., Salas-Salvadó, J., Gómez-Gracia, E., Lapetra, J., Arós, F., Fiol, M., Ros, E., Serra-Majem, L., Pintó, X., Saez, G. T., Basora, J., Sorlí, J. V., Martínez, J. A., Vinyoles, E., … Lamuela-Raventós, R. M. (2014). Inverse association between habitual polyphenol intake and incidence of cardiovascular events in the PREDIMED study. Nutrition, Metabolism and Cardiovascular Diseases, 24(6), 639–647. https://doi.org/10.1016/j.numecd.2013.12.014

Worley, B., & Powers, R. (2016). PCA as a predictor of OPLS-DA model reliability. Current Metabolomics, 4(2), 97–103. https://doi.org/10.2174/2213235X04666160613122429.PCA

Zhang, H., Chen, X., Zong, B., Yuan, H., Wang, Z., Wei, Y., Wang, X., Liu, G., Zhang, J., Li, S., Cheng, G., Wang, Y., & Ma, Y. (2018). Gypenosides improve diabetic cardiomyopathy by inhibiting ROS-mediated NLRP3 inflammasome activation. Journal of Cellular and Molecular Medicine, 22(9), 4437–4448. https://doi.org/10.1111/jcmm.13743

CAPITULO 4: RESULTADOS

4.1 El extracto del fruto de *Berberis microphylla* G. Forst (calafate) reduce el estrés oxidativo y la peroxidación lipídica de LDL humana.

En esta sección se presentan los resultados que dieron origen al primer paper de esta tesis doctoral. Antioxidants 2020, 9(12), 1171; https://doi.org/10.3390/antiox9121171 .

Article

Berberis microphylla G. Forst (calafate) berry extract reduces oxidative stress and lipid peroxidation of human LDL

Lia Olivares [1,2], Claudia Radojkovic [2], Si Yen Chau [2], Daniela Nova [1], Luis Bustamante [1], Yamil Neira [1], Andy Perez [1] and Claudia Mardones [1*]

1 Departamento de Análisis Instrumental, Facultad de Farmacia, Universidad de Concepción, Concepción, Chile; liaolivares@udec.cl, daninovabaza@gmail.com, lbust85@gmail.com, yneira@udec.cl, aperezd@udec.cl, cmardone@udec.cl

2 Departamento de Bioquímica Clínica e Inmunología, Facultad de Farmacia, Universidad de Concepción, Concepción, Chile; cradojkovic@udec.cl, schau@udec.cl

* Correspondence: cmardone@udec.cl; Tel.: +56 983616340 (F.L.), C. M.

Abstract

Calafate (*Berberis microphylla* G. Forst) is a Patagonian barberry very rich in phenolic compounds. Our aim was to demonstrate, through *in vitro* models, that a comprehensive characterized calafate extract has a protective role against oxidative processes associated to cardiovascular disease development. Fifty-three phenolic compounds (19 of them not previously reported in calafate), were identified by HPLC-DAD-ESI-QTOF. Fatty acids profile and metals content were for first time studied, by GC-MS and Total-X-ray-Fluorescence respectively. Linolenic and linoleic acid, and Cu, Zn, and Mn were the main relevant compounds from these groups. The bioactivity of calafate extract associated to the cardiovascular protection was evaluated using human umbilical vein endothelial cells and human low density lipoprotein (LDL) to measure oxidative stress and lipid peroxidation. The results showed that calafate extract reduced intracellular ROS production (51%) and completely inhibited LDL oxidation and malondialdehyde (MDA) formation. These findings demonstrated the potential of the relevant mix of compounds found in calafate extract on lipoperoxidation and suggest a potential protective effect for reducing the incidence of cardiovascular disease.

Keywords: *Berberis microphylla* G. Forst, UHPLC-QTOF, Phenolic compounds, HUVEC, cardiovascular disease, antioxidant capacity

4.1.1. Introduction

Polyphenols are natural antioxidants that reduce oxidation processes and inhibit the production of free radicals [1]. They are commonly found in vegetables, fruits, and many other foods; moreover, they are responsible for the color and flavor of these foods [2]. Phenolic compounds have been described as molecules with antibiotic, antitumoral, antioxidant and antiviral properties, among other bioactivities [3]. Many studies have demonstrated that certain polyphenols (delphinidin, resveratrol, quercetin, etc.) can contribute to the prevention of chronic non-communicable diseases, such as obesity, Alzheimer's disease, cancer and cardiovascular disease (CVD) [4].

CVD is the main cause of death both in Chile and around the world [4]: 27% of total deaths in Chile (MINSAL) and 31% worldwide (WHO) are caused by stroke or acute myocardial infarction. Hypertension, dyslipidemias, obesity, and metabolic syndrome, among others, have been described as risk factors of CVD; their common denominator is endothelial dysfunction [1].

This condition is produced by an imbalance in the normal function of endothelial cells, which leads to the hallmark of CVD, a vasoconstricted, inflammatory and pro-coagulative state [5]. The chronic exposure to harmful physical and chemical stimuli, such as oxidized low density lipoprotein (LDL), can result in endothelial dysfunction by increasing levels of reactive oxygen species (ROS) and oxidative stress in endothelial cells [5].

According to several studies, the consumption of polyphenolic compounds can reduce CVD risk [6]. The PREDIMED (Prevención con Dieta Mediterránea) study demonstrated an inverse relationship between anthocyanin consumption and CVD risk [6]. Notably, decreased ROS production, lower expression of inflammatory markers, and decreased blood pressure have been described as important effects of certain polyphenols [4,7].

Calafate is an endemic evergreen shrub of the Berberidaceae family from Chilean-Argentine Patagonia. The shrub has 1 to 2 meters high, with leaves grouped in rosettes and yellowish spines. Its flowers are solitary, with a long peduncle that is born from each rosette of leaves. Its bloom is in September and the fruit is edible. The shrub produces a dark skinned barberry with a

high polyphenol content and antioxidant capacity [8-10], which are normally consumed fresh or as juices, marmalade and infusions. Anthocyanins, hydroxycinnamic acids and flavonols are the main phenolic compounds described in the fruit [11-13]. Anthocyanins can trap free radicals, reducing oxidative stress, a common factor in the development of chronic non-communicable diseases [14]. In a study carried out by Ramirez et al. [14], using erythrocytes obtained from healthy humans, researchers demonstrated that a methanolic calafate extract inhibited 90% of the lipidic peroxidation caused by tert-butylhydroperoxide. Lipidic peroxidation is crucial in the induction and/or propagation of oxidative stress related diseases [15]. Additionally, calafate berry extract increased the ratio of reduced/oxidized glutathione (GSH/GSSG), which led to decreased oxidative stress in murine adipocytes treated with macrophage conditioned medium [16]. Another study reported inhibition of TNF-α gene expression (a cytokine related to proinflammatory state) in murine macrophages stimulated with lipopolysaccharides in the presence of calafate extract [17]. Finally, in a recent study, Calfío & Huidobro-Toro described a vasodilatory effect of an hydroalcoholic calafate berry extract, which was 89.6% ($p<0.01$) inhibited by L-NNA (150 μM), an inhibitor of endothelial nitric oxide synthase

(eNOS) [18]. These findings suggest that nitric oxide, one of the most important endothelium-derived vasodilatory molecule, participates in the vascular response induced by calafate. Altogether, these studies suggest that calafate can contribute to reduce endothelial dysfunction, which is the basis of cardiovascular disease. However, none of them included the study of lipid peroxidation based on a LDL model, which is directly associated with the atheroma formation [1].

Some fatty acids, mainly poliinsaturated are other compounds associated with the prevention of CVD through inhibitory effects on inflammation, oxidation and thrombosis [19]. On the other hand, certain metals (Mn, Cu and Zn) have shown an activating effect on enzymes involved in antioxidant protection in humans [20]. To our knowledge, neither fatty acids nor metals have been studied in calafate.

To fill this gap, we studied the effect of a comprehensive characterized calafate extract against oxidative stress using human umbilical vein endothelial cells (HUVEC) and lipoperoxidation on human LDL, as biological models directly related with CVD. The main objective was to demonstrate that the relevant mix of compounds found in calafate extract,

determined by LC-MS, GC-MS and Total Reflection X-ray Fluorescence (TXRF), reduces ROS production and lipoperoxidation, both processes related with the prevention of cardiovascular disease incidence.

4.1.2. Materials and Methods

4.1.2.1. Reagents and vegetable material

Reagents: Commercially available delphinidin 3-glucoside, 3-cafeoylquinic acid, BF3-methanol 10% LiChropure for fatty acid derivatization, Miristic acid d27 and Supelco 37 Component FAME Mix were obtained from Sigma-Aldrich (Steinheim, Germany). Formic acid, ammonia (25%), sodium hydroxide, sodium chloride, hydrochloric acid, acetonitrile, methanol, ethanol, water (HPLC-MS grade or hypergrade), and Hexane (SupraSolv®) for gas chromatography, Dimethyl sulfoxide (DMSO) and Vitamin C were provided by Merck (Darmstadt, Germany). Chloroform (Optima® GC/MS) and BCA (bicinchoninic acid) Protein Assay Kit were provided by Fisher Scientific (Waltham, MA, USA). SPE 150 mg Oasis MCX 6 cm3 mixed phase cartridges from Waters (Milford, MA, USA). 2',7'-Dichlorodihydrofluorescein diacetate (H2DCF-DA) was obtained from Invitrogen (Waltham,MA,USA) and malondialdehyde (MDA) was

purchased from Sigma-Aldrich (St. Louis,MO,USA). M199 medium, fetal bovine serum (FBS), and other cell culture reagents were obtained from Gibco Life Technologies (Grand Island, NY, USA). Penicillin-streptomycin solution and Trypsin 0.25% were purchased from HyClone Co. (Logan, UT, USA). 3-(4,5 Dimethylthiazol 2)-2,5-diphenylterazolium bromide (MTT) was purchased from Cayman Chemical Company (Ann Arbor,MI,USA).

Vegetable material: Calafate berries (Berberys microphylla G. Forst) were collected near Punta Arenas, Chile (53.1548309,-70.911293). Berries were collected between February and May 2019 at maturity stage, and were frozen at -80°C until their analyses. Approximately 1 Kg of fruit was collected, which was homogenized before analysis. A taxonomical identification, by comparison of the species with those from the University of Concepcion Herbarium, was carried out in order to assure the identity of the samples. The moisture (%) of the fruits was 69,4 ± 2,7%.

4.1.2.2. Instrumentation

An ultrasonic bar homogenizer Cole Palmer series 4710 (Chicago,IL,USA), a mechanical shaker (Edyman KL2), a desktop centrifuge Heraeus-Christ GmbH (Osterode,Germany), an Alpha 2–4 LD plus lyophilizing system from

Martin Christ (Osterode,Germany), a centrifuge Heraeus-Fresco17 from Thermo Fisher (Waltham,MA,USA), a laboratory stirrer/hotplate CORNING model PC420 (Durham,NC,USA), an analytical balance from Denver Instrument Company (NY,USA), a rotavapor with a V-700 vacuum pump and V-850 controller system from Büchi (Flawil,Switzerland), and a MM 400 mixer mill from Retsch GmbH (Haan, Germany) were used for sample preparation. An Epoch™ microplate reader from Biotek Instruments (Winooski,VT,USA) was used for antioxidant and cellular assays. A Beckman Optima TM LE 80 K (Palo Alto,CA,USA) was used for ultracentrifugation.

The identity assignment of phenolic compounds was carried out with a UHPLC-DAD Bruker Elute LC system, coupled in tandem with a Q-TOF spectrometer Compact, Bruker (Bremen,Germany). The control system used was Compass HyStar (Bruker), the acquisition software was Bruker otofControl 4.1.402.322-7977-vc110 6.3.3.11, and data analysis was performed with Compass DataAnalysis 4.4.200 (Bruker) software.

The quantitative analysis of phenolic compounds was carried out with a Shimadzu HPLC system equipped with a quaternary LC-10ADVP pump, an

FCV-10ALVP elution unit, a DGU-14A degasser unit, a CTO-10AVP oven, and a UV-vis diode array spectrophotometer model SPD-M10AVP. The control system and data collection were performed using Shimadzu Chromatography Data System CLASS-VP software (Kyoto,Japan).

The fatty acid profile was determined using an Agilent 7890A GC (Palo Alto,CA,USA) with a multimode injector, interfaced to an Agilent 7000 GC/MS Triple Quad detector, fitted with an Agilent CTC PAL autosampler and controlled by Agilent MassHunter GC/MS acquisition software (Version B.05.00/Build 5.0.291.0).

Metal profile analysis was performed using a bench top TXRF system (S4 TStar, Bruker® AXS Microanalysis GmbH, Berlin, Germany) equipped with a 50 W X-ray tube with a molybdenum (Mo) anode and a multilayer monochromator (17.5 keV).

4.1.2.3 Full chemical characterization of calafate

4.1.2.3.1 Extraction protocols

The extraction was carried out according to a protocol previously described by Ruiz et al., 2013 [11]. Briefly, 5 g of calafate berries were triturated, mixed with 10 mL of methanol/formic acid (97:3 ratio) and sonicated (60 s,

40% A). The sample was then stirred for 16 h and centrifuged at 1,730 g for 10 min. Subsequently, the supernatant was removed and added to a 25 mL flask. An additional 5 mL of solvent was added to the sample and stirred for 30 min; the sample was then centrifuged, and the supernatant was transferred to a 25 mL flask. This procedure was repeated 3 times. Finally, the flask was filled with the same solvent, obtaining the crude extract. Additionally, the same procedure was developed using ethanol/formic acid (97:3 ratio), in order to compare the effect of the extraction solvents (methanol vs ethanol) on the polyphenolic composition and on the biological assays (Raw extracts).

Hydroxycinnamic acid determination required a purification step using solid phase extraction with cation exchange columns (Oasis MCX Water, USA), as previously described by Ruiz et al., 2013 (Purified extract) [12]. Briefly, 1 mL of crude extract was evaporated and resuspended in 5 mL of 0.1 M HCl. Subsequently, the MCX SPE-column was conditioned with 5 mL of methanol and 5 mL of ultrapure water. The resuspended crude extract was loaded onto the SPE column and subsequently washed with 5 mL of 0.1 M HCl and 5 mL of ultrapure water. The elution of hydroxycinnamic acids was done with 5 mL of solvent and repeated 3 times, obtaining an extract rich in hydroxycinnamic acids (Purified extract).

Raw extracts (methanolic and ethanolic) were used for the analysis of anthocyanins in fruit by LC-MS, metal profiling by TXRF, fatty acids by GC-MS and *in vitro* assays. Purified extract was used for hydroxycinnamic acid identification and quantitation.

4.1.2.3.2 Identification and quantitation of anthocyanins

The identification of anthocyanins by LC-MS was based on the method previously described by Ruiz et al., 2013 [12]. This method uses a mobile phase with lower formic acid concentration than the common method for anthocyanin [8], because the ESI system of the spectrometer does not allow the use of high formic acid concentrations (Compact User Manual, Bruker DaltonikGmbH). Chromatographic separation conditions were as follows: a Kromasil column 100 5 C18 250x4.6 mm with a C-18 precolumn (Nova-Pak Waters, 22×3.9 mm, 4 μm), mobile phase A: formic acid 0.1% in water, and mobile phase B: 0.1% formic acid in acetonitrile. A flow rate of 0.3 mL/min and an injection volume of 10μL were used. The acetonitrile gradient ranged from 15% to 25% for 14 min, from 25% to 35% for 11 min, from 35% to 100% for 1 min, 100% for 9 min and from 100% to 15% for 1 min with a stabilization period of 25 min. The spectrophotometric detection was set at

520 nm, and MS detection was set using the base peak chromatogram (BPC), both obtained in the LC-MS. The MS conditions for anthocyanin identification were as follows: positive ionization ESI +4500 V, dry gas: 9 L/min, nebulizer: 4 Bar, T°: 200°C, end capillary 500V, collision energy at 10-25eV in stepping mode, Auto MS/MS mode (4 precursor/cycle), 50-1500 m/z (scan 0.2s centroid mode) and internal calibration using sodium formate (10% formic acid, 1 M) with a mass accuracy <3 ppm.

Quantitative analysis was carried out using a Shimadzu HPLC system by external calibration curve using a delphinidin 3-glucoside standard at 518 nm as described by Ruiz et al., 2010 [8].

4.1.2.3.3 Hydroxycinnamic acid derivatives (HCAD) analysis by LC-MS

Identification was performed as previously described Ruiz et al., 2013 [12].The same column, precolumn and chromatographic separation used for anthocyanin analysis were used . The spectrophotometric detection was set at 320 nm, and MS detection was set using the BPC, both obtained in the LC-MS. The same spectrometric conditions used in section 2.3.2 were used, with exception negative ionization ESI -3500V. The quantitative analysis was

carried out using a Shimadzu LC-DAD system by an external calibration curve prepared with 3-caffeoylquinic acid standard and measured at 326 nm.

4.1.2.3.4 Metal profile analysis

The identification and quantitation of metals in calafate was carried out by a previous siliconization procedure for TXRF measurement. For this purpose, 10µL of silicone solution in isopropanol was dropped onto the surface of quartz carriers and dried at 110°C on a hot plate. Separately, 10µL of methanolic and ethanolic extracts (dilution 1/100) containing 0.5 mg/L Ga as an internal standard were dropped onto the siliconized carriers. After drying the samples at 80°C, they were placed into the TXRF equipment. The characteristic radiation emitted by each element was detected by a silicon drift detector with an area of 60 mm2 and an energy resolution < 145 eV, working at 50 kV and 750 µA in the air. The measurement live time was 1,200 s. Elements were identified automatically by referring to the software database. The quantitative analysis was carried out by a standard internal method using Ga [21].

4.1.2.3.5 Analysis of fatty acid profile

The fatty acid profile and concentration were carried out on lyophilized calafate fruit and in the methanolic and ethanolic extracts (described in section 2.3.1). The lyophilized fruit was homogenized using a ball mill (30 cycles/s for 1.5 min). Subsequently, 100 mg of homogenized calafate (or 250µL of extracts) mixed with 1 mL of methanol/chloroform 2/1%v/v solution were transferred to a 1.5 mL centrifuge tube and shaken (ball mill 30 cycles/s during 1.5 min), followed by a centrifugation step (9600 g for 2 min at 4°C). A mix of 780µL of the resulting supernatant, 260µL of chloroform, and 468µL of water was transferred to a 4mL vial and vortexed. Finally, 400µL of the organic phase was transferred to a new 4 mL glass vial and evaporated under a nitrogen stream for derivatization.

Fatty acid methyl ester (FAME) derivatization was achieved using the AOAC 969.33 protocol for fatty acids [22] with Myristic-d-27 acid (75 mg/L) as the internal standard. The GC-MS analysis was performed using a 30 m×0.25 mm×0.2 µm ionic liquid SLB-IL-111 column from Supelco. The injection volume was 1µL, the injection temperature was 250°C, the split mode was 10:1, and the gas carrier flow was 1.5 mL/min. The oven temperature program started at 40°C for 4 min, with a 5°C/min ramp up to 260°C for a total analysis time of 48 min. The transference line was set at 275°C, with an

ionization source of 70 eV and 230°C with a Quadrupole temperature of 150°C. Mass spectra acquisition was performed in scan mode from 20 to 450 m/z, with 140 ms scan time. Fatty acids were identified by comparing the retention times (RT) with a FAME mix, the mass spectra and NIST05 library.

Extracted ions at m/z 74 and 87 were used for the saturated and monounsaturated fatty acids. The ions at m/z 79 and 81 were used for the di- and tri-unsaturated fatty acids. The areas corrected by the internal standard of the samples and the standard mix (Supelco pn: CRM47885, XA18647V) were compared by applying a response factor method, according to the AOAC 996.06. The concentration of the different fatty acids was expressed as mg/g FW or mg/mL extract.

4.1.2.4. *In vitro* assays

All *in vitro* assays were carried out using the characterized extracts obtained in 2.3.1. (methanolic and ethanolic extracts).

4.1.2.4.1 Antioxidant capacity and total phenolic compounds

$TEAC_{CUPRAC}$ and $TEAC_{ABTS}$ were determined as previously described by Ruiz et al., 2010 [8] and Ruiz et al., 2013 [11]. $TEAC_{ORAC}$ was carried out according to Ou et al., 2013 [23]. Total phenolic compounds were quantified

using the Folin-Ciocalteu method [8], and all methodologies were carried out in 96-well microplate.

4.1.2.4.2 Cell culture

HUVECs (Lonza Group) were cultured on gelatin-coated plastic dishes with M199 medium supplemented with 20% FBS at 37 ºC in 5% CO2 [24]. For experiments, cells were recovered with Trypsin/EDTA and seeded in 96-well plates. All experiments were performed between passages 3-8 and treatments were added at 90% confluence.

4.1.2.4.2.1 Viability assay

Cell viability was determined by the MTT method [25]. HUVECs were seeded at a density of 30,000 cells/well into 96-well plates (100µL) and were cultured for 1 day in M199 medium supplemented with 20% FBS. Then, cells were pretreated for 48 h with different dilutions of calafate extracts in culture medium supplemented with 2% FBS or with phosphate buffered saline (PBS) 10 mM (145 mM NaCl, 7.5mM Na_2HPO_4, 2.5mM NaH_2PO_4, pH 7.2-7.4), which was used as a positive control to induce cell death by serum deprivation. After the incubation period, cells were incubated with the MTT solution at a final concentration of 0.5 mg/mL for 4 h at 37 °C. Next, 85µL

of medium was removed and DMSO (50µL) was added to each well. Absorbance was measured at 540 nm with a microplate reader. Viability was expressed as a percentage as compared to nontreated cells cultured in M199 medium with 2% FBS (viability control).

4.1.2.4.2.2 ROS measurement

The intracellular ROS measurement was based on ROS-mediated conversion of a nonfluorescent H_2DCFH-DA probe into DCF, whose intensity of fluorescence reflected enhanced oxidative stress. For these experiments, HUVECs were seeded in 96-well plates at a density of 30,000 cells/well, and after 1 day, they were incubated with calafate dilutions for another 24 h. After washes with PBS 10 mM, cells were incubated with H_2DCFH-DA (10µM) in 10 mM PBS at 37°C for 45 min. At the end of the incubation period, cells were washed and stimulated with H_2O_2 (200 µM), and DCF fluorescence was measured at 540 nm (emission) and 485 nm (excitation) over 45 min with a microplate fluorescence reader. Cells exposed to H_2O_2 (200 µM) but not to calafate were used as a positive control of oxidative stress. The results were expressed as fold change of fluorescence intensity compared to nonstimulated HUVECs (negative control: cells not exposed to either

calafate or H_2O_2) [5]. As antioxidant control, vitamin C (250 µg/mL) was added to cell cultures at the same time as H_2O_2.

4.1.2.4.3 LDL isolation

Low density lipoprotein (LDL) extraction was done as described by Havel, Eder, & Bragdon, 1955 [26]. Peripheral blood was obtained from healthy donors (6) after 10 h of starvation. All participants signed a written informed consent form before sample collection. LDL samples were collected, dialyzed in PBS 10 mM pH 7.4, and quantified by BCA assay kit for further studies. This protocol conforms to the Declaration of Helsinki, and it was revised and approved by the University of Concepción Ethics Committee (CEBB-427-2-2019).

4.1.2.4.3.1 LDL oxidation

LDL (500 µg/mL) was incubated at 37ºC in PBS 10 mM with or without CuSO4 (7 µM) (positive and negative controls, respectively), in a final reaction volume of 100µL. For some experiments, different dilutions of calafate extract were incubated together with LDL and $CuSO_4$. Kinetics of oxidation were recorded every minute by absorbance at 232 nm in a microplate reader [5].

4.1.2.4.3.2 MDA assay

To evaluate lipoperoxidation, LDL was incubated at 37°C with $CuSO_4$ (7 µM) (positive control) with or without calafate extract or an antioxidant control (vitamin C 250 µg/mL) for 1 h 20 min. Then reaction was stopped with 1µL of BHT 5% p/v. MDA quantification was carried out by the TBARS method as described by Richard in 1992, with some modifications [27]. Briefly, 100µL of MDA standard or LDL, 100µL trichloroacetic acid 10% w/v and 800µL thiobarbituric acid 0.53% w/v were added in cryotubes and vortexed. The cryotubes were boiled for 60 min at 95°C, and the reaction was stopped in ice for 15 min. Finally, the mix was transferred to a 96-well plate and the absorbance was read at 540 nm. Quantification was carried out by external calibration with MDA standard. Negative control consisted in LDL incubated only with PBS 10mM.

4.1.2.5 Statistical Analysis

All results were expressed as arithmetic means and standard errors. Data were subjected to one-way ANOVA to evaluate the statistical significance of intergroup differences with Bonferroni post hoc tests, considering $\alpha < 0.05$.

Graphics were performed using GraphPad Prism software version 5.0 and statistical analyses were carried out using IBM SPSS software version 20.

4.1.3. Results and discussion

4.1.3.1 Phenolic profile in calafate fruit by UHPLC-DAD-ESI-QTOF-MS/MS

Anthocyanins were analyzed in positive mode (ESI +) by LC-MS and the profiles of HCADs and other phenolic compounds were analyzed in negative mode (ESI -). The assignment of identity was carried out using PUBCHEM (P), METFRAG (M), HMDB (H) and KEEG (K) databases, as well as comparing results with other publications. The level of annotation, in almost all case, was at least level 2, according with the definition of Sumner et al [28]

The anthocyanins identified in calafate are presented in Table 4.1.1. The main anthocyanins detected in this study were the same as those described by Ruiz et al., 2010 [8]; however, minor anthocyanins reported in the cited publication were not detected by us, despite the high sensitivity of the MS system. This could be due to the low concentration of formic acid used in the mobile phase (0.1%), which did not allow the anthocyanin structures to

stabilize (between flavylium cation, quinoidal base, carbinol and chalcone forms) [29]. This nonequilibrium state can also explain the peak widening and the low chromatographic resolution, responsible for a lower sensitivity (chromatogram in supplementary material, Figure S1). Additionally, in the same chromatogram, a mass of [M]+ 336.1213 m/z (Signal 14) was found, which was assigned as berberine, an alkaloid previously described in calafate [10]. The fragments of 321.0996 m/z $[C_{19}H_{15}NO_4]$+ and 306.0761 m/z $[C_{18}H_{12}NO_4]$+ are products of demethylations of the berberine structure. The fragment 292.0968 m/z $[C_{18}H_{12}NO_3$+2H]+ was obtained from a cross fragmentation in the cyclic ether. Signal 13 was tentatively annotated as protoberberine (jatrorrhizine) with [M+] 338.1371 m/z and fragments 294.1099 m/z $[C_{18}H_{16}NO_3]$+ and 323.1121 m/z $[C_{19}H_{17}NO_4]$+.

Table 4.1.1: Metabolic profile of calafate obtained by UHPLC-DAD-ESI-QTOF-MS/MS in positive and negative ionization modes

Nº peak	t_R (min)	λ (nm)	Molecular Formula	$[M]^+$ or $[M-H]^-$	ESI	Fragments[e]	Error (ppm)	m_σ[f]	Annotation	Ref or DB
1[c]	7.6	276; 523	$C_{27}H_{31}O_{17}^+$	627.1527	+	303.0499; 229.0495; 465.1028	4.6	4.2	delphinidin-3,7-*β*-*O*-diglucoside	8, 9, 18, M, K

2[b]	8.1	276; 524	$C_{28}H_{33}O_{17}^+$	641.1678	+	317.0656	5.4	5.5	petunidin-3,7-*β*-*O*-diglu-coside	8, 9, 18
3[b]	8.7	-	$C_{29}H_{35}O_{17}^+$	655.1840	+	331.0812	4.3	18.1	malvidin-3,7-*β*-*O*-diglucoside	8, 9, 18
4[c]	9.8	277; 525	$C_{27}H_{31}O_{16}^+$	611.1582	+	303.0499; 229.0495	4.1	4.3	delphinidin 3-rutinoside	8, 11, M, K
5[c]	9.9	276; 525	$C_{21}H_{21}O_{12}^+$	465.0989	+	303.0499; 229.0495	8.4	5.6	delphinidin 3-glucoside	8, 11, 14, 18 M, K
6[c]	12.0	280; 519	$C_{27}H_{31}O_{15}^+$	595.1646	+	287.0550; 242.0574	1.9	14.0	cyanidin 3-rutinoside	8, 11, 14, M, K
7[c]	12.1	279; 519	$C_{21}H_{21}O_{11}^+$	449.1059	+	287.0550; 115.0542	4.3	0.9	cyanidin 3-glucoside	8, 11, 14, 18, M, K
8[c]	12.1	279; 519	$C_{22}H_{23}O_{12}^+$	479.1170	+	317.0656;217.0495; 302.0421;245.0444; 174.0311;192.0417; 229.0495; 274.0472	3.0	6.0	petunidin 3-glucoside	8, 11, 14, 18, H
9[b]	12.3	281; 524	$C_{28}H_{33}O_{16}^+$	625.1764	+	317.0656	0.1	4.9	petunidin 3-rutinoside	8, 11, 14
10[b]	14.7	277; 529	$C_{29}H_{35}O_{16}^+$	639.1923	+	331.0812	-0.5	3.1	malvinidin 3-rutinoside	8, 11
11[c]	14.7	278; 529	$C_{22}H_{23}O_{11}^+$	463.1228	+	301.0707;286.0472; 229.0495;187.0390; 213.0546; 203.0339	1.5	4.0	peonidin 3-glucoside	8, 11, 14, 18, M, K
12[c]	14.8	277; 529	$C_{23}H_{25}O_{12}^+$	493.1338	+	331.0812;287.0550; 316.0578;242.0574; 245.0444; 217.0495	0.6	5.3	malvidin 3-glucoside	8, 11, 18, M, K
13[b]	28.3	221; 251; 350	$C_{20}H_{20}NO_4^+$	338.1371	+	294.1099;323.1191; 280.0955	5.5		jatrorrhizine	10
14[c]	32.4	221; 251; 350	$C_{20}H_{18}NO_4^+$	336.1213	+	292.0968;306.0761; 321.0996;278.0812;	5.3	16.7	berberine	10, M, K
15[c]	11.3	326	$C_{15}H_{16}O_{11}$	371.0606	-	209.0303; 191.0197; 147.0299	3.8	4.3	3-trans-caffeoyl-glucaric acid or 4-trans-caffeoyl-glucaric acid	9, 12, 30, M, K

16[c]	12.1	326	$C_{15}H_{16}O_{11}$	371.0619	-	209.0303;191.0197; 135.0452;147.0299; 179.0350;129.0193; 193.0506	0.1	9.0	3-trans-caffeoyl-glucaric acid or 4-trans-caffeoyl-glucaric acid	9, 12, 30, M, K
17[c]	12.7	325	$C_{15}H_{16}O_{11}$	371.0619	-	209.0303;163.0401; 191.0197;119.0502; 135.0452;147.0299; 179.0350	0.1	10.8	2- or 5-trans-caffeoyl-glucaric acid	9, 12, 30, M, K
18[c]	13.4	-	$C_{16}H_{18}O_9$	353.0889	-	191.0561;135.0452; 179.0350; 93.0346; 161.0244	-3.0	18.3	caffeoylquinic acid isomer	12, 30, 31, M, K
19[a]	13.7[A]	-	$C_{15}H_{18}O_{11}$	355.0660 $[M\text{-}H_2O\text{-}H]^-$	-	209.0303;147.0299; 239.0561; 119.0502	3.0	16.9	syringic acid glucuronide	H
20[c]	13.8	-	$C_{15}H_{16}O_{11}$	371.0619	-	209.0303;191.0197; 135.0452;147.0299; 115.0037; 173.0092	0.1	9.4	caffeoyl glucaric isomer	12, 30, M, K
21[c]	14.1[B]	-	$C_{15}H_{16}O_{11}$	371.0626	-	209.0303;191.0197; 135.0452; 173.0092	-1.7	2.6	caffeoyl glucaric isomer	12, 30, M, K
22[a]	14.7	-	$C_{15}H_{12}O_9$	335.0409	-	183.0299;177.0193	-0.2	4	3-hidroxy-4-metoxy-5-(3,4,5-trihidroxybenzoyloxy)benzoic acid	H
23[a]	14.9	327	$C_{15}H_{14}O_{10}$	353.0521	-	191.0197;135.0452; 147.0299;179.0350; 161.0244	-2.0	18.4	caffeoyl isocitrate isomer	P, M, K
24	15.6	-	$C_{13}H_{24}O_9$	323.1345	-	113.0244;179.0561; 101.0244;161.0455	0.8	2.4	unidentified	
25[d]	16.0	326	$C_{16}H_{18}O_9$	353.0866	-	191.0561;127.0401; 161.0244; 93.0346	3.3	1.5	3-caffeoylquinic acid	12, 30, 31, M, K
26[a]	16.6	-	$C_{15}H_{14}O_{10}$	353.0506	-	161.0244;191.0197; 147.0299;135.0452; 117.0346	2.4	4.2	caffeoyl lisocitrate isomer	P, M, K
27[c]	16.8	-	$C_{15}H_{18}O_8$	325.0920	-	119.0502; 163.0401	1.6	2.7	*p*-coumaric acid *O*-glucose	31, M, K
28[a]	17.5	329	$C_{15}H_{14}O_{10}$	353.0491	-	191.0197;147.0299; 135.0452; 179.0350	6.5	12.0	caffeoyl isocitrate isomer	P, M, K

29[a]	17.5[A]	329	$C_{16}H_{18}O_{11}$	385.0758	-	191.0197;223.0459; 179.0350	4.8	10.9	*O*-feruloyl galactaric acid	M, K
30[c]	18.1	-	$C_{18}H_{26}O_{10}$	401.1425	-	161.0455	7.1	4.6	benzyl *O*-[arabino furanosyl-(1→6)-glucoside)	31, H
31[b]	18.3	-	$C_{24}H_{22}O_{14}$	533.0911	-	209.0303; 191.0197	4.9	9.0	dicaffeoyl glucaric acid isomer	12, 30
32[b]	18.6	-	$C_{24}H_{22}O_{14}$	533.0896	-	209.0303; 191.0197	7.6	4,1	dicaffeoyl glucaric acid isomer	12, 30
33[c]	18.7	-	$C_{15}H_{18}O_{8}$	325.0904	-	145.0295; 117.0346	7.6	15.5	*p*-coumaric acid *O*-glucose	31, M, K
34[c]	19.0	-	$C_{16}H_{18}O_{9}$	353.0851	-	191.0561; 161.0244; 93.0346; 127.0401; 133.0295	7.6	19.4	caffeoylquinic acid isomer	12, 30, 31, M, K
35[a]	20.1	-	$C_{21}H_{22}O_{11}$	449.1064	-	259.0612; 191.0561; 97.0295	5.6	17.2	2',3,4,4',6'-Pentahydroxy chalcone 4'-*O*-glucoside	M, K
36[c]	20.4	-	$C_{16}H_{18}O_{8}$	337.0899	-	191.0561;119.0502; 93.0346; 163.0401; 145.0295; 155.0350	8.9	5.1	*p*-coumaroyl quinic acid	12, 30, 31, M, K
37[a]	21.9	-	$C_{17}H_{20}O_{11}$	399.0911	-	161.0244;191.0197; 173.0092; 367.0671	5.6	5.1	sinapinic acid-*O*-glucuronide	H
38[c]	22.5	354	$C_{27}H_{30}O_{16}$	609.1435	-	301.0354;255.0299; 151.0037; 178.9986	4.3	5.7	rutin	10, 18, 30, 31, M, K
39	23.1	-	$C_{18}H_{32}O_{12}$	439.1799	-	149.0455;179.0561; 119.0350;101.0244; 251.0772	5.0	15.3	unidentified	
40[c]	23.4[A]	-	$C_{17}H_{20}O_{9}$	367.1003	-	135.0452;161.0244; 179.0350;191.0561; 137.0244;127.0401; 117.0346	8.6	8.2	feruloylquinic acid isomer	12, 30, 31, M, K
41[a]	23.4	-	$C_{15}H_{14}O_{10}$	353.0489	-	135.0452;129.0193; 179.0350;161.0244; 173.0092;219.0299; 151.0401; 335.0409	7.1	15.1	caffeoyl isocitrate isomer	P, M, K

42[d]	24.6	354	$C_{21}H_{20}O_{12}$	463.0861	-	271.0248;301.0354; 255.0299;151.0037; 245.0455; 178.9986	4.5	7.5	quercetin 3-glucoside	18, 30, 31, M, K
43	25.0	-	$C_{18}H_{32}O_{10}$	407.1903	-	227.1289; 138.1050	4.7	10.4	Unidentified	
44[c]	25.4	-	$C_{27}H_{30}O_{15}$	593.1499	-	285.0405;257.0397; 549.1250;	2.1	19.1	kaempferol-3-*O*-rutinoside	30, M, K
45[b]	25.8	355	$C_{28}H_{32}O_{16}$	623.1592	-	315.0510;300.0276; 287.0561	4.1	2.6	isorhamnetin 3-*O*-(6-*O*-rhamnosyl-glucoside	31
46[a]	26.5	-	$C_{24}H_{22}O_{15}$	549.0878	-	301.0354;255.0299; 464.0960;109.0295; 163.0037	1.4	18.7	quercetin 3-*O*-(6-*O*-malonyl-beta-D-glucoside)	M, K
47[a]	26.5	-	$C_{21}H_{20}O_{12}$	463.0872	-	301.0354;273.0405; 191.0350;215.0350; 215.0409;163.0037; 257.0455;230.0221; 197.0244;197.0303; 288.0851	2.1	8.2	quercetin 7-*O*-beta-D-glucoside	M, K
48[a]	27.1	353	$C_{24}H_{22}O_{15}$	549.0895	-	271.0248;255.0299; 151.0037	-1.6	18.9	quercetin 3-*O*-(6-*O*-malonyl-beta-D-glucoside)	M, K
49[b]	27.8	-	$C_{22}H_{22}O_{12}$	477.1033	-	243.0299;271.0248; 257.0455;286.0483; 300.0276; 215.0350	1.2	9.9	isorhamnetin-3-glucoside	10, 30, 31
50[c]	28.5	348	$C_{21}H_{20}O_{11}$	447.0929	-	271.0248;301.0354; 255.0299;151.0037; 245.0397;178.9986; 109.0295;121.0295; 135.0088	0.9	2.9	quercetin 3-L-rhamnoside	10, 30, 31, M, K
51[c]	29.6	-	$C_{25}H_{24}O_{12}$	515.1194	-	353.0878;173.0455; 179.0350;191.0561; 135.0452;155.0350; 93.0346; 161.0244; 318.0686;137.0244; 203.0350;356.0902; 111.0452	0.1	16.0	3,5-dicaffeoyl quinic acid	12, 31, M, K
52[b]	30.0	-	$C_{24}H_{24}O_{13}$	519.1134	-	300.0276;315.0510; 227.0350;177.0193; 204.0428; 204.0487	2.0	3.2	isorhamnetin-3-malonyl-hexoside	10
53[c]	31.7	-	$C_{21}H_{20}O_{10}$	431.0974		285.0405;255.0299; 244.0377; 267.0358	2.3	6.4	kaempferol rhamnoside	10, 30, 31, M, K

[A] Compounds detected only in the methanolic extract. [B] Compounds detected only in the ethanolic extract. Peaks identified with [a]Database (DB) (PUBCHEM (P), METFRAG (M), HMDB (H) and KEEG (K)), [b]bibliography, [c]Database plus bibliography, [d]Database (DB), bibliography and commercial standards. [e]Higher to lower intensity. [f]mσ: Bruker parameter.

The phenolic compounds profile obtained by negative mode (ESI -) showed mainly HCADs (chromatogram as supplementary material, Figure S2). Other compounds assigned as flavonols, chalcone, depsides and hydrolysable tannins were detected. 3-caffeoylquinic acid and caffeoylglucaric isomers were the main compounds detected, which were in accordance with previous findings [9,12,30].

Additionally, we assigned identities for the following compounds that have not been detected before in calafate: caffeoylisocitrate isomers (signals 23, 26, 28, 41) that showed a [M-H]- (deprotonated molecule) of 353.0521 m/z and the following fragments: 191.0197 m/z [$C_6H_7O_7$]- corresponding to an isocitrate group, 179.0350 m/z [$C_9H_7O_4$]- associated with caffeic acid and 161.0244 m/z [$C_9H_6O_3$-H]- corresponding to caffeoyl group moiety. O-

feruloylgalactaric acid (signal 29) was tentatively assigned by its ion [M-H]- of 385.0758 m/z with fragments 191.0197 m/z [$C_6H_8O_7$-H]- (galactaroyl), 223.0459 m/z [$C_7H_{11}O_8$]- (methylated isocitrate) and 179.0350 m/z [$C_9H_6O_4$+H]- (caffeic acid). All these signals showed a maximum absorbance at 329 nm, which is characteristic of HCADs. Syringic acid glucuronide, a hydrolyzable tannin (signal 19), showed a pseudomolecular ion of [M-H2O-H]- 355.0660 m/z, and a fragment of 147.0299 m/z [$C_5H_7O_5$]- (glucuronide group moiety). 3-Hydroxy-4-metoxy-5-(3,4,5-trihidroxybenzoyloxy)benzoic acid (signal 22), known as depside or depsidone, was characterized by [M-H]- 335.0409 m/z and a fragment of 183.0299 m/z [$C_8H_7O_5$]- corresponding to 3-hidroxy-4-metoxybenzoic acid by rupture of an ester bond. Benzyl O-(arabinofuranosyl-(1->6)-glucoside) (signal 30), an O-glycosyl compound, was characterized by a [M-H]- of 401.1425 m/z [31] and a fragment of 161.0455 m/z [$C_6H_9O_5$]- (a fragment from the glucoside group modified in the oxygen of ether bond). p-Coumaric acid O-glucose (signals 27 and 33) with [M-H]- 325.0920 m/z and fragments 119.0502 m/z [C_8H_7O]- (coumaric acid decarboxylated), 163.0401 m/z [$C_9H_7O_3$]- (coumaric acid) [31] and 145.0295 m/z [$C_9H_7O_2$-2H]- (coumaroyl group) was identified. Sinapinic acid-O-glucuronide isomer (signal 37)

corresponded to HCADs with an ion [M-H]- of 399.0911 m/z and fragments 161.0244 m/z [$C_9H_5O_3$]- (demethoxylated sinapinic acid), 191.0197 m/z [$C_{10}H_7O_4$]- (sinapinic acid moiety) and 173.0092 m/z [$C_{10}H_5O_3$]-, corresponding to [$C_{10}H_7O_4$-H_2O]-. Isorhamnetin 3-O-(6-O-rhamnosylglucoside (signal 45) corresponded to a flavonol characterized by λmax 355 nm, a [M-H]- 623.1592 m/z, fragments of 315.0510 m/z [$C_{16}H_{11}O_7$]- (isorhamnetin aglycone) [31], and 300.0276 m/z [$C_{15}H_8O_7$]- (demethylated aglycone). Finally, we found 2',3,4,4',6'-pentahydroxychalcone 4'-O-glucoside (signal 35), a product of the equilibrium of cyanidin-glucoside flavylium-hemiketal-chalcone. This compound was explained by the ion [M-H]- 449.1064 m/z and fragment 259.0612 m/z [$C_{14}H_{11}O_5$]- (aglycone moiety). In total, we found 53 compounds, 19 of them detected in calafate fruit for first the time.

4.1.3.2 Fatty acid profile of calafate berry by GC-MS

In this study, we were the first to describe the fatty acid profile of a calafate berry. Table 4.1.2 displays the main fatty acid methyl ester (FAME) detected, and the chromatogram is shown as supplementary material (Figure S3).

Seven fatty acids were detected in calafate, two of which were essential poly-unsaturated fatty acids, linoleic acid (LA) (12.7%) and linolenic acid (ALA) (15.6%), and monounsaturated fatty acids (oleic and erucic acids, 19.9%). Several studies suggest a favorable relationship between cardiovascular health and unsaturated fatty acid consumption. Regular intake of these fatty acids has been associated with a lower content of total plasma cholesterol and LDL levels, as well as a reduction of atherosclerosis and a decreased incidence of cardiovascular disease [32]. A study carried out with HUVECs demonstrated that the incubation of cells with an Ω 3 fatty acid (DHA) decreased the expression of adhesion molecules, such as VCAM-1, and the generation of NADPH oxidase-induced ROS in response to IL-1β [33]. Furthermore, it has been demonstrated that LA; 18:2, n-6 and ALA; 18:3, n-3 decrease ROS levels in cells exposed to high glucose [34]. Considering these antecedents and the fatty acid profile, although low in total concentration, these properties, together with the other detected compounds, can explain the beneficial effects of calafate consumption in the context of CVD.

Table 4.1.2: Fatty acids profile of calafate fruit (GC-MS)

t_R (min)	Formula	Assigned identity	Mass (Da)	Concentration (mg/g FW[a])
19.972	$C_{15}H_{30}O_2$	Methyl tetradecanoate (Myristic acid methyl ester)	242.2	0.16 ± 0.01
22.443	$C_{17}H_{34}O_2$	Hexadecanoic acid, methyl ester	270.3	0.08 ± 0.02
24.708	$C_{19}H_{38}O_2$	Octadecanoic acid, methyl ester	298.3	0.06 ± 0.00
25.507	$C_{19}H_{36}O_2$	9-Octadecenoic acid, methyl ester, (Z) (Oleic acid methyl ester)	296.3	0.04 ± 0.01
26.783	$C_{19}H_{34}O_2$	9,12-Octadecadienoic acid (Z,Z)-, methyl ester (Linoleic acid methyl ester ω6)	294.3	0.07 ± 0.03
28.160	$C_{19}H_{32}O_2$	9,12,15-Octadecatrienoic acid, methyl ester, (Z,Z,Z)- (Linolenic acid methyl ester ω3)	292.2	0.09 ± 0.04
29.473	$C_{23}H_{44}O_2$	13-Docosenoic acid, methyl ester, (Z)- (Erucic acid methyl ester)	352.3	0.08 ± 0.01

a FW: Fresh Weight. Data presented as the mean ± standard error.

4.1.3.3 Metal contents in calafate berry by TXRF.

The metal profile of calafate fruit has not been previously described. TXRF is a surface elemental analysis technique often used for ultratrace analysis [35]. The methanolic calafate extract was analyzed in order to identify and quantify the main metals. Corresponding X-ray fluorescence spectra are shown in the supplementary material (Figure S4).

The metals detected in calafate were K, Ca, P, S, Mn, Cu, Pb and Zn. Heavy metals, such as As and Se, were not detected; moreover, Al was under the LOD. The estimated concentrations are listed in Table 4.1.3. Due to cross contamination in the TXRF system, Fe was not measured using this technique and its quantitation was carried out by atomic absorption spectroscopy (supplementary material). However, Fe had a concentration below the quantification limit of the method (<0.71 μg/g).

Zn, Cu and Mn play important roles in the regulation of oxidative stress. They form complexes with superoxide dismutase (SOD) that transform superoxide anions into H_2O_2, which is subsequently transformed into water and oxygen by catalase. Mn is the main activator of enzymes involved in the antioxidant protection of the human body, such as mitochondrial SOD [20].

Interestingly, when comparing Mn concentration in calafate to that in other fruits, such as grapes or raspberries, calafate showed higher levels. In grape varieties, concentrations range from 0.0006 to 0.0004 mg/g (as fresh weight), while raspberries have between 0.041 and 0.015 mg/g (dry weight) [36,37]. Considering Mn consumption has been associated with beneficial effects, this

finding also contributes to the understanding of the potential benefits of calafate fruit in prevention of CVD.

Finally, it is important to highlight that the estimated concentration of Cu and Pb was below the maximum limit allowed in food (0.01 and 0.002 mg/g, respectively) (http://www.diariooficial.interior.gob.cl/media/2013/12/17/do-20131217.pdf). This consideration is important in a product for human consumption.

Table 4.1.3: Estimated concentration of metals in calafate berry by TXRF

	Calafate mg/g FW[b]
Aluminium	ND
Phosphorus	0.830±0.040
Sulfur	0.610±0.010
Potassium	3.460±0.110
Calcium	0.550±0.020
Manganese	0.006±0.000
Copper	0.006±0.000
Zinc	0.007±0.000
Lead	0.001±0.000
Iron[a]	< 0.00071

[a]Determined by atomic absorption spectroscopy. [b] FW: fresh weigh

4.1.3.4 Concentration of main compounds in the extracts

The full characterization of calafate fruit was carried out using methanol as an extraction solvent, as previously described [8,11,12]. However, considering the cellular toxicity of this solvent, we also evaluated an ethanolic extract obtained under the same conditions as the methanolic extract.

The ethanolic extract showed a similar profile of compounds as that observed for the methanolic extract, with minor differences (see Table 4.1.1). The comparative results from the quantitative analyses for the main compounds are presented in the supplementary material (Table S1, S2). The results were expressed as μmol/mL for phenolic compounds and mg/mL for fatty acids and showed no significant difference for the main anthocyanins, HCADs or fatty acid contents ($p > 0.05$), which indicates a similar capacity for extraction. Furthermore, total concentration of anthocyanins, HCADs and fatty acids did not show a significant difference either ($p > 0.05$) (Table 4.1.4). However, the observed anthocyanin concentration was lower than previously reported [8], but this can be explained by different edaphoclimatic

conditions [8]. The important figures of the quantitative method are included in the supplementary material (Table S3).

Table 4.1.4: Total polyphenol concentration and antioxidant capacity in calafate extracts.

Extract	Total Anthocyanins	Total Hydroxycinnamic acids	Total Fatty acids	ABTS	CUPRAC	ORAC	Folin-Ciocalteu
	(μmol/mL)	(μmol/mL)	(mg/mL)	(eq.trolox μmol/mL)			(eq. Gallic acid mg/mL)
Methanolic	2.22 ± 0.18	0.35 ± 0.01	0.37 ± 0.04	13.74 ± 0.76	21.14 ± 0.28	21.38 ± 0.64	1.90 ± 0.04
Ethanolic	2.16 ± 0.07	0.28 ± 0.02	0.51 ± 0.04	10.88±0.72 *	19.36±0.14 *	21.60 ± 0.86	1.60 ± 0.02*

*$p < 0.05$ vs methanolic extract. Data presented as the mean ± standard error. Figures of merit are presented as supplementary material (Table S3).

4.1.3.5 Antioxidant capacity of calafate extracts

The antioxidant capacity of methanolic and ethanolic extracts was determined by $TEAC_{ABTS}$, $TEAC_{CUPRAC}$, $TEAC_{ORAC}$, and Folin-Ciocalteu (Table 4.1.4), which was a complementary screening battery to obtain a global view of the antioxidant potential of the extracts. The results showed high antioxidant capacity for both extracts, with no significant differences

between them. The concentration of metals also showed no differences between extracts (data not shown). Metals can have an important role because free ions catalyze Fenton-type reactions, which reduce antioxidant capacity. However, Zúñiga et al., 2014 demonstrated that Fe and Mn concentrations may increase antioxidant capacity by 11.0 and 8.9%, respectively (results obtained for both free and complexed metals) [38]. Calafate extracts contained 6.0 µg/g FW of Mn but an undetected concentration of Fe. The contribution of Mn to the high antioxidant capacity of this fruit is unknown, as such it is necessary to perform further studies in order to better understand the effects of these metals on the antioxidant capacity of calafate, which could be through interactions with polyphenols or enzymes.

4.1.3.6 Calafate extracts reduced ROS production caused by H_2O_2 in HUVECs

Despite the high antioxidant capacity of calafate extracts demonstrated by chemical methods, these results do not necessarily correlate with antioxidant effects in biological systems. To evaluate the potential of calafate extracts on oxidative stress, which is an important factor involved in the development of CVD, we assessed intracellular ROS production using HUVECs. The cells

were preincubated with the extracts and then exposed to H_2O_2, an oxidizing agent that generates oxidative stress in cells [39].

In a first set of experiments, we evaluated whether calafate extracts had any effect on cell viability. This is important since cell viability can interfere with further ROS quantification. As shown in supplementary material (Figure S5), neither methanolic nor ethanolic extract dilutions affected cell viability after 48 h of incubation ($p > 0.05$). In contrast, cells exposed to PBS for 48 h (positive control for cell lysis by serum deprivation) showed a significant reduction of cell viability (approximately 96%).

Since calafate extracts did not change cell viability, we next evaluated the antioxidant effect of calafate extracts on cells exposed to H_2O_2. In this model, we assessed the ability of calafate to prevent ROS production since cells were preincubated with extracts for 24 h and then, they were removed from culture before the addition of H_2O_2. As determined with the H_2DCF-DA probe (Figure 4.1.1), 200 µM H_2O_2 induced a 1.8-fold increase in ROS production when compared with nontreated cells (negative control) ($p < 0.05$). The addition of vitamin C together with H_2O_2 restored radical production to the

basal levels, which is due to the ability of ascorbic ion to react with radicals, producing the ascorbyl radical [20].

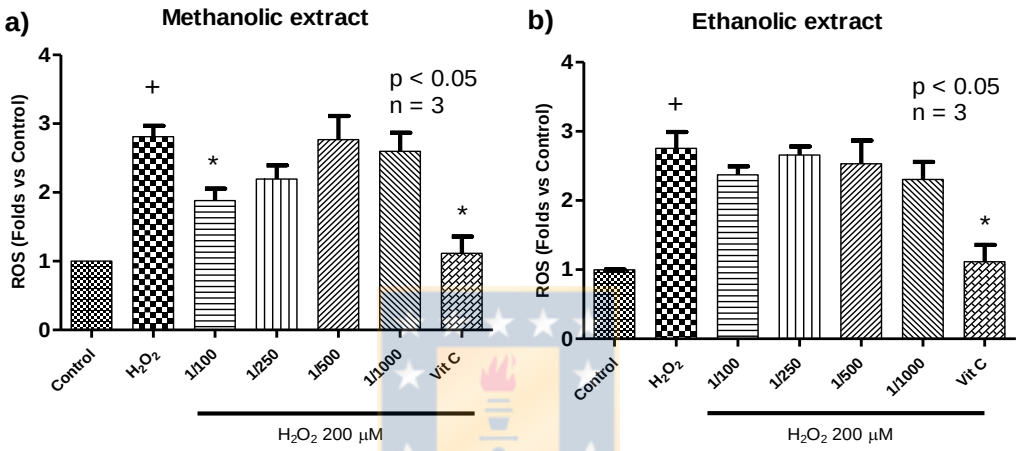

Figure 4.1. 1: Protective effect of calafate extract on ROS production upon H_2O_2 stimulation. a) Methanolic extract diluted at 1/100 (2 mg FW/mL), 1/250 (0.8 mg FW/mL), 1/500 (0.4 mg FW/mL) and 1/1000 (0.2 mg FW/mL). b) Ethanolic extract diluted at 1/100 (2 mg FW/mL), 1/250 (0.8 mg FW/mL), 1/500 (0.4 mg FW/mL) and 1/1000 (0.2 mgFW/mL). Intracellular ROS levels were determined by H_2DCF-DA fluorescence (10 µM) (λex 485 nm; λem540 nm) in cells previously incubated with extract and then exposed to H_2O_2. Vitamin C (250 µg/mL) was used as the antioxidant control. Data

are presented as the mean ± standard error values. + $p < 0.05$ vs control (negative control). * $p < 0.05$ vs H_2O_2 control (positive control).

In these experiments, the oxidative effect of H_2O_2 was reduced by 51% in cells preincubated with the methanolic calafate extract at a dilution of 1/100 (equivalent to 2.22 nmol of anthocyanins and 0.035 nmol of HCAD) ($p < 0.05$) (Figure 4.1.1a). As extract dilution increased, the antioxidant effect was reduced and was no longer detected at a dilution of 1/500. For the ethanolic extract, this antioxidant effect was minor (approximately 22% reduction for 1/100 dilution) and did not reach statistical significance (Figure 4.1.1b). Due to the lack of a significant difference in the phenolic composition and fatty acids content of the ethanolic and methanolic extracts (Table 4.1.4), we hypothesize that minor changes in other compounds may be relevant for the protective effect observed.

It is important to note that the antioxidant protection exerted by the methanolic extract was only detected after long incubations (24 h), since experiments performed with shorter periods (4 h) did not reduce oxidative stress (data not shown). This suggests that the calafate extract induces cell responses resulting in higher expression/activity of molecules/enzymes

involved in the protection against oxidative stress, such as reduced glutathione (GSH) and superoxide dismutase (SOD). This is consistent with findings reported for delphinidin (the main anthocyanin found in calafate extract), which is able to protect SOD activity in HUVECs treated with an oxidant agent for 24 h. In the absence of delphinidin, SOD activity is significantly attenuated by oxidative stress [40]. Moreover, the antioxidant properties of calafate could be related to the effect of metals on the activity of some antioxidant enzymes, as mentioned above. Additionally, despite the low concentration of fatty acids found in calafate extracts, they could still contribute to this antioxidant effect, as reported by Jiang et al., 2017, where ALA and LA reduced ROS in HK-2 cells treated with a high glucose concentration [34].

4.1.3.7 Calafate extract reduced lipidic peroxidation caused by $CuSO_4$ in human LDL

Oxidative stress is closely related to LDL oxidation and endothelial dysfunction, two important factors contributing to atherosclerosis and CVD [5]. Thus, we evaluated the effect of calafate extracts on lipidic peroxidation of LDL. In Figure 4.1.2, the kinetics of human LDL oxidation are presented,

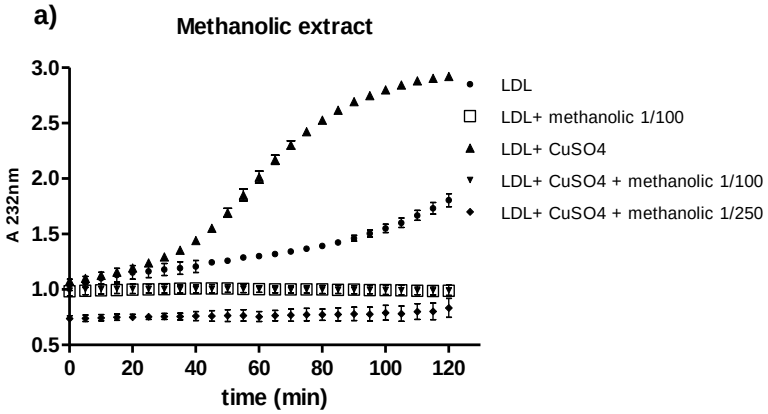
a)
Methanolic extract
A 232nm
time (min)
LDL
LDL+ methanolic 1/100
LDL+ CuSO4
LDL+ CuSO4 + methanolic 1/100
LDL+ CuSO4 + methanolic 1/250

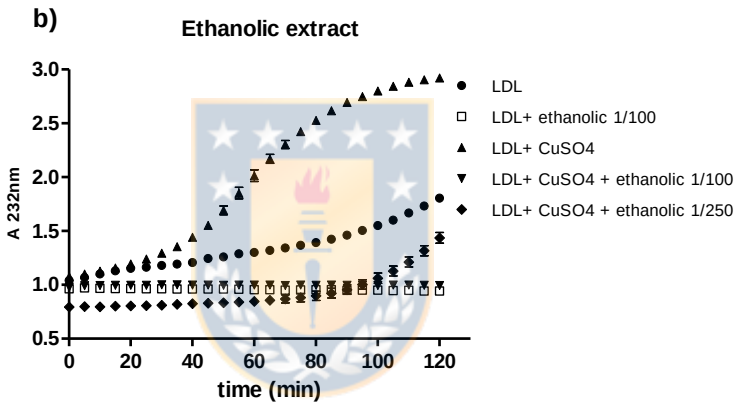
b)
Ethanolic extract
A 232nm
time (min)
LDL
LDL+ ethanolic 1/100
LDL+ CuSO4
LDL+ CuSO4 + ethanolic 1/100
LDL+ CuSO4 + ethanolic 1/250

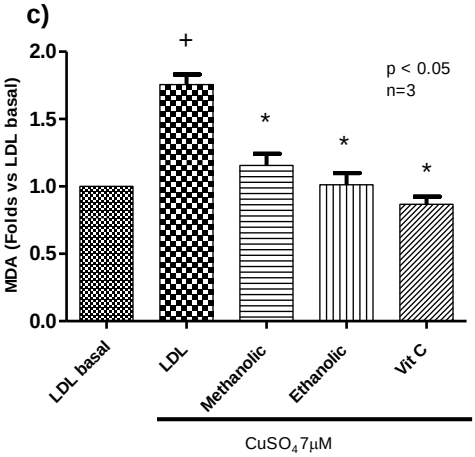
c)
MDA (Folds vs LDL basal)
p < 0.05
n=3
LDL basal
LDL
Methanolic
Ethanolic
Vit C
CuSO4 7µM

Figure 4.1.2: Effect of calafate extract on lipidic peroxidation of LDL. a) Kinetic curve of LDL oxidation with or without methanolic extract (dilution 1/100 and 1/250). b) Kinetic curve of LDL oxidation with or without ethanolic extract (dilution 1/100 and 1/250). Figures A and B are representative of three LDL assays obtained from different volunteers. c) MDA production in relation to LDL basal control (methanolic and ethanolic extract dilution at 1/100). Data are presented as the mean ± standard error values. Vitamin C (250 µg/mL) was used as the antioxidant control. + $p < 0.05$ vs LDL basal (negative control). * $p < 0.05$ vs LDL $CuSO_4$ control (positive control).

as determined by intermediate oxidation products (conjugated dienes measured at 232 nm).

The results showed that native LDL is gradually oxidized by incubation at 37ºC (autoxidation), and after 120 min, conjugated dienes increased approximately 50%. This reaction speed is rapidly increased with $CuSO_4$, as oxidation products began to increase after 40 min of incubation (while LDL without $CuSO_4$ was not oxidized yet). They reached the plateau after 90 min

with a 3-fold increase in absorbance, compared to time 0. The methanolic extract inhibited LDL oxidation induced by $CuSO_4$ at dilutions of 1/100 (2 mg FW/mL) and 1/250 (0.8 mg FW/mL) throughout the incubation period (Figure 4.1.2a). Interestingly, the methanolic extract also inhibited the auto-oxidation of LDL, since it was able to maintain the absorbance at the same values as at time 0, while native LDL (without $CuSO_4$) absorbance was increased at the end of the incubation period. Regarding the ethanolic extract, dilutions 1/100 (2 mg FW/mL) and 1/250 (0.8 mg FW/mL) produced the same effect as the methanolic extract by completely inhibiting LDL oxidation (Figure 4.1.2b). However, at the end of the incubation, dilution 1/250 began to increase absorbance in the condition with $CuSO_4$ to the level of native LDL, suggesting the consumption of antioxidant molecules by this reaction. These results are in concordance with ROS production experiments in which the ethanolic extract showed a lower protective effect than the methanolic extract and confirm that other compounds present in calafate, other than phenolic compounds, can contribute to the antioxidant effect.

Additionally, we measured MDA in LDL, as a final product of the oxidation process. In these experiments, MDA was assessed after 80 min of oxidation. Under these conditions, calafate extracts reduced MDA produced by $CuSO_4$

to the levels found in native LDL (Figure 4.1. 2c). This effect was comparable to the effect obtained with vitamin C ($p < 0.05$). This is an interesting finding attributed to the total compounds present in the extracts, which are responsible for total antioxidant capacity.

The effect of the extracts against LDL oxidation may be produced by the ability of polyphenols (flavonoids) to eliminate free radicals or chelate metal ions, such as copper in this case (oxidant agent) [41]. However, to establish which compounds are responsible for these effects, it is necessary to carry out complementary experiments.

In a biological context, LDL oxidation plays a very important role in cardiovascular disease [15]. Oxidized LDL is atherogenic, as it causes direct oxidative damage to endothelial cells, promotes the inflammatory response and accumulates in the intima of blood vessels, where it is recognized and endocytosed by macrophages, promoting their transformation to foam cells, one of the main components of the atherosclerotic plaque [1]. Compounds that can prevent oxidative processes have been demonstrated to attenuate or prevent the development of atherosclerosis. Our findings suggest that consumption of calafate fruit could have a potential anti-atherosclerotic

effect, which can be mainly attributed to the phenolic compounds composition and additionally to the metals and poly-unsaturated fatty acids which may also have an important role in the beneficial effect of calafate.

4.1.4. Conclusions

Calafate fruit has a broad profile of bioactive compounds, mainly including phenolic compounds, which compose more than 53 chromatographic signals (anthocyanins, HCADs, flavonols and other phenolics and alkaloids such as berberine), fatty acids (mainly linolenic and linoleic acids), and certain metals (Mn, Cu and Zn, among others). This composition constitutes a product with remarkable nutraceutical characteristics for human consumption. Calafate extracts have a high chemical antioxidant capacity, can decrease ROS production in a cellular model of endothelium, and protect LDL against oxidation, which is one of the main factors responsible for the progression of atherosclerosis. Finally, based on our results, we propose that the consumption of calafate can play a role in the prevention of cardiovascular disease, the main cause of death in Chile and around the world; however, in order to confirm the effect of calafate in preventing CVD,

further studies must be carried out, including animal, clinical or preclinical trials".

Supplementary Materials: The following are available online at www.mdpi.com/xxx/s1, Figure S1: Base peak chromatogram ESI + crude extract calafate (black) and DAD chromatogram to 520 nm (red), Figure S2: Base peak chromatogram ESI- extract previously purify with solid extraction for hydroxycinnamic acid derivatives (red), DAD chromatogram 320 nm (yellow) and DAD chromatogram 360 nm (green), Figure S3: Extracted ion chromatogram (EIC) of fatty acids profile in calafate fruit (81 m/z; 87 m/z; 91 m/z), Figure S4: X-ray fluorescence spectra of calafate fruit. Internal standard Ga 0.5 mg/L Scans 1,200 s, Table S1: Comparative concentration of main polyphenolic compounds identified in calafate berry extracts, Table S2: Comparative concentration of FAME identified in calafate berry extracts, Table S3: Figure of merit of the quantitative method, Figure S5: *In vitro* viability assay determined by MTT method, and Method "Determination of Fe in calafate extract by atomic absorption spectroscopy (AAS)".

Author Contributions: "Conceptualization, C.R. and C.M.; methodology, L.O., C.R, and S.C.; validation, L.O; formal analysis, L.O. and D.N.;

investigation, L.O., S.C, D.N., and L.B.; resources, C.R. and C.M.; data curation, L.O. and L.B.; writing—original draft preparation, L.O.; writing—review and editing, C.R., L.B., Y.N., A.P. and C.M.; visualization, L.O., C.R. and C.M.; supervision, C.R. and C.M.; project administration, L.O, C.R. and C.M.; funding acquisition, L.O. and C.M. All authors have read and agreed to the published version of the manuscript."

Funding: This research was funded by ANID Chile: Beca Doctorado Nacional, grant number 21170812; FONDECYT, number 1191276; FONDEQUIP, number 170023; and AFB, number 1700017. The APC was funded by FONDECYT, number 1191276.

Acknowledgments: We thank Mr. César Busolich from Secretos de la Patagonia, Punta Arenas, Chile, who provided calafate samples.

Conflicts of Interest: The authors declare no conflict of interest.

References

1. Lobo, V.; Patil, A.; Phatak, A.; Chandra, N. Free radicals, antioxidants and functional foods: Impact on human health. Pharmacogn, Rev. 2010, 4(8), 118–126. https://doi.org/10.4103/0973-7847.70902

2. Soares, S.; Silva, M. S.; García-Estevez, I.; Groβmann, P.; Brás, N.; Brandão, E.; Nuno, M.; Freitas, V de.; Behrens, M .; Meyerhof, W. Human Bitter Taste Receptors Are Activated by Different Classes of Polyphenols. J. Agric. Food Chem 2018, 66, 8814–8823. https://doi.org/10.1021/acs.jafc.8b03569

3. Abbas, M.; Saeed, F.; Anjum, F. M.; Afzaal, M.; Tufail, T.; Bashir, M. S.; Ishtiag, A.; Hussain, S.; Suleria, H. A. R. Natural polyphenols: An overview. Int. J. Food Prop. 2017, 20(8), 1689–1699. https://doi.org/10.1080/10942912.2016.1220393

4. Andriantsitohaina, R.; Auger, C.; Chataigneau, T.; Étienne-Selloum, N.; Li, H.; Martínez, M. C.; Schini-Kerth, V.B.; Laher, I. Molecular mechanisms of the cardiovascular protective effects of polyphenols. Br. J. Nutr. 2012, 108(9), 1532–1549. https://doi.org/10.1017/S0007114512003406

5. Campos, J.; Schmeda-Hirschmann, G.; Leiva, E.; Guzmán, L.; Orrego, R.; Fernández, P.; González, M.; Radojkovic, C.; Lamperti, L.; Pastene, E.; Aguayo, C. Lemon grass (Cymbopogon citratus (D.C) Stapf) polyphenols protect human umbilical vein endothelial cell (HUVECs) from oxidative damage induced by high glucose, hydrogen peroxide and oxidised low-density lipoprotein. Food Chem. 2014, 151, 175–181. https://doi.org/10.1016/j.foodchem.2013.11.018

6. Tresserra-Rimbau, A.; Rimm, E. B.; Medina-Remón, A.; Martínez-González, M. A.; de la Torre, R.; Corella, D.; Salas-Salvadó, J.; Gómez-Gracia, E.; Lapetra, J.; Arós, F.; Fiol, M.; Ros, E.; Serra-Majem, L.; Pintó, X.; Saez, G. T.; Basora, J.; Sorlí, J. V.; Martínez, J. A.; Vinyoles, E.; Ruiz-Gutiérrez, V.; Estruch, R.; Lamuela-Raventós. Inverse association between habitual polyphenol intake and incidence of cardiovascular events in the PREDIMED study. Nutr. Metab. Cardiovasc. Dis. 2014, 24(6), 639–647. https://doi.org/10.1016/j.numecd.2013.12.014

7. Sarr, M.; Chataigneau, M.; Martins, S.; Schott, C.; El Bedoui, J.; Oak, M. H.; Muller, B.; Chataigneau,T.; Schini-Kerth, V. B. Red wine polyphenols prevent angiotensin II-induced hypertension and endothelial

dysfunction in rats: Role of NADPH oxidase. Cardiovasc. Res. 2006, 71, 794–802. https://doi.org/10.1016/j.cardiores.2006.05.022

8. Ruiz, A.; Hermosín-Gutiérrez, I.; Mardones, C.; Vergara, C.; Herlitz, E.; Vega, M.; Dorau, C.; Winterhalter, P.; Von Baer, D. Polyphenols and antioxidant activity of calafate (berberis microphylla) fruits and other native berries from Southern Chile. J. Agric. Food Chem. 2010, 58(10), 6081–6089. https://doi.org/10.1021/jf100173x

9. Ruiz, A.; Mardones, C.; Vergara, C.; Von Baer, D.; Gómez-Alonso, S.; Gómez, M. V.; Hermosín-Gutiérrez, I. Isolation and structural elucidation of anthocyanidin 3,7-β-O- diglucosides and caffeoyl-glucaric acids from calafate berries. J. Agric. Food Chem. 2014, 62, 6918–6925. https://doi.org/10.1021/jf5012825

10. Ruiz, A.; Zapata, M.; Sabando, C.; Bustamante, L.; Von Baer, D.; Vergara, C.; Mardones, C. Flavonols, Alkaloids, and Antioxidant Capacity of Edible Wild Berberis Species from Patagonia. J. Agric. Food Chem. 2014, 62, 12407–12417. https://doi.org/10.1021/jf502929z

11. Ruiz, A.; Hermosín-Gutiérrez, I.; Vergara, C.; Von Baer, D.; Zapata, M.; Hitschfeld, A.; Obando, L.; Mardones, C. Anthocyanin profiles in south Patagonian wild berries by HPLC-DAD-ESI-MS/MS. Food Res. Int. 2013, 51(2), 706–713. https://doi.org/10.1016/j.foodres.2013.01.043

12. Ruiz, A., Mardones, C.; Vergara, C.; Hermosín-gutiérrez, I.; Von Baer, D.; Hinrichsen, P.; Rodriguez, R.; Arribillaga, D.; Dominguez, E. Analysis of hydroxycinnamic acids derivatives in calafate (Berberis microphylla G . Forst) berries by liquid chromatography with photodiode array and mass spectrometry detection. J. Chromatogr. A 2013, 1281, 38–45. https://doi.org/10.1016/j.chroma.2013.01.059

13. Schmeda-Hirschmann, G.; Jiménez-Aspee, F.; Theoduloz, C.; Ladio, A. Patagonian berries as native food and medicine. J. Ethnopharmacol. 2019, 241, 111979. https://doi.org/10.1016/j.jep.2019.111979

14. Ramirez, J. E.; Zambrano, R.; Sepúlveda, B.; Kennelly, E. J.; Simirgiotis, M. J. Anthocyanins and antioxidant capacities of six Chilean berries by HPLC-HR-ESI-ToF-MS. Food Chem. 2015, 176, 106–114. https://doi.org/10.1016/j.foodchem.2014.12.039

15. Shao, D.; Lian, Z.; Di, Y.; Zhang, L.; Rajoka, M.S.R.; Zhang, Y.; Kong, J.; Jiang C.; Shi, J. Dietary compounds have potential in controlling atherosclerosis by modulating macrophage cholesterol metabolism and inflammation via miRNA. Npj Science of Food 2018, 2, 13. https://doi.org/10.1038/s41538-018-0022-8

16. Reyes-Farias, M.; Vasquez, K.; Fuentes, F.; Ovalle-Marin, A.; Parra-Ruiz, C.; Zamora, O.; Pino, M. T.; Quitral, V.; Jimenez, P.; Garcia, L.; Garcia-Diaz, D. F. Extracts of Chilean native fruits inhibit oxidative stress, inflammation and insulin-resistance linked to the pathogenic interaction between adipocytes and macrophages. J. Funct. Foods 2016, 27, 69–83. https://doi.org/10.1016/j.jff.2016.08.052

17. Reyes-farias, M.; Vasquez, K.; Ovalle-marin, A.; Fuentes, F.; Parra, C.; Quitral, V.; Jimenez, P.; Garcia-diaz, D. F. Chilean Native Fruit Extracts Inhibit Inflammation Linked to the Pathogenic Interaction Between Adipocytes and Macrophages. J. Med. Food, 2015 18(5), 601–608. https://doi.org/10.1089/jmf.2014.0031

18. Calfío, C.; Huidobro-Toro, J. P. Potent vasodilator and cellular antioxidant activity of endemic patagonian calafate berries (Berberis microphylla) with nutraceutical potential. Molecules 2019, 24(15). https://doi.org/10.3390/molecules24152700

19. Casas, R.; Castro-Barquero, S.; Estruch, R.; Sacanella, E. Nutrition and cardiovascular health. Int. J. Mol. Sci. 2018, 19(12), 3988. https://doi.org/10.3390/ijms19123988

20. Fukai, T.; Ushio-Fukai, M. Superoxide dismutases: Role in redox signaling, vascular function, and diseases. Antioxid. Redox Signaling. 2011, 15 (6), 1583-1606. https://dx.doi.org/10.1089%2Fars.2011.3999

21. Medina, G.; Castillo, R. del P.; Neira, J. Y. Multivariate calibration for the improvement of the quantification of cadmium in the presence of potassium as interferent by total reflection X - ray fluorescence. X-Ray Spectrom. 2019, 48(6), 700–707. https://doi.org/10.1002/xrs.3113

22. Pino Ramos, L. L.; Jiménez-Aspee, F.; Theoduloz, C.; Burgos-Edwards, A.; Domínguez-Perles, R.; Oger, C.; Durand, T.; Gil-Izquierdo, Á.; Bustamante, L.; Mardones, C.; Márquez, K.; Contreras, D.; Schmeda-Hirschmann, G. Phenolic, oxylipin and fatty acid profiles of the Chilean hazelnut (Gevuina avellana): Antioxidant activity and inhibition of pro-inflammatory and metabolic syndrome-associated enzymes. Food Chem. 2019, 298. https://doi.org/10.1016/j.foodchem.2019.125026

23. Ou, B.; Chang, T.; Huang, D.; Prior, R. L. Determination of Total Antioxidant Capacity by Oxygen Radical Absorbance Capacity (ORAC) Using Fluorescein as the Fluorescence Probe: First Action 2012.23. J. AOAC Int. 2013, 96(6), 1372–1376. https://doi.org/10.5740/jaoacint.13-175

24. González, M.; Rojas, S.; Avila, P.; Cabrera, L.; Villalobos, R.; Palma, C.; Aguayo, C.; Peña, E.; Gallardo, V.; Guzmán-Gutiérrez, E.; Sáez, T.; Salsoso, R.; Sanhueza, C.; Pardo, F.; Leiva, A.; Sobrevia, L. Insulin reverses D-glucose-increased nitric oxide and reactive oxygen species generation in human umbilical vein endothelial cells. PLoS ONE 2015, 10(4), 1–23. https://doi.org/10.1371/journal.pone.0122398

25. Mosmann, T. Rapid colorimetric assay for cellular growth and survival: Application to proliferation and cytotoxicity assays. J. Immunol. Methods 1983, 65, 55–63. https://doi.org/10.1016/0022-1759(83)90303-4

26. Havel, R. J.; Eder, H. A.; Bragdon, J. H. The distribution and chemical composition of ultracentrifugally separated lipoproteins in human serum. J. Clin. Invest. 1955, 34(9), 1345–1353. https://doi.org/10.1172/JCI103182

27. Richard, M. J.; Portal, B., Meo; J.; Coudray, C.; Hadjian, A.; Favier, A. Malondialdehyde kit evaluated for determining plasma and lipoprotein

fractions that react with thiobarbituric acid. Clinical Chemistry 1992, 38(5), 704–709. https://doi.org/10.1093/clinchem/38.5.704

28. Sumner, L.W.; Amberg, A.; Barrett, D.; Beale, M.H.; Beger, R.; Daykin, C.A.; Fan, T.W.M.; Fiehn, O.; Goodacre, R.; Griffin, J.L.; Hankemeier, T.;Hardy, N.; Harnly, J.; Higashi, R.; Kopka, J.; Lane, A.N.; Lindon, J.C.; Marriott, P.; Nicholls, A.W.; Reily, M.D.; Thaden, J.J.; Viant, M.R. Proposed minimum reporting standards for chemical analysis: Chemical Analysis Working Group (CAWG) Metabolomics Standards Initiative (MSI). Metabolomics 2007, 3(3), 211-221. https://doi.org/10.1007/s11306-007-0082-2

29. Fang, J. Bioavailability of anthocyanins. Drug Metab. Rev. 2014, 46(4), 508–520. https://doi.org/10.3109/03602532.2014.978080

30. Chamorro, M. F.; Reiner, G.; Theoduloz, C.; Ladio, A.; Schmeda-Hirschmann, G.; Gómez-Alonso, S.; Jiménez-Aspee, F. Polyphenol composition and (bio)activity of Berberis species and wild strawberry from the Argentinean Patagonia. Molecules 2019, 24(18), 1–24. https://doi.org/10.3390/molecules24183331

31. Elsadig Karar, M. G.; Kuhnert, N. UPLC-ESI-Q-TOF-MS/MS Characterization of Phenolics from Crataegus monogyna and Crataegus laevigata (Hawthorn) Leaves, Fruits and their Herbal Derived Drops (Crataegutt Tropfen). Journal of Chemical Biology & Therapeutics 2016, 1, 102. https://doi.org/10.4172/2572-0406.1000102

32. Jones, P. J. H.; Senanayake; V. K., Pu, S.; Jenkins, D. J. A.; Connelly, P. W.; Lamarche, B.; Couture, P.; Charest, A.; Baril-Gravel, L.; West, S. G.; Liu, X.; Fleming, J. A.; McCrea, C.E.; Kris-Etherton, P. M. DHA-enriched high-oleic acid canola oil improves lipid profile and lowers predicted cardiovascular disease risk in the canola oil multicenter randomized controlled trial. Am. J. Clin. Nutr., 2014, 100(1), 88–97. https://doi.org/10.3945/ajcn.113.081133

33. Massaro, M.; Scoditti, E.; Carluccio, M. A.; De Caterina, R. Nutraceuticals and prevention of atherosclerosis: Focus on ω-3

polyunsaturated fatty acids and mediterranean diet polyphenols. Cardiovasc. Ther., 2010, 28(4), 13–19. https://doi.org/10.1111/j.1755-5922.2010.00211.x

34. Jiang, M.; Zhang, H.; Zhai, L.; Ye, B.; Cheng, Y.; Zhai, C. ALA/LA ameliorates glucose toxicity on HK-2 cells by attenuating oxidative stress and apoptosis through the ROS/p38/TGF-β1 pathway. Lipids Health Dis. 2017, 16, 216. https://doi.org/10.1186/s12944-017-0611-6

35. Gama, E. M.; Nascentes, C. C.; Matos, R. P.; Rodrigues, G. D. C.; Rodrigues, G. D. A simple method for the multi-elemental analysis of beer using total reflection X-ray fluorescence. Talanta 2017, 174, 274–278. https://doi.org/10.1016/j.talanta.2017.05.059

36. Snežana S. M.; Mirjana V. O; Milan N. M., Danijela A. K.; Aleksandra N. P.; Snežana B. T.; Milan D. S. Elemental Composition of Various Sour Cherry and Table Grape Cultivars Using Inductively Coupled Plasma Atomic Emission Spectrometry Method (ICP-OES). Food Analytical Methods 2012, 5, 279–286. https://doi.org/10.1007/s12161-011-9232-2

37. Castilho Maro, L.; Pio, R.; Santos Guedes; M., Patto de Abreu, C.; Nogueira Curi, P. Bioactive compounds, antioxidant activity and mineral composition of fruits of raspberry cultivars grown in subtropical areas in Brazil. Fruits 2013, 68(3), 209-217. https://doi.org.10.1051/fruits/2013068

38. Zúñiga, M. C.; Pérez-Roa, R. E.; Olea-Azar, C.; Laurie, V. F.; Agosin, E. Contribution of metals, sulfur-dioxide and phenolic compounds to the antioxidant capacity of Carménère wines. J. Food Compos. Anal. 2014, 35(1), 37–43. https://doi.org/10.1016/j.jfca.2014.04.003

39. Zhu, Y.; Zhang, Y. J.; Liu, W. W.; Shi, A. W.; Gu, N. Salidroside suppresses HUVECs cell injury induced by oxidative stress through activating the Nrf2 signaling pathway. Molecules 2016, 21, 1033. https://doi.org/10.3390/molecules21081033

40. Chen, C. ye; Yi, L.; Jin, X.; Mi, M. tian.; Zhang, T.; Ling, W. hua; Yu, B. Delphinidin attenuates stress injury induced by oxidized low-density lipoprotein in human umbilical vein endothelial cells. Chem.-Biol. Interact. 2010, 183(1), 105–112. https://doi.org/10.1016/j.cbi.2009.09.024

41. Saravanan, S.; Parimelazhagan, T. In vitro antioxidant, antimicrobial and anti-diabetic properties of polyphenols of Passiflora ligularis Juss. fruit pulp. Food Science and Human Wellness 2014, 3, 56–64. https://doi.org/10.1016/j.fshw.2014.05.001

4.2 La ingesta de *Berberis microphylla* G. Forst reduce el impacto de una dieta alta en grasas sobre factores de riesgo plasmáticos relacionados con la patología cardiovascular

En esta sección se presentan los resultados que dieron origen al segundo artículo de investigación de esta tesis doctoral enviado para publicación a Food Chemistry (FOODCHEM-D-22-05672).

Article

Berberis microphylla G. Forst intake reduces the impact of a high-fat diet on plasma cardiovascular disease factors

Lia OLIVARES-CARO[a,b], Daniela NOVA[a], Claudia RADOJKOVIC[b], Daniel DURAN[b], Daniela MENNICKENT[a,b], Luis BUSTAMANTE[a], Victoria MELIN[d], David CONTRERAS[e], Andy PEREZ[a], Claudia MARDONES[a,c]*

[a] Departamento de Análisis Instrumental, Facultad de Farmacia, Universidad de Concepción, Concepción, Chile

[b] Departamento de Bioquímica Clínica e Inmunología, Facultad de Farmacia, Universidad de Concepción, Concepción, Chile

[c] Unidad de Desarrollo Tecnológico, Universidad de Concepción, Coronel, Chile

[d] Departamento de Ingeniería Mecánica, Facultad de Ingeniería, Universidad de Tarapacá, Avda. General Velásquez 1775, Arica 1000007, Chile

[e] Facultad de Ciencias Químicas, Universidad de Concepción, Concepción 4070386, Chile

*Corresponding author. Tel.: +56 983616340. E-mail address cmardone@udec.cl (C. Mardones).

Abstract

Polyphenols are bioactive substances that participate in the prevention of chronic illnesses. High content has been described in *Berberis microphylla* (calafate), a wild berry extensively distributed in Chilean-Argentine Patagonia. We evaluated its beneficial effect through the study of mouse plasma metabolome changes after its consumption. Characterized calafate extract was administered in water to a group of mice fed a high-fat diet and a control diet. Metabolome changes were studied using UHPLC-DAD-QTOF-based untargeted metabolomics. Thirteen features were identified with a maximum annotation level-A. Metabolome perturbation was contrasted with changes in plasma biomarkers related to inflammation and cardiovascular disease, with the more relevant being thrombomodulin and adiponectin followed by sE-selectin, sICAM-1 and proMMP-9. Metabolomics revealed an increase in succinic acid, activating tricarboxylic acid and reducing carnitine accumulation. These changes could be associated with protection against atherosclerosis due to calafate consumption, which is discussed from a holistic and integrative point of view.

Keywords: *Berberis microphylla*, calafate, Polyphenols, cardiovascular disease risk, metabolomic

4.2.1. Introduction

Cardiovascular disease (CVD) is the main cause of death both in Chile and in the world: 27% of total deaths in Chile (MINSAL) and 31% worldwide (WHO) are caused by stroke or acute myocardial infarction. Hypertension, dyslipidemias, obesity, and metabolic syndrome, among other conditions, have been described as risk factors for CVD. Obesity is a condition characterized by an abnormal or excessive accumulation of fat, which leads to an altered metabolism and physiology (Curtasu et al., 2019). A high-fat diet (HFD) in association with a sedentary lifestyle increases the probability of obesity. A high-fat high-calorie diet has been related to increased oxidative stress, increased p47phox expression, reactive oxygen species (ROS) generation, NF-κB transcription, and a consequent elevation of TNF-α levels (a cytokine related to a proinflammatory state) (Biobaku et al., 2019). In addition, Shai et al., 2006 described an imbalance of cytokines and inflammatory proteins in obesity and CVD. For instance, soluble forms of

adhesion molecules, such as sICAM-1 and sVCAM-1, have been associated with obesity and other risk factors for coronary heart diseases (CHDs) (Shai et al., 2006). Moreover, Ruel et al., 2008 demonstrated an association between oxidized LDL and sVCAM-1 plasma levels and an inverse correlation with sICAM-1 (Ruel et al., 2008). Furthermore, plasma E-selectin levels have been significantly correlated with hyperinsulinemia and insulin resistance assessed by HOMA-IR in men with abdominal obesity (Couillard et al., 2005). Leptin, a peptide hormone produced predominantly by white adipose cells, increases in obese individuals and could promote inflammation related to chronic pathologies (Zunino et al., 2012). Finally, a review published by Bartekova et al., 2018 showed a large number of cytokines involved in heart disease: TNF-α, related to vascular dysfunction and atherogenesis, NF-kB, associated with the expression of pro-inflammatory markers, IL-2 and IL-4, which increase in plasma from stable angina pectoris patients, IL-6 increased in acute myocardial infarction and IL-18 in oxidative stress, among others (Bartekova et al., 2018).

Polyphenols are natural antioxidants that reduce oxidation processes and inhibit free radical production (Lobo et al., 2010). Calafate (*Berberis microphylla*) is a barberry that is rich in polyphenols and that has a high

antioxidant capacity obtained from an endemic shrub of Chilean-Argentine Patagonia (Ruiz et al., 2013)[ab]. It has been reported that calafate extract increased the ratio of reduced/oxidized glutathione (GSH/GSSG), which led to decreased oxidative stress in murine adipocytes treated with macrophage-conditioned medium. This is considered an obesity *in vitro* model because obesity increases the macrophage population in white adipose tissue, with a proinflammatory phenotype (Reyes-Farias et al., 2016). Another study reported the inhibition of TNF-α gene expression by a calafate extract in murine macrophages stimulated with 5 μg/mL lipopolysaccharides. Finally, our research group recently described that calafate extract reduces intracellular ROS production (51%) in human umbilical vein endothelial cells (HUVECs) and completely inhibits LDL oxidation and malondialdehyde (MDA) formation, demonstrating a potential role for preventing oxidative stress and lipoperoxidation (Olivares-Caro et al., 2020). These studies suggest that calafate could contribute to reducing the proinflammatory and oxidative state induced by cardiovascular risk factors, such as a HFD. However, *in vivo* studies are needed to evaluate the effect of calafate from an integral biological response point of view.

Metabolomics is a tool that directly relates a measurable chemical response to a biological event, allowing a simultaneous semiquantitative comparison of hundreds to thousands of metabolites in a living system and linking the genotype and phenotype of an organism (Marshall & Powers, 2017). The metabolome represents a wide range of metabolites with different chemical and physical properties, which can be modified by internal and/or external factors. Metabolomics compares patterns or "fingerprints" of metabolites that change in response to disease, exposure to toxins, and environmental or genetic alterations. Mass spectrometry (MS)-based metabolomics offers analyses with high selectivity and sensitivity and the potential to identify detected metabolites (Marshall & Powers, 2017).

Using LC–MS-based untargeted metabolomics, we evaluated the effect of chronic consumption of a calafate fruit extract on the metabolome of mice exposed to a high-fat diet. Additionally, we quantified the main inflammatory proteins and molecules associated to cardiovascular diseases, such as IL-6, insulin, leptin, MCP-1, total PAI-1, resistin, TNF-α, E-selectin, ICAM-1, PECAM-1, P-selectin, proMMP-9, thrombomodulin and adiponectin, in plasma. Finally, we developed an integrative biological analysis to obtain a holistic interpretation of the calafate extract effect *in vivo*.

4.2.2. Materials and Methods

4.2.2.1. Reagents and vegetable material

Formic acid (LiChropur®) for LC–MS (98-100%), acetonitrile (hyper grade), methanol (hyper grade), ethanol, and water (HPLC–MS), and ammonium formate for mass spectrometry (>99.0%) were provided by Merck (Darmstadt, Germany). DL-2-aminoadipic acid, stearoyl-L-carnitine, propionyl-L-carnitine, trans-2-hexadecenoyl-L-carnitine, cis, cis-9,12-octadecadienoyl-L-carnitine, deoxycholic acid and succinic acid were obtained from Sigma–Aldrich (Steinheim, Germany).

Vegetable material: calafate berries (Berberis microphylla) were collected near Punta Arenas, Chile (53.1548309, -70.911293).

4.2.2.2. Instrumentation

A Heraeus-Fresco17 centrifuge from Thermo Fisher (Waltham, MA, USA), an analytical balance from Denver Instrument Company (NY, USA), and a refrigerated CentriVap concentrator from LABCONCO (Kansas City, MO, USA) were used for sample preparation.

The untargeted metabolomics was carried out with a UHPLC-DAD Bruker Elute LC system coupled in tandem with a Q-TOF spectrometer Compact, Bruker (Bremen, Germany). The control system used was Compass HyStar (Bruker), and the acquisition software was Bruker to control 4.1.402.322-7977-vc110 6.3.3.11. Data analysis was performed with Compass DataAnalysis 4.4.200 (Bruker) software, Compass QuantAnalysis 4.4 (Bruker Daltonics, Bremen, Germany), MetaboScape 3.0 (Bruker Daltonics, Bremen, Germany), and freely accessible software MetaboAnalyst (https://www.metaboanalyst.ca/).

Cytokine quantification was carried out in a MAGPIX instrument by Luminex XMAP Technology (Life Technologies, Grand Island, NY, USA) using a MILLIPLEX® MAP Mouse Adipokine Magnetic Bead Panel, MILLIPLEX® MAP Mouse Adipokine Magnetic Single Bead and MILLIPLEX® MAP Mouse CVD Magnetic Bead Panel 1. Data analysis and data acquisition were carried out with Luminex xPONENT® version 4.3229.0 (Luminex Corporation, TX, USA). Plate shaking for wash and incubation time was carried out in Thermomixer® C serial number 5382KG639268 (Eppendorf, Hamburg, Germany).

4.2.2.3.1 Calafate extract

The extraction was carried out as previously described by (Ruiz et al., 2013)a, using ethanol/formic acid (97:3) as solvent extraction (raw extract), which was subsequently characterized. Hydroxycinnamic acid (HCA) and flavonol determination required a purification step using solid-phase extraction with cation exchange columns (Oasis MCX Water, USA), as previously described by Ruiz et al. (purified extract)(Ruiz, et al., 2013)[b]. The raw extract was evaporated, posteriorly lyophilized and suspended in ultrapure water for the *in vivo* study in C57BL/67 mice (5 mg dry extract/mL). The calafate extract was characterized by HPLC-DAD-MS (Bustamante et al., 2018). The sugar and ascorbic acid contents of the calafate extract were determined according to Morlock & Vega-Herrera, 2007.

4.2.2.3.2 *In vivo* assay

Ten- to twelve-week-old outbred C57BL/6J mice (n= 24) purchased from the Instituto de Salud Pública (ISP, Santiago, Chile) were housed in a conventional animal facility maintained at 25±1 °C under a 12 h light:12 h dark photoperiod in accordance with the Guidelines for the Care and Use of Laboratory Animals (https://grants.nih.gov/grants/olaw/Guide-for-the-Care-

and-use-of-laboratory-animals.pdf) (Morton & Griffiths, 1985). After the acclimation period, mice were randomized and were fed ad libitum with a D12450H low-fat diet (10% fat; Open Source Diets - Research Diets, Inc, New Brunswick, NJ, EEUU), which is named a normal diet (N), or with a D12451 high-fat isocaloric diet (45% fat; Open Source Diets - Research Diets, Inc, New Brunswick, NJ, EEUU), which was named a high-fat diet (H) (n=12 mice per group). After three months, each group was randomized into another two subgroups (n=6 mice per group) that received either water (N and H groups) or calafate extract in water, freshly prepared every 2 days, as the only source of liquid (called the Ncal and Hcal subgroups). Both calafate extract and water had similar pH values and sugar contents (pH 3 and 1.8 mg/mL of sugar) (Bustamante et al., 2018). Pellet and liquid consumption were quantified daily, and animal weight was assessed weekly. At the end of the study, animals were fasted for 12 h at the beginning of the dark cycle, then were anesthetized with isoflurane and sacrificed through exsanguination at the fourth month after calafate extract supplementation. Blood samples were collected by cardiac puncture in EDTA tubes and centrifuged at 2,500 g x 15 min at 5 °C (Bustamante et al., 2018). Aliquots

of 20 μL plasma were frozen in liquid nitrogen and stored at −80 °C in Eppendorf tubes for metabolomic analysis.

4.2.2.3.3 Biochemical analyses and protein quantification

Cytokine quantification was performed using MAGPIX instruments with different immunological-based panels (MILLIPLEX MAP KIT) (See 2.2) for the following proteins: IL-6, insulin, leptin, MCP-1, total PAI-1, resistin and TNF-α, adiponectin, E-selectin, ICAM-1, PECAM-1, P-selectin, proMMP-9 and thrombomodulin. The assay was conducted following the manufacturer's instructions using the MAGPIX system. Protein concentrations were calculated using the best-fitting parameter logistic on xPONENT® software (Logistic 5P Weighted).

Biochemical analyses in plasma were carried out by colorimetric assay kits for plasma triglycerides (TGs) and total cholesterol (TC) (Valtek Diagnostics, Chile). Alanine aminotransferase (ALT/GPT) and aspartate aminotransferase (AST/GOT) were measured using kinetic kits (Valtek Diagnostics, Chile). Blood glucose was measured using the OneTouch Ultra2 glucometer (Johnson & Johnson Medical). Measurements were performed in duplicate or triplicate according to the availability of samples using control

sera (Valtrol N, Valtrol P; Valtek Diagnostics, Chile). The results are expressed as arithmetic means and standard deviations. Data were subjected to one-way ANOVA to evaluate the statistical significance of intergroup differences with the Levene test of homogeneity of variances and Bonferroni and Dunnett T3 post hoc tests, considering $\alpha < 0.05$. Graphics were generated using the software Microsoft Excel for Microsoft 365 MSO version 2205, and statistical analyses were carried out using the software IBM SPSS version 20.

4.2.2.3.4 Metabolite extraction from plasma samples

Plasma samples were extracted for metabolomic analysis according to the protocol described below. Briefly, 50 µL of plasma was mixed with 1000 µL of methanol (-20 °C). The samples were shaken for 1 min, stored for 5 min at 4 °C, and then vortexed for 5 s. Finally, the extracts were centrifuged at 15,700 × g for 20 min at 4 °C. Then, 800 µL of each extract was transferred to a vial, and methanol was removed by vacuum centrifugal evaporation at 4 °C. Samples were reconstituted in 200 µL of methanol (-20 °C). A quality control sample (QC) was obtained with 30 µL of each plasma sample. It was extracted as described previously and was injected between samples for

robustness and repeatability evaluation of the instrumental system. The entire extraction procedure was performed in glass vials to avoid plastic contamination. Methods showed a different number of samples because some were lost in the extraction procedure.

4.2.2.3.5 UHPLC-DAD-ESI-QTOF-MS/MS metabolomics analysis

Plasma extracts were analyzed by reversed-phase chromatography UHPLC-DAD-ESI-QTOF-MS/MS based on the method previously described by Laursen et al., 2017 (Method 1) and Patterson et al., 2015 (Method 2) for compounds with medium polarity and non-polar, respectively. A Phenomenex column Kinetex® C18 100 x 4.6 mm 2.6 µm (Torrance, CA, USA), oven temperature 50 °C, autosampler temperature 4 °C, and partial loop injection mode were used for both methods. The chromatographic separation conditions were as follows.

Method 1: Mobile phase A was composed of 0.1% formic acid in water, and mobile phase B was composed of 0.1% formic acid in acetonitrile, with a flow rate of 0.5 mL/min and an injection volume of 20 µL. The acetonitrile gradient ranged from 0% for 2 min, from 0% to 5% for 4 min, from 5% to 60% for 0.5 min, from 60% to 88% for 6.5 min, from 88% to 100% for 0.5

min, from 100% for 1 min and from 100 to 0% for 1 min with a stabilization period of 7.5 min.

Method 2: Mobile phase A: 60:40 acetonitrile:water, 0.1% formic acid , and 10 mM ammonium formate; and mobile phase B: 90:10 isopropanol:acetonitrile, 0.1% formic acid, 10 mM ammonium formate, a flow rate of 0.2 mL/min and an injection volume of 20 µL. The mobile phase B gradient ranged from 32 to 43% for 2 min, 43% for 2 min, from 43% to 75% for 6 min, 75% for 2 min, 75% to 100% for 2 min, 100% for 1 min and from 100 to 32% for 1 min with a stabilization period of 5 min.

Method 3: Plasma extract analysis by normal phase chromatography UHPLC-DAD-ESI-QTOF-MS/MS was based on the method described by Armirotti et al., 2014 for polar metabolites. A HILIC BEH Amide 100 x 2.1 mm y de 1.7 µm (Waters, Milford, MA, EEUU), oven temperature 40 °C, autosampler temperature 4 °C, and partial loop injection mode were used. The chromatographic separation conditions were as follows: Mobile phase A was composed of 10 mM ammonium formate in water, and mobile phase B was composed of 95:5 ammonium formate in acetonitrile:water. A flow rate of 0.4 mL/min and an injection volume of 20 µL were used. The gradient

ranged from 100% B for 1 min, from 100% to 70% B for 16 min, 70% B for 1 min, and from 70 to 100% for 1 min with a stabilization period of 5 min.

The MS conditions in all the metabolomic studies were positive ionization ESI +4500 V and negative ionization ESI -3500 V, dry gas: 9 L/min, nebulizer: 4 Bar, T°: 200 °C, end capillary 500 V, collision energy at 10-25 eV in stepping mode, Auto MS/MS mode (2 precursor/cycle), 50-1500 m/z (scan 0.2 s centroid mode) and internal calibration using sodium formate (0.01 M) with a mass accuracy < 3 ppm.

All metabolomic sequences started with 5 blank injections (solvent only), followed by 3 technical blanks (considering extraction process) and 3 QC. Then, every 11 samples, a QC was injected (Alseekh et al., 2021).

4.2.2.3.6 Data Processing and Data Analysis

Bucket Table: UHPLC-ESI-QTOF-MS/MS was processed in MetaboScape 3.0 (T-ReX 3D algorithm) under the parameters shown in Table S1. This software transformed the raw data into a matrix with the features (m/z – retention time (t_R) pairs and normalized peak intensity) (file: .csv). The workflow included mass recalibration, t_R alignment, feature extraction (m/z

– t_R pairs), adduct and neutral loss administration, import of MS/MS spectra, and generation of the bucket table.

Data Prefilter: The matrix was processed in MetaboAnalyst software, and the data were filtered considering RSDs > 20% compared to QC. The purpose of data filtering is to identify and remove variables that are unlikely to be of use when modeling the data. Principal component analysis (PCA) and volcano plot (fold change threshold: 1.5 and p value threshold: 0.05 FDR-adjusted) were used to select characteristic features of each group (comparisons between 2 group were: N-Ncal, H-Hcal, N-H and Ncal-Hcal). Peak area integration was manually curated with Compass QuantAnalysis 4.4 software.

Filter and feature selection: The new bucket table was processed in MetaboAnalyst 5.0, and data filtering and Pareto scaling were performed again. All variables were Pareto scaled to reduce the relative importance of large values and keep the data structure partially intact (Curtasu et al., 2019). ANOVA ($p < 0.05$) was used to select the significant characteristic features of each group (Figure S1).

Metabolite annotation workflow: In DataAnalysis software, the molecular formula with the smallest mass error was selected. The spectra were sent to

databases such as MetFrag (In silico fragmentation for computer-assisted identification of metabolite mass spectra) (https://msbi.ipb-halle.de/MetFrag/), HMDB (The human metabolome database) (https://hmdb.ca/), and METLIN (https://metlin.scripps.edu/landing_page.php?pgcontent=mainPage) by comparing the accurate mass and fragments information obtained from UHPLC-QTOF/MS (Laursen et al., 2017). Furthermore, the theoretical isotopic pattern was compared with the experimental isotopic pattern. Finally, identity confirmation of the most important metabolites was carried out by standard comparison (retention time (t_R) and/or fragmentation spectrum). Metabolite annotation was based on the guide for annotation, quantification and best reporting practices proposed by Alseekh et al., 2021. Tolerance to the m/z value was set to 10 ppm.

Heatmap analysis was carried out by Euclidean distance between samples to observe the group separation due to the differences in the metabolites identified in calafate consumption.

4.2.3. Results and Discussion

The effect of chronic consumption of calafate fruit extract on the plasma metabolome and its possible relationship with cardiovascular protection was evaluated by a metabolomic study of 24 plasma samples obtained from 4 groups of mice fed normal-fat and high-fat diets supplemented or not with calafate extract for 4 months (N, H, Ncal, Hcal) (see 4.2.2.3.2). The dose studied is equivalent to the intake of 210 g of fruit, which is within the recommended consumption of fruits and vegetables for the prevention of chronic diseases by the WHO.

4.2.3.1 Calafate berry extract composition

The calafate extract contained anthocyanins (225 ± 3 µmol/g dry weight), flavonols (12.0 ± 0.5 µmol/g dry weight) and HCA (28.4 ± 0.9 µmol/g dry weight). Major anthocyanins were delphinidin-3-glucoside (35%), petunidin-3-glucoside (19%) and malvidin-3-glucoside (13%). Major flavonols and HCA identified were quercetin-3-rutinoside (36%) and quercetin-3-rhamnoside (27%), caffeoylquinic acid (25%) and 3 or 4-trans-caffeoyl-glucaric acid (15%). The sugar, glucose and fructose contents in the extract were 64.3% w/w.

4.2.3.2 Animal characteristics

According to the Guidelines for the Care and Use of Laboratory Animals (https://grants.nih.gov/grants/olaw/Guide-for-the-Care-and-use-of-laboratory-animals.pdf) (Morton & Griffiths, 1985), mice showed no signs of stress. The average food and water intake per day in each group was 29.7 ± 6.8 g and 57.3 ± 7.7 mL, respectively. A significant increase in weight was observed for the group fed a high-fat diet H and Hcal (5.8%) ($p < 0.05$) (Table S2) compared to initial weight. The average daily intake of calafate extract per group was 299.10 ± 51.94 mg of dry extract. The Hcal and Ncal groups did not show changes in body weight due to the consumption of calafate (Table S2).

4.2.3.3 Biochemical analysis

4.2.3.3.1 Clinical Biochemistry

Biochemical analysis of plasma showed that total cholesterol (TC) was higher by 51% in the H groups than in the N groups ($p < 0.05$), which is similar to the results reported by Miao et al., 2016 and Guzmán & Sánchez, 2021 for high-fat diet rats. No changes in TC were observed after chronic calafate intake; however, this cannot exclude modifications in lipoprotein

composition. Guzmán & Sánchez, 2021 reported an increase in the concentration of HDL and a decrease in the atherogenic index (−81%) and coronary risk index (−62%) posterior to calafate intake in a high-fat diet mouse model (Guzmán & Sánchez, 2021). On the other hand, our results do not show significant differences for triglycerides, glycemia, and transaminase enzymes (GOT, GPT) ($p > 0.05$) (Table S2).

4.2.3.3.2 Inflammation and cardiovascular risk markers

Concerning the plasma concentration of biomarkers associated with inflammation and cardiovascular disease, we observed significant changes, which are presented in Figure 4.2.1. The Ncal group showed a lower thrombomodulin concentration in plasma than the N group ($p<0.05$), an effect that was not observed in the high-fat diet group. Thrombomodulin is a biomarker of vascular endothelial damage, whose increase has been associated with metabolic syndrome and CVD in children with risk factors for CVD (Kikuchi et al., 2021). Thrombomodulin plasma levels increase by approximately 43% in different groups of patients with atheromatous arterial disease (ischemic heart disease and polyvascular lesions) (Seigneur et al., 1993). On the other hand, we observed an increase in adiponectin

concentration in the Hcal ($p<0.05$) and Ncal groups. Adiponectin is an endocrine factor mainly synthesized and released from adipose tissue that is signaled through specific receptors in the skeletal muscle, vascular endothelium, liver, and myocardium. Studies have reported that adiponectin has insulin-sensitizing, vasodilator, antiatherogenic, and anti-inflammatory properties (Shabalala et al., 2020). Okamoto et al., 2008 found that adiponectin knockout mice developed 61% larger atherosclerotic lesions and accumulated 63% more CD4 T lymphocytes than control mice (Okamoto et al., 2008). According to Masumi et al., 2011 adiponectin reduction in plasma markedly increases CHD risk in men and shows that the hazard ratio does not change after adjusting for BMI (Masumi Ai et al., 2011).

IL-6, insulin, leptin, MCP-1, total PAI-1, resistin, TNF-α, sE-selectin, sICAM-1, PECAM-1, P-selectin and proMMP-9 did not show significant changes associated with calafate intake (Figure S2 and S3); however, sE-selectin, sICAM-1 and proMMP-9 showed tendency to decreased in Hcal compared with those of the H group (Figure 4.2.1). Additionally, leptin decreased in the Ncal group compared to the N group, and this change was not observed in the H group (Figure 4.2.1). Adhesion molecule cell surface glycoproteins are expressed in endothelial cells and epithelial cells and have

a role in epithelial injury-resolution responses, innate and adaptive immune responses in inflammation, and tumorigenesis. Shai et al., 2006 showed that the soluble forms of adhesion molecules, such as sICAM-1 and sVCAM-1, are increased in plasma during endothelial injury and are useful as predictors of CHD (Shai et al., 2006).

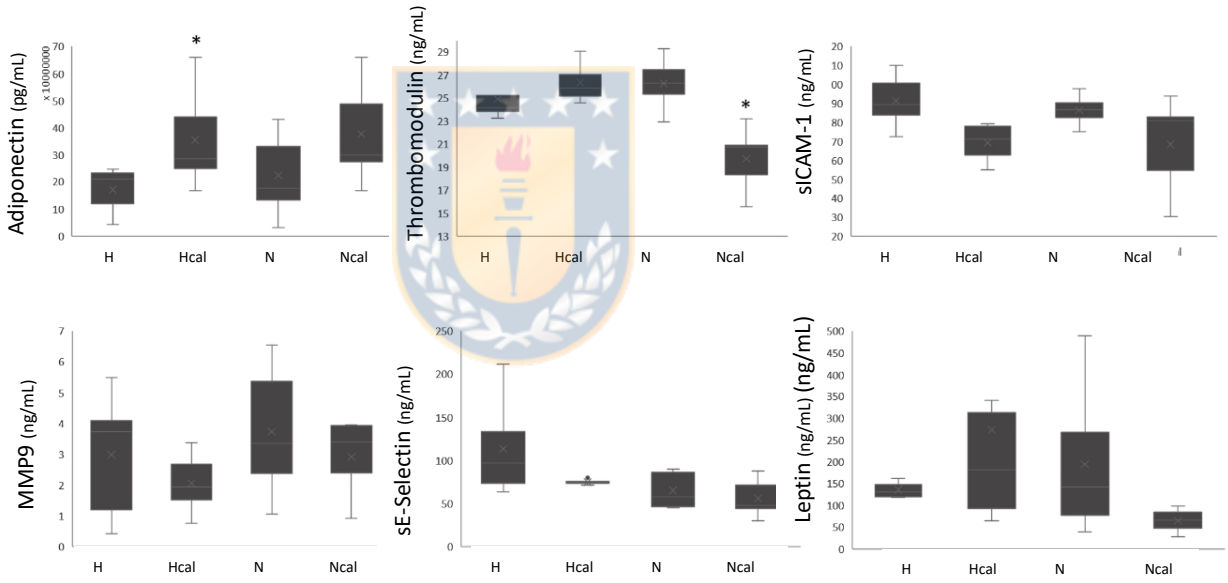

Figure 4.2.1: Box-plot proteins markers in endothelial dysfunction and adipokines related with metabolic risk factors. Data expressed as concentration in plasma samples (ng/mL or pg/mL) in different groups (mean X, median line and interquartile range in box-plot, * $p < 0.05$ H-Hcal N-Ncal)

High plasma levels of sICAM-1 and sVCAM-1 correlate with a 2.5-fold increase in CVD risk, and the sE-selectin concentration is increased in stroke (Pawelczyk et al., 2018). In addition, these proteins were directly associated with body mass index (BMI), inflammatory biomarkers (IL-6, PCR, sTNF), and triglycerides and were inversely associated with high-density lipoprotein levels (HDL) ($p < 0.05$) (Shai et al., 2006). MMP-9 is a proteolytic enzyme (gelatinase) involved in the degradation of extracellular matrix, is secreted by various cells, including macrophages and endothelial cells, and contributes to atherosclerotic plaque susceptibility and rupture, leading to cardiovascular events such as myocardial infarction (Olejarz et al., 2020). Boumiza et al., 2021 reported an inverse correlation between plasma levels of MMP-9 and the MMP-9/TIMP-1 ratio with the endothelium-dependent response, which was associated with endothelial dysfunction in obese patients or with metabolic syndrome (Boumiza et al., 2021). Altogether, these results suggest that calafate extract intake would have beneficial effects on endothelial function and cardiovascular protection.

Finally, leptin is an adipokine produced by white adipose tissue, and its disruption marks a milestone in the development of metabolic diseases, such as obesity, type 2 diabetes, and hypertension (Kim et al., 2020). Agostinis-

Sobrinho et al., 2017 showed a positive correlation between leptin and the leptin/adiponectin ratio and all metabolic risk factors (MRFs), such as triglycerides, HOMA-IR, and blood pressure. In addition, ROC curve analyses showed that adiponectin, leptin, and the L/A ratio were predictive biomarkers of MRFs (Agostinis-Sobrinho et al., 2017). According to our results and based on these antecedents, regulation of these biomarkers produced by calafate extract consumption could reduce the risk factors for CVD in mice.

4.2.3.4 Metabolomics

Typical base peak chromatograms of the plasma extract obtained with the different chromatographic methods are illustrated in Figures S4 and S5. After applying the described workflow (Section 4.2.2.3.6), the bucket table presented 39227, 5464 and 15778 features for methods 1, 2 and 3, respectively, in negative mode and 11028, 19929 and 11070 in positive mode. After QC feature filtration, a total of 32181 and 7652 features were deleted for negative and positive methods 1, 4030 and 16657 for method 2, and 11012 and 7844 for method 3. This supports the quality of the metabolomics data.

First, PCA examined spontaneous clustering patterns in the datasets, and as seen in Figures S6 and S7, the QCs were clustered in the center of the models. PCA models obtained with method 1 in negative ionization mode explained a total variance of 65.6% between principal component PC 1 and PC 2. In method 2, these components explained 80%, and method 3 explained 79.2%. In positive ionization, PCA showed values of 71.3% and 74.6% for methods 2 and 3, respectively. Method 1 was excluded because no significant features were obtained in the following analyses.

The cluster distribution of plasma samples denoted a separation between the N and H groups (Figure S8). Moreover, the PCA score plot of N-Ncal and H-Hcal (Figure 4.2.2) showed clustering of the samples due to calafate consumption. Relevant features were preselected by loadings plot and volcano plot analysis, and lately significant features were selected by ANOVA ($p < 0.05$). The significant features in the negative mode were 17, 11, and 37 for methods 1, 2, and 3, respectively, and in positive mode 7 and 44 for methods 2 and 3 (supplementary material).

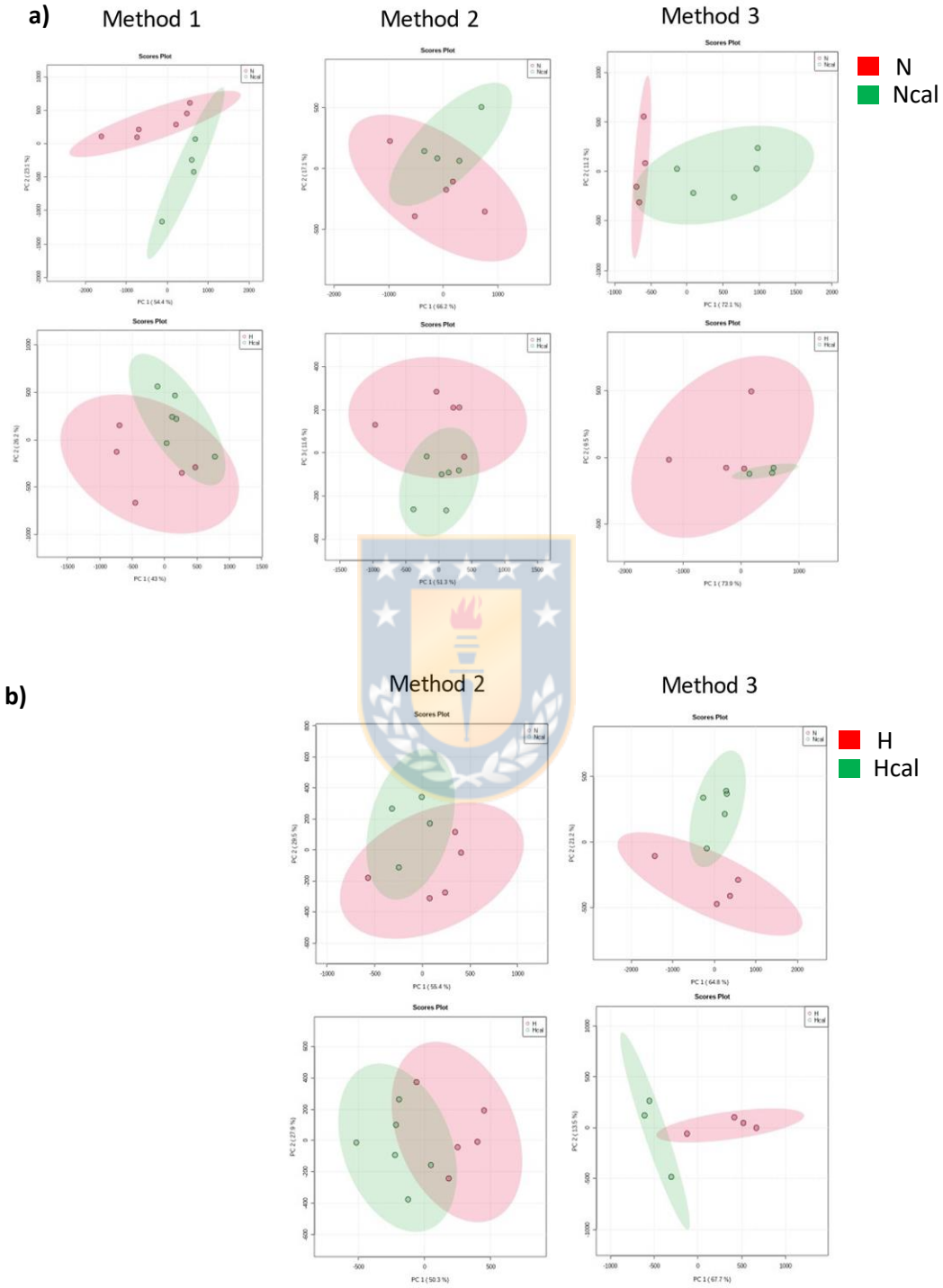
a)
Method 1
Method 2
Method 3
N
Ncal
b)
Method 2
Method 3
H
Hcal

Figure 4.2.2: Principal component analysis (PCA). a) Score plot in negative mode and b) Score plot in positive mode for method 1, method 2 and method 3. N and H in red, and Ncal and Hcal in green for each ionization mode.

4.2.3.4.1 Metabolite annotation and observational changes

Metabolite annotation was carried out using the HMDB, METFRAG, METLIN, and PubChem databases and/or by comparison with the standards. The time retention, pseudomolecular ion, and fragments of significantly annotated plasma metabolites, related to cardiovascular disease, are presented in Table 4.2.1.

Tabla 4.2.1: Significant metabolites identified by UHPLC-DAD-QTOF which are related with CVD (positive and negative ionization modes).

Feature N°	Ion	molecular ion formula	m/z	fragments with intensity	error ppm	identification	Identification level (A-D)[1]	International identifier[2]	Method[3]
1	[M-H]-	$[C_{24}H_{39}O_4]$-	391.2849	391.2872; 345.2823 $C_{23}H_{37}O_2$; 392.2978	-1.9	deoxycholic acid	A	METLIN 265 HMDB00626	1
2	[M-H]-	$[C_6H_{10}NO_4]$-	160.0612	116.0709 $C_5NO_2H_{10}$; 142.0510 $C_6H_8NO_3$	3.5	DL- 2-aminoadipic acid	A	METLIN 324 HMDB00510	3
3	[M-H]-	$[C_4H_5O_4]$-	117.0192		-2.4	succinic acid	A t_R	METLIN 114	2 3
4	[M + FA-H]-	$[C_{25}H_{49}NO_9P]$-	538.3140	253.2184 palmitoleic acid $C_{16}H_{29}O_2$;	-2.5	LysoPC(16:1/0:0)	B	HMDB0010383	1, 2 and 3

				478.2965 $C_{23}H_{45}NO_7P$; 479.3015; 254.2202; 224.0688 $C_7H_{15}NO_5P$; 538.3203; 152.9954 $C_6H_4NO_2$; 242.0767 $C_7H_{17}NO_6P$; 168.0431 $C_4H_{11}NO_4P$; 255.2270 palmitic acid $C_{16}H_{31}O_2$; 480.3119; 134.9973 82 C_7H_4OP				METLIN 40288	
5	[M+FA-H]-	[$C_{29}H_{49}NO_9P$]-	586.3142	526.2964 $C_{27}H_{45}NO_7P$; 527.2954; 301.2199; 224.0732; 586.3142; 587.3137; 303.2374 $C_{16}H_{34}NO_2P$; 302.2256; 152.9942; 528.2938; 301.2686 Eicosapentaenoic acid $C_{20}H_{29}O_2$; 529.3097; 168.0459; 228.2245; 257.2409 $C_{16}H_{34}P$; 242.0797 $C_7H_{17}NO_6P$; 257.0238 $C_{13}H_8NO_3P$	-0.9	LysoPC (20: 5 / 0: 0)	B	HMDB10397	1
6	[M-H]-	[$C_{21}H_{41}NO_7P$]-	450.2619	253.2162 palmitoleic acid $C_{16}H_{29}O_2$; 450.2641; 254.2229; 451.2742; 196.0359 $C_5H_{11}NO_5P$; 121.9994 $C_2H_5NO_3P$; 197.0393; 140.0115 $C_2H_7NO_4P$; 262.9691; 451.3470	4.2	LysoPE (16: 1 / 0: 0) LysoPE (0: 0/16: 1)	B	HMDB0011504 HMDB0011474	1
7	[M-H]-	[$C_{25}H_{43}NO_7P$]-	500.2775		-2.9	LysoPE(20:4)	D	METLIN 62302, 62275 or 62276	3
8	[M+H]+	[$C_{23}H_{43}NO_4$]+	398.3251	85.0260 182 $C_5H_4O_2$; 125.0717; 144.1003 $C_7H_{14}NO_2$	-1.9	trans-2-hexadecenoyl-L-carnitine	A	METLIN 58388 HMDB06317	2
9	[M+H]+	[$C_{25}H_{50}NO_4$]+	428.3702		9.1	stereoyl-L-carnitine	A (t_R)	METLIN 5811	2
10	[M+H]+	[$C_{26}H_{47}NO_7P$]+	516.3046	184.0733 $C_5H_{15}NO_4P$; 124.9998; 98.9853; 104.1061; 457.2327; 458.2310; 86.0967;	7	LysoPC (18:4)	B (family Standard D)	HMDB10389 METLIN 61699 (Park et al., 2015)	2

				185.0763 $C_5H_{12}N$; 146.9791; 311.2591					
11	[M+H]+	$[C_{25}H_{46}NO_4]+$	424.3407	97.1010	2.1	cys,cys-9,12-octadecadienoyl-L-carnitine linoleoyl-L-carnitine	A	METLIN 58412-58418	2 and 3
12	[M+H]+	$[C_{24}H_{37}O_2]+$	357.2767		-3.7	tetracosahexaenoic acid	D	METLIN 6430	2
13	[M+H]+	$[C_{10}H_{20}NO_4]+$	218.1388		3.8	propionyl-L-carnitine	A (tR)	METLIN 965	2 and 3
14	[M + H]+	$[C_6H_{12}NO_4]+$	162.0758	98.0587 C_5H_8NO	1.7	aminoadipic acid	B	HMDB00510 METLIN 324	3

[1]Identification level based in (Alseekh et al., 2021).[2]Data base used for identification. [3]Method of analysis

An increase in deoxycholic acid (N°1: [M-H]- 391.2849 m/z) was found in Group H, and this effect was reduced by calafate intake (Hcal), reaching a similar level found in the normal diet groups ($p < 0.05$) (Figure 4.2.3). This metabolite was detected by two chromatographic methods (1 and 2) in negative mode. Deoxycholic acid is a secondary bile acid generated by the 7α-dehydroxylation of cholic acid in gut microbiota (Yoshimoto et al., 2013). Shimizu et al., 2014 demonstrated that this metabolite (5 µM) incubated for 48 h with vascular smooth muscle cells (VSMCs) promoted cellular migration and proliferation, related to endothelial dysfunction, vascular

inflammation and atherosclerosis development (Shimizu et al., 2014). Additionally, Haeusler et al., 2013 reported that plasma 12α-hydroxylated biliary acids are increased in association with insulin resistance, a risk factor for CVD (Haeusler et al., 2013).

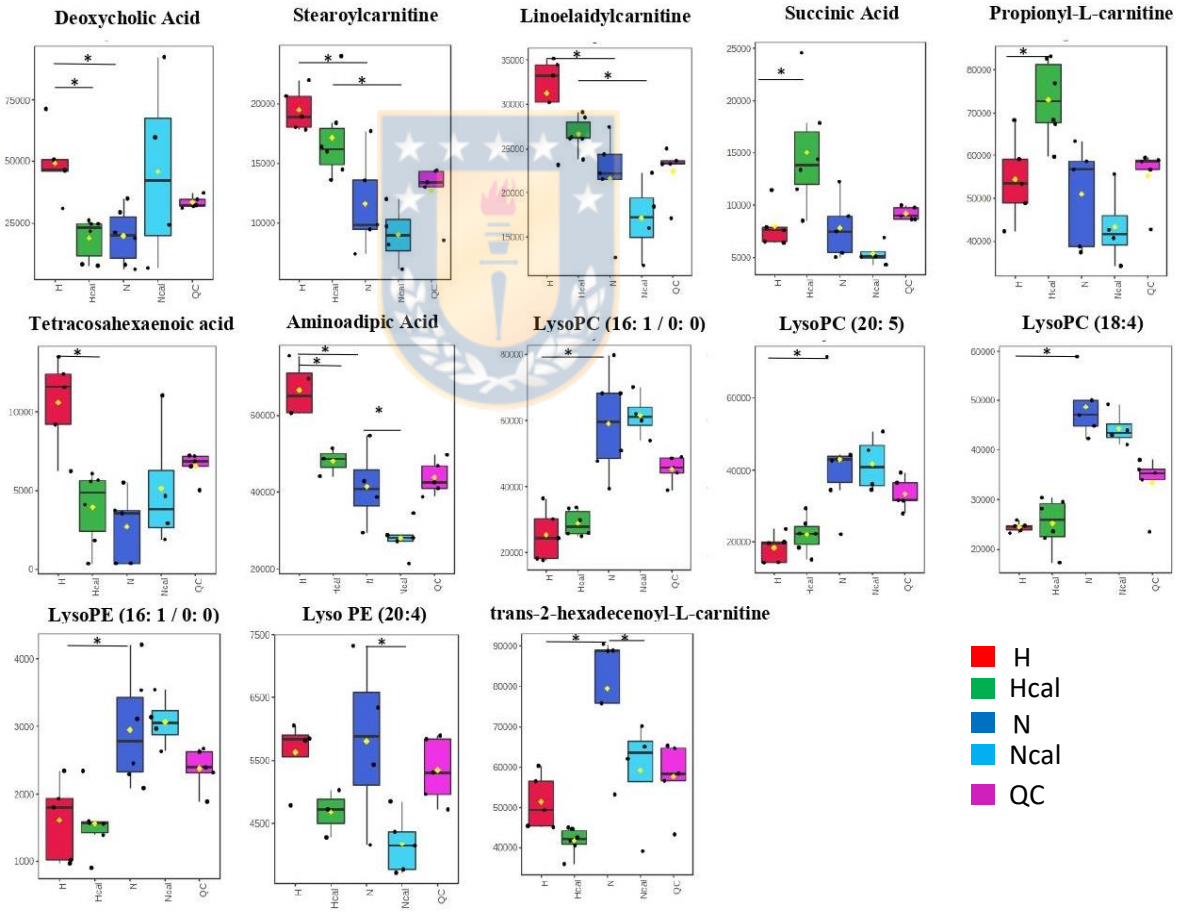

Figure 4.2.3: Box plot features significative ($p<0.05$) identified. H in red, Hcal in green, N in blue, Ncal in light blue and QC in pink.

A metabolomic study in the plasma of humans (60 control and 40 diabetic volunteers) showed deoxycholate or cholanoic acid in 68% of diabetic patients and 45% of control volunteers (Suhre et al., 2010). Finally, the increase in deoxycholic acid in the serum of high-fat diet-fed mice analyzed by liquid chromatography–mass spectrometry has been previously reported (Yoshimoto et al., 2013), which is concordant with our findings.

DL-2-Aminoadipic acid (2AAA) (N°2: [M-H]- 160.0612 m/z and N°14: [M+H]+ 162.0758 m/z) was also identified in a negative and positive mode in the HILIC method. 2-AAA was increased in the H group compared to the N group, and calafate extract intake reduced its concentration in the H group and N group ($p < 0.05$) (Figure 4.2.3). 2-AAA is an oxidized derivative from the amino acid lysine. This metabolite has been strongly associated with diabetes development in the Framingham Heart Study (risk factor for CVD), where individuals with high plasmatic 2-AAA showed a 4-fold higher probability of developing diabetes after a 12-year follow-up period than those with the lowest concentration (Wang et al., 2013). In addition, Estaras et al., 2020 demonstrated that the incubation of pancreatic acinar cells with 2-AAA induced oxidative stress and lipid peroxidation, both processes related to diabetes and CVD (Estaras et al., 2020). Finally, this metabolite has also been

related to obesity, where 2-AAA levels are higher in the obese group than in the normal-weight group (Lee et al., 2019). Plasma 2-AAA was positively associated with adiposity indices (fat mass, fat percent, waist circumference, BMI, and BMI z score; all $p \leq 0.0336$) (Lee et al., 2019). In the same study, researchers reported that 2-AAA levels increased in the adipose tissue of mice fed a high-fat diet compared with mice fed a standard diet, which is concordant with our results

Stereoyl-L-carnitine (N°9: [M+H]+ 428.3702 m/z) and linoleoyl-L-carnitine (N°11: [M+H]+ 424.3407 m/z) were identified in positive mode. A tendency to decrease was observed from the H to the Ncal group (Figure 4.2.3). Significant differences were found between the N-H group and the Ncal-Hcal group ($p < 0.05$). Similar results have been reported by Mihalik et al., 2010, who described an increase in acylcarnitines in the plasma of obese volunteers and participants with type 2 diabetes mellitus, suggesting a defect in the use of succinyl-CoA in the tricarboxylic acid cycle and an increase in incomplete β-oxidation in skeletal muscle (Mihalik et al., 2010). On the other hand, a metabolomic study of Langerhans islets (LH) in mice and humans with type 2 diabetes mellitus described acylcarnitine accumulation in LH, which could result from excessive β-oxidation in the presence of abundant fatty acids

(Aichler et al., 2017), which is consistent with our results. This study also noted specific stearoylcarnitine and linoleoylcarnitine accumulation and impaired the tricarboxylic acid (TCA) cycle in mitochondrial energy metabolism due to a decrease in succinate and ATP (Aichler et al., 2017). Our results showed that calafate extract intake diminished the increased stereoyl-L-carnitine and linoleoyl-L-carnitine observed in the H and N groups (Figure 4.2.3); these results, together with the increased succinate (N°3 117.0192 m/z) and propionyl-L-carnitine (N°13: [M+H]+ 218.1388 m/z) concentrations in the H group (H-Hcal $p < 0.05$) (Figure 4.2.3), suggest a beneficial effect on oxidative phosphorylation and the TCA cycle. These results did not cause an increase in oxidative stress, since we observed a decrease of 17 % in hydroxyl radical in Hcal plasma compared with H ($p < 0.05$), determined by electron paramagnetic resonance (EPR) spectroscopy (data not shown) (Tarifeño-Saldivia et al., 2018). Propionyl-L-carnitine has high affinity for carnitine acyltransferase, producing propionyl-coenzyme A and L-carnitine, essential cofactors in the transport of long-chain fatty acids from the cytosol to the mitochondria (Ferrari et al., 2004). On the other hand, treatment with propionyl-L-carnitine decreased lipid peroxidation (malondialdehyde formation) in SHRs (hypertensive mice) by 40% in the

liver and 34% in the heart (Gómez-Amores et al., 2005). The same tendency to decrease from H to Ncal was not found for trans-2-hexadecenoyl-L-carnitine (N° 8: [M+H]+ 398.3251 m/z), although it is from the same family of compounds.

Considering the abnormal metabolism of fatty acids found in the H group, we also found a significant increase in tetracosahexaenoic acid in the H group (N° 12: [M+H]+ 357.2767 m/z) ($p < 0.05$), similar to the report of Miao et al., 2016 (Figure 4.2.3). The group that received the calafate extract (Hcal) showed a reduction in this metabolite, supporting the improvement of β-oxidation.

These findings suggest that the intake of calafate favors β-oxidation and may have an FFA-lowering effect in prolonged consumption. Moreover, calafate intake reduced metabolites associated with inflammation and CVD, which supports its beneficial effects on cardiovascular health. These results can also be observed in the heatmap analysis (Figure 4.2.4), where the H group is totally separated from Hcal, N and Ncal, highlighting a tendency of the Hcal group to be closer to the N group. These metabolites are associated with a high-fat diet and are modified by calafate consumption.

Additionally, it is worth noting that metabolites with no significant differences between paired group comparisons (H-Hcal and N-Ncal) showed differences between the normal and high-fat diets (Figure 4.2.3). These metabolites were Lyso PC (16:1/0:0) (N°4: [M+FA-H]- 538.3140 m/z) and Lyso PC (20:5) (N°5: [M+FA-H]- 586.3142 m/z), which were tentatively identified in negative mode, and Lyso PC (18:4) (N°10: [M+H]+ 516.3046), which was detected in positive mode. Ganna et al., 2014 associated Lyso PC (18:2) and (18:1) with high HDL-C and total cholesterol levels and with low BMI and subclinical CVD markers. They also found a strong negative association between LysoPC and coronary heart disease (Ganna et al., 2014). Additionally, an atherogenic diet decreased Paraoxonase-1 ARNm and activity, an enzyme responsible for producing LysoPC from phosphatidylcholine (PC), which is capable of limiting the synthesis of cholesterol in macrophages with antiatherogenic effects (Rozenberg et al., 2003).

In addition, we identified Lyso PE (16:1) (N°6: [M-H]- 450.2619 m/z) and Lyso PE (20:4) (N°7: [M-H]- 500.2775 m/z) (Figure 4.2.3). The first was higher in the N and Ncal groups than in the H and Hcal groups ($p < 0.05$). However, LysoPE (20:4) showed significant differences between the N and

Ncal groups ($p < 0.05$) and between the H and Hcal groups ($p < 0.1$). Lyso PEs containing unsaturated fatty acids, which have been related to coronary artery disease (CAD), and have higher levels in patients with CAD than in control subjects (Park et al., 2015). In this context, these differences are associated with the high-fat diet model.

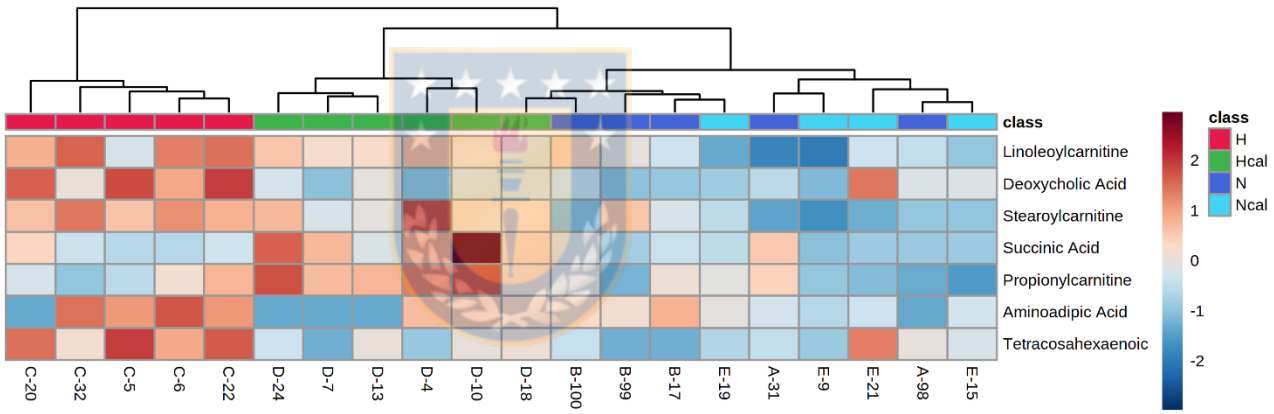

Figure 4.2.4: Heatmap of significant metabolites

Altogether, these results demonstrate that high-fat fed-mice display metabolomic changes that suggest an impairment of β-oxidation and mitochondrial energy related to cardiovascular disease development. Calafate consumption can modify this profile, reducing the impact of a high-fat diet on metabolism.

4.2.3.5 Biological interpretation

Phenol compounds are the main compounds in calafate berries and have been reported to have effects such as ROS scavenging, induction of enzymes that scavenge ROS and synthesize endogenous antioxidants, metal chelation, inhibition of ROS-producing enzymes such as NADPH oxidase, effects on the electron transport chain, among others (Sandoval-Acuña et al., 2014). Anthocyanins (the main polyphenols in calafate) can trap free radicals, reducing oxidative stress. Delphinidin is able to protect SOD activity in HUVECs and attenuate ox-LDL-induced generation of ROS, p38MAPK protein expression, NF-kB activity and protein expression, IκB-α degradation and expression of adhesion molecules (P-selectin and ICAM-1) in endothelial cells (Chen et al., 2011). Flavonols such as quercetin decrease the levels of MMP-9 and NF-kB in mice fed 0.2% quercetin-fortified rodent chow (Ballmann et al., 2017) and significantly increase the oxygen consumption rate and energy metabolism (glycolysis and mitochondrial respiration) in AML12 hepatocytes, suggesting enhanced fatty acid β-oxidation. It has also been demonstrated that quercetin affects the expression levels of lipid metabolism-related genes (PPAR-α and PPAR-γ) (Fukaya et al., 2021). Finally, chlorogenic acid (the main hydroxycinnamic acid from

calafate) and berberine (alkaloid in calafate) have been reported to increase adiponectin levels in visceral adipose tissue and serum, respectively (Shabalala et al., 2020). Adiponectin drastically increases the expression and activity of PPAR-α, promoting fatty acid oxidation and tricarboxylic cycle activation in the liver. Adiponectin inhibits NF-kB activation that mediates vascular cell adhesion molecule-1 expression in endothelial cells (Shabalala et al., 2020). These findings did not consider the antagonistic and synergistic effects that could be present in calafate, so studies with the complete composition of fruit are necessary.

Previously, our research group reported that calafate extract reduced oxidative stress by reducing intracellular ROS production (51%) and completely inhibiting LDL oxidation, which is attributed to its complex composition of bioactive compounds (Olivares-Caro et al., 2020). Calfío and Huidobro-Toro, 2019 described a vasodilator effect of calafate berry extract through nitric oxide production, one of the most important endothelium-derived vasodilator molecules (Calfío & Huidobro-Toro, 2019). Reyes-Farias et al., 2016 demonstrated that calafate berry extract increased the ratio of reduced/oxidized glutathione (GSH/GSSG), which led to decreased oxidative stress in murine adipocytes treated with macrophage-conditioned

medium (Reyes-Farias et al., 2016). Finally, in this work, we demonstrated that calafate extract decreases endothelial dysfunction and inflammatory markers, acylcarnitines and metabolites associated with cardiovascular disease. Additionally, we showed an increase in succinic acid, that is related to TCA activation, and the adiponectin hormone, which has been shown to have pleiotropic effects.

In accordance with the results described previously, we propose in Figure 4.2.5 that calafate could have an effect on three main organs: adipose tissue, liver, and vascular endothelium. calafate fruit decreases oxidative stress and can activate transcription factors, such as NF-kB and PPAR-α, decreasing vascular adhesion molecules and activating fatty acid oxidation and the TCA cycle in the liver. On the other hand, this fruit could stimulate an increase in adiponectin levels in adipose tissue. Transcriptional studies in *in vivo* models should be carried out to corroborate this new hypothesis.

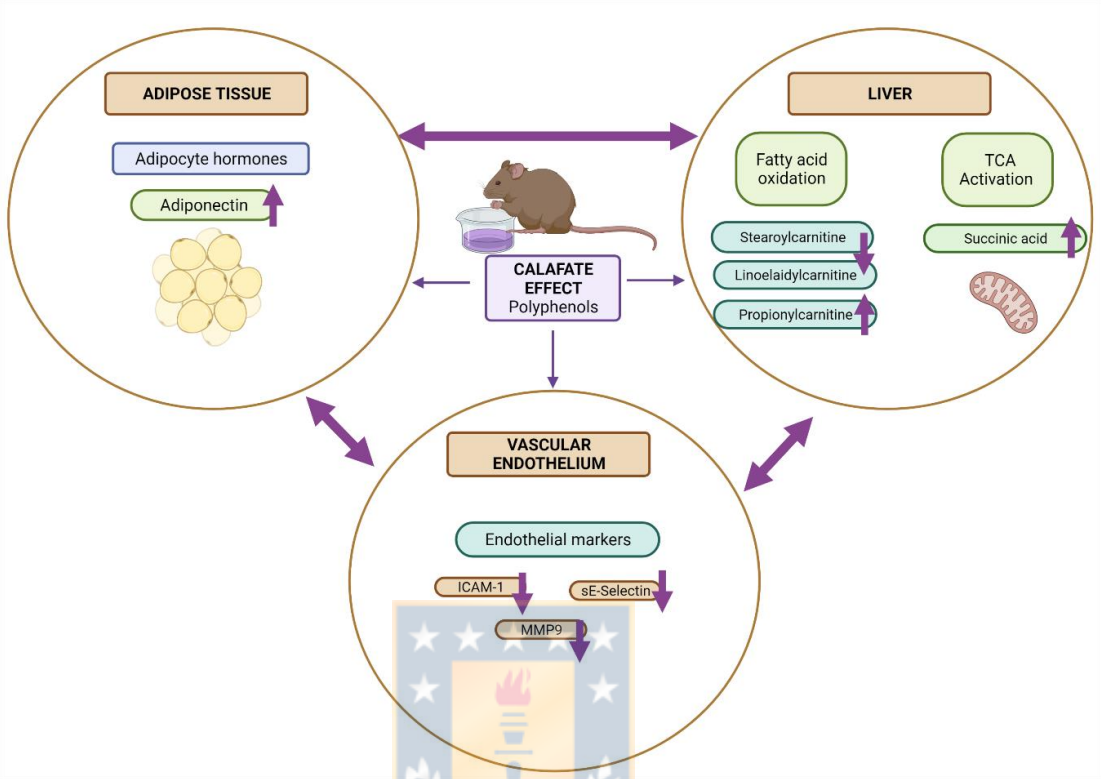

Figure 4.2.5: Proposal of the systemic effect caused by *Berberis microphylla* (calafate) berries.

4.2.4. Conclusion

The current study presents for the first time the beneficial impact of *ad libitum* feeding of calafate berry extract on the plasma proteins and metabolome in mice exposed to a high-fat diet. Calafate intake produced a change in plasma proteins and the metabolome of mice fed a HFD, both related to a reduced risk of CVD associated with the HFD. A reduction in

thrombomodulin, sE-selectin, sICAM-1 and proMMP-9, which are associated with endothelial dysfunction and inflammation as bases of atherosclerosis, was observed. Additionally, a reduction in leptin and an increase in adiponectin were found, both positively associated with a functional adipose tissue and the reduction in CDV risk. Significant changes in the metabolome could explain the role of calafate in the β-oxidation of fatty acids. These changes include an increase in succinic acid levels, activating tricarboxylic acid and reducing carnitine accumulation. Additionally, other metabolites associated with endothelial dysfunction, oxidative stress and lipid peroxidation, such as deoxycholic and aminoadipic acid, were also detected. All these findings can explain an effective role of calafate consumption in reducing the risk of cardiovascular disease caused by a high-fat diet.

4.2.5. Acknowledgment

This work was supported by ANID Chile: Beca Doctorado Nacional [21170812]; FONDECYT [1191276]; and FONDEQUIP [170023], CENTROS BASALES ACE210012. The graphical abstract and figure 4.2.5 were created with BioRender.com. We thank Mr. César Busolich from

Secretos de la Patagonia, Punta Arenas, Chile, who provided calafate samples.

4.2.6. Conflict of interest

The authors declare they have no conflicts of interest.

4.2.7. CRediT author statement

Lia OLIVARES-CARO: Validation, Methodology, Formal analysis, Investigation, Data Curation, Writing - Original Draft, Funding acquisition. Daniela NOVA: Validation, Investigation, Data Curation. Claudia RADOJKOVIC: Writing - Review & Editing, Visualization. Daniel DURAN: Methodology, Investigation, Supervision. Daniela MENNICKENT: Investigation, Data Curation. Luis BUSTAMANTE: Writing - Review & Editing, Visualization, Data Curation. Victoria MELIN: Methodology. David CONTRERAS: Methodology. Andy PEREZ: Methodology. Claudia MARDONES: Conceptualization, Data Curation, Resources, Writing - Original Draft, Writing - Review & Editing, Supervision, Project administration, Funding acquisition.

4.2.8. References

Agostinis-Sobrinho, C. A., Lacerda Mendes, E., Moreira, C., Abreu, S., Lopes, L., Oliveira-Santos, J., Skurvydas, A., Mota, J., & Santos, R. (2017). Association between Leptin, Adiponectin, and Leptin/Adiponectin Ratio with Clustered Metabolic Risk Factors in Portuguese Adolescents: The LabMed Physical Activity Study. Annals of Nutrition and Metabolism, 70(4), 321–328. https://doi.org/10.1159/000477328

Aichler, M., Borgmann, D., Krumsiek, J., Buck, A., MacDonald, P. E., Fox, J. E. M., Lyon, J., Light, P. E., Keipert, S., Jastroch, M., Feuchtinger, A., Mueller, N. S., Sun, N., Palmer, A., Alexandrov, T., Hrabe de Angelis, M., Neschen, S., Tschöp, M. H., & Walch, A. (2017). N-acyl Taurines and Acylcarnitines Cause an Imbalance in Insulin Synthesis and Secretion Provoking β Cell Dysfunction in Type 2 Diabetes. Cell Metabolism, 25(6), 1334-1347.e4. https://doi.org/10.1016/j.cmet.2017.04.012

Alseekh, S., Aharoni, A., Brotman, Y., Contrepois, K., D'Auria, J., Ewald, J., C. Ewald, J., Fraser, P. D., Giavalisco, P., Hall, R. D., Heinemann, M., Link, H., Luo, J., Neumann, S., Nielsen, J., Perez de Souza, L., Saito, K., Sauer, U., Schroeder, F. C., Schuster, S., Siuzdak, G., Skirycz, A., Sumner, L.W., Snyder, M. P., Tang, H., Tohge, T., Wang, Y., Wen, W., Wu, S., Xu, G., Zamboni, N., & Fernie, A. R. (2021). Mass spectrometry-based metabolomics: a guide for annotation, quantification and best reporting practices. Nature Methods, 18(7), 747–756. https://doi.org/10.1038/s41592-021-01197-1

Armirotti, A., Basit, A., Realini, N., Caltagirone, C., Bossù, P., Spalletta, G., & Piomelli, D. (2014). Sample preparation and orthogonal chromatography for broad polarity range plasma metabolomics: Application to human subjects with neurodegenerative dementia. Analytical Biochemistry, 455(1), 48–54. https://doi.org/10.1016/j.ab.2014.03.019

Ballmann, C., Denney, T. S., Beyers, R. J., Quindry, T., Romero, M., Amin, R., Selsby, J. T., & Quindry, J. C. (2017). Lifelong quercetin enrichment and cardioprotection in Mdx/Utrn+/-mice. American Journal of Physiology -

Heart and Circulatory Physiology, 312(1), H128–H140. https://doi.org/10.1152/ajpheart.00552.2016

Bartekova, M., Radosinska, J., Jelemensky, M., & Dhalla, N. S. (2018). Role of cytokines and inflammation in heart function during health and disease. Heart Failure Reviews, 23(5), 733–758. https://doi.org/10.1007/s10741-018-9716-x

Biobaku, F., Ghanim, H., Batra, M., & Dandona, P. (2019). Macronutrient-Mediated Inflammation and Oxidative Stress: Relevance to Insulin Resistance, Obesity, and Atherogenesis. Journal of Clinical Endocrinology and Metabolism, 104(12), 6118–6128. https://doi.org/10.1210/jc.2018-01833

Boumiza, S., Chahed, K., Tabka, Z., Jacob, M. P., Norel, X., & Ozen, G. (2021). MMPs and TIMPs levels are correlated with anthropometric parameters, blood pressure, and endothelial function in obesity. Scientific Reports, 11(1), 1–12. https://doi.org/10.1038/s41598-021-99577-2

Bustamante, L., Pastene, E., Duran-Sandoval, D., Vergara, C., Von Baer, D., & Mardones, C. (2018). Pharmacokinetics of low molecular weight phenolic compounds in gerbil plasma after the consumption of calafate berry (Berberis microphylla) extract. Food Chemistry, 268(February), 347–354. https://doi.org/10.1016/j.foodchem.2018.06.048

Calfío, C., & Huidobro-Toro, J. P. (2019). Potent vasodilator and cellular antioxidant activity of endemic patagonian calafate berries (berberis microphylla) with nutraceutical potential. Molecules, 24(15). https://doi.org/10.3390/molecules24152700

Chen, C. ye, Yi, L., Jin, X., Zhang, T., Fu, Y. jie, Zhu, J. dong, Mi, M. tian, Zhang, Q. yong, Ling, W. hua, & Yu, B. (2011). Inhibitory Effect of Delphinidin on Monocyte-Endothelial Cell Adhesion Induced by Oxidized Low-Density Lipoprotein via ROS/p38MAPK/NF-κB Pathway. Cell Biochemistry and Biophysics, 61(2), 337–348. https://doi.org/10.1007/s12013-011-9216-2

Couillard, C., Ruel, G., Archer, W. R., Pomerleau, S., Bergeron, J., Couture, P., Lamarche, B., & Bergeron, N. (2005). Circulating levels of oxidative stress markers and endothelial adhesion molecules in men with abdominal obesity. Journal of Clinical Endocrinology and Metabolism, 90(12), 6454–6459. https://doi.org/10.1210/jc.2004-2438

Curtasu, M. V., Knudsen, K. E. B., Callesen, H., Purup, S., Stagsted, J., & Hedemann, M. S. (2019). Obesity Development in a Miniature Yucatan Pig Model: A Multi-compartmental Metabolomics Study on Cloned and Normal Pigs Fed Restricted or Ad Libitum High-Energy Diets. Journal of Proteome Research, 18(1), 30–47. https://doi.org/10.1021/acs.jproteome.8b00264

Estaras, M., Ameur, F. Z., Estévez, M., Díaz-Velasco, S., & Gonzalez, A. (2020). The lysine derivative aminoadipic acid, a biomarker of protein oxidation and diabetes-risk, induces production of reactive oxygen species and impairs trypsin secretion in mouse pancreatic acinar cells. Food and Chemical Toxicology, 145(May). https://doi.org/10.1016/j.fct.2020.111594

Ferrari, R., Merli, E., Cicchitelli, G., Mele, D., Fucili, A., & Ceconi, C. (2004). Therapeutic effects of L-carnitine and propionyl-L-carnitine on cardiovascular diseases: A review. Annals of the New York Academy of Sciences, 1033, 79–91. https://doi.org/10.1196/annals.1320.007

Fukaya, M., Sato, Y., Kondo, S., Adachi, S. ichi, Yoshizawa, F., & Sato, Y. (2021). Quercetin enhances fatty acid β-oxidation by inducing lipophagy in AML12 hepatocytes. Heliyon, 7(6), e07324. https://doi.org/10.1016/j.heliyon.2021.e07324

Ganna, A., Salihovic, S., Sundström, J., Broeckling, C. D., Hedman, Å. K., Magnusson, P. K. E., Pedersen, N. L., Larsson, A., Siegbahn, A., Zilmer, M., Prenni, J., Ärnlöv, J., Lind, L., Fall, T., & Ingelsson, E. (2014). Large-scale Metabolomic Profiling Identifies Novel Biomarkers for Incident Coronary Heart Disease. PLoS Genetics, 10(12). https://doi.org/10.1371/journal.pgen.1004801

Gómez-Amores, L., Mate Barrero, A., Revilla Torres, E., Santa-María Pérez, C., & Vázquez Cueto, C. M. (2005). El tratamiento con propionil-L-carnitina

mejora el estrés oxidativo asociado a la hipertensión arterial. Hipertensión y Riesgo Vascular, 22(3), 109–116. https://doi.org/10.1016/s1889-1837(05)71545-2

Guzmán, C., & Sánchez, R. (2021). Effect of calafate (Berberis microphylla) supplementation on lipid profile in rats with diet-induced obesity. Functional Foods in Health and Disease, 11(10), 512–521. https://doi.org/10.31989/FFHD.V11I10.823

Haeusler, R. A., Astiarraga, B., Camastra, S., Accili, D., & Ferrannini, E. (2013). Human insulin resistance is associated with increased plasma levels of 12a-hydroxylated bile acids. Diabetes, 62(12), 4184–4191. https://doi.org/10.2337/db13-0639

Kikuchi, T., Lin, L., & Horigome, H. (2021). Soluble thrombomodulin and cardiovascular disease risk factors in Japanese children. Blood Coagulation & Fibrinolysis, 32(4), 273–277. https://doi.org/10.1097/MBC.0000000000001035

Kim, J. G., Lee, B. J., & Jeong, J. K. (2020). Temporal leptin to determine cardiovascular and metabolic fate throughout the life. Nutrients, 12(11), 1–14. https://doi.org/10.3390/nu12113256

Laursen, M. R., Hansen, J., Elkjær, C., Stavnager, N., Nielsen, C. B., Pryds, K., Johnsen, J., Nielsen, J. M., Bøtker, H. E., & Johannsen, M. (2017). Untargeted metabolomics reveals a mild impact of remote ischemic conditioning on the plasma metabolome and α-hydroxybutyrate as a possible cardioprotective factor and biomarker of tissue ischemia. Metabolomics, 13(67), 1–13. https://doi.org/10.1007/s11306-017-1202-2

Lee, H. J., Jang, H. B., Kim, W. H., Park, K. J., Kim, K. Y., Park, S. I., & Lee, H. J. (2019). 2-Aminoadipic acid (2-AAA) as a potential biomarker for insulin resistance in childhood obesity. Scientific Reports, 9(1), 1–10. https://doi.org/10.1038/s41598-019-49578-z

Lobo, V., Patil, A., Phatak, A., & Chandra, N. (2010). Free radicals, antioxidants and functional foods: Impact on human health. Pharmacognosy Reviews, 4(8), 118–126. https://doi.org/10.4103/0973-7847.70902

Marshall, D. D., & Powers, R. (2017). Beyond the Paradigm: Combining Mass Spectrometry and Nuclear Magnetic Resonance for Metabolomics. Progress in Nuclear Magnetic Resonance Spectroscopy, 100, 1–16. https://doi.org/10.1016/j.pnmrs.2017.01.001

Masumi Ai, Otokozawa, S., Asztalos, B. F., White, C. C., Banjaw, S. D.-, Cupples, L. A., Nakajima, K., Wilson, P. W., & Schaefer, E. J. (2011). Adiponectin: an Independent Risk Factor for Coronary Heart Disease in the Framingham Offspring Study. Atherosclerosis, 217(2), 543–548. https://doi.org/10.1016/j.atherosclerosis.2011.05.035.Adiponectin

Miao, H., Zhao, Y. H., Vaziri, N. D., Tang, D. D., Chen, H., Chen, H., Khazaeli, M., Tarbiat-Boldaji, M., Hatami, L., & Zhao, Y. Y. (2016). Lipidomics Biomarkers of Diet-Induced Hyperlipidemia and Its Treatment with Poria cocos. Journal of Agricultural and Food Chemistry, 64(4), 969–979. https://doi.org/10.1021/acs.jafc.5b05350

Mihalik, S. J., Goodpaster, B. H., Kelley, D. E., Chace, D. H., Vockley, J., Toledo, F. G. S., & Delany, J. P. (2010). Increased levels of plasma acylcarnitines in obesity and type 2 diabetes and identification of a marker of glucolipotoxicity. Obesity, 18(9), 1695–1700. https://doi.org/10.1038/oby.2009.510

Morlock, G. E., & Vega-Herrera, M. A. (2007). Two new derivatization reagents for planar chromatographic quantification of sucralose in dietetic products. Journal of Planar Chromatography - Modern TLC, 20(6), 411–417. https://doi.org/10.1556/JPC.20.2007.6.4

Morton, D. ., & Griffiths, P. H. . (1985). Guidelines in the recognition of pain, distress anddisconform in experimental animal and an hypothesis for assessment. Veterinary Record, 116, 431–436. https://doi.org/http://dx.doi.org/10.1136/vr.116.16.431

Okamoto, Y., Folco, E. J., Minami, M., Wara, A. K., Feinberg, M. W., Sukhova, G. K., Colvin, R. A., Kihara, S., Funahashi, T., Luster, A. D., & Libby, P. (2008). Adiponectin inhibits the production of CXC receptor 3 chemokine ligands in macrophages and reduces T-lymphocyte recruitment in atherogenesis. Circulation Research, 102(2), 218–225. https://doi.org/10.1161/CIRCRESAHA.107.164988

Olejarz, W., Łacheta, D., & Kubiak-Tomaszewska, G. (2020). Matrix metalloproteinases as biomarkers of atherosclerotic plaque instability. International Journal of Molecular Sciences, 21(11). https://doi.org/10.3390/ijms21113946

Olivares-Caro, L., Radojkovic, C., Chau, S. Y., Nova, D., Bustamante, L., Neira, J. Y., Perez, A. J., & Mardones, C. (2020). Berberis microphylla G. Forst (calafate) berry extract reduces oxidative stress and lipid peroxidation of human LDL. Antioxidants, 9(12), 1–20. https://doi.org/10.3390/antiox9121171

Park, J. Y., Lee, S. H., Shin, M. J., & Hwang, G. S. (2015). Alteration in metabolic signature and lipid metabolism in patients with angina pectoris and myocardial infarction. PLoS ONE, 10(8), 1–15. https://doi.org/10.1371/journal.pone.0135228

Patterson, R. E., Ducrocq, A. J., McDougall, D. J., Garrett, T. J., & Yost, R. A. (2015). Comparison of blood plasma sample preparation methods for combined LC-MS lipidomics and metabolomics. Journal of Cromatography B, Analytical Technologies in the Biomedical and Life Sciences, 1002, 260–266. https://doi.org/10.1016/j.jchromb. 2015.08.018

Pawelczyk, M., Glabiński, A., Kaczorowska, B., & Baj, Z. (2018). sP- and sE-selectin in stroke patients with metabolic disorders. Neurologia i Neurochirurgia Polska, 52(5), 599–605. https://doi.org/10.1016/j.pjnns.2018.08.004

Reyes-Farias, M., Vasquez, K., Fuentes, F., Ovalle-Marin, A., Parra-Ruiz, C., Zamora, O., Pino, M. T., Quitral, V., Jimenez, P., Garcia, L., & Garcia-Diaz, D. F. (2016). Extracts of Chilean native fruits inhibit oxidative stress,

inflammation and insulin-resistance linked to the pathogenic interaction between adipocytes and macrophages. Journal of Functional Foods, 27, 69–83. https://doi.org/10.1016/j.jff.2016.08.052

Rozenberg, O., Shih, D. M., & Aviram, M. (2003). Human serum paraoxonase 1 decreases macrophage cholesterol biosynthesis: Possible role for its phospholipase-A2-like activity and lysophosphatidylcholine formation. Arteriosclerosis, Thrombosis, and Vascular Biology, 23(3), 461–467. https://doi.org/10.1161/01.ATV.0000060462.35946.B3

Ruel, G., Pomerleau, S., Couture, P., Lemieux, S., Lamarche, B., & Couillard, C. (2008). Low-calorie cranberry juice supplementation reduces plasma oxidized LDL and cell adhesion molecule concentrations in men. British Journal of Nutrition, 99(2), 352–359. https://doi.org/10.1017/S0007114507811986

Ruiz, A., Hermosín-Gutiérrez, I., Vergara, C., von Baer, D., Zapata, M., Hitschfeld, A., Obando, L., & Mardones, C. (2013). Anthocyanin profiles in south Patagonian wild berries by HPLC-DAD-ESI-MS/MS. Food Research International, 51(2), 706–713. https://doi.org/10.1016/j.foodres.2013.01.043

Ruiz, A., Mardones, C., Vergara, C., Hermosín-gutiérrez, I., Baer, D. Von, Hinrichsen, P., Rodriguez, R., Arribillaga, D., & Dominguez, E. (2013). Analysis of hydroxycinnamic acids derivatives in calafate (Berberis microphylla G . Forst) berries by liquid chromatography with photodiode array and mass spectrometry detection. Journal of Chromatography A, 1281, 38–45. https://doi.org/10.1016/j.chroma.2013.01.059

Sandoval-Acuña, C., Ferreira, J., & Speisky, H. (2014). Polyphenols and mitochondria: An update on their increasingly emerging ROS-scavenging independent actions. Archives of Biochemistry and Biophysics, 559, 75–90. https://doi.org/10.1016/j.abb.2014.05.017

Seigneur, M., Dufourcq, P., Conri, C., Constans, J., Mercié, P., Pruvost, A., Amiral, J., Midy, D., Baste, J. C., & Boisseau, M. R. (1993). Levels of plasma thrombomodulin are increased in atheromatous arterial disease. Thrombosis Research, 71(6), 423–431. https://doi.org/10.1016/0049-3848(93)90116-6

Shabalala, S. C., Dludla, P. V., Mabasa, L., Kappo, A. P., Basson, A. K., Pheiffer, C., & Johnson, R. (2020). The effect of adiponectin in the pathogenesis of non-alcoholic fatty liver disease (NAFLD) and the potential role of polyphenols in the modulation of adiponectin signaling. Biomedicine and Pharmacotherapy, 131(May), 110785. https://doi.org/10.1016/j.biopha.2020.110785

Shai, I., Pischon, T., Hu, F. B., Ascherio, A., Rifai, N., & Rimm, E. B. (2006). Soluble intercellular adhesion molecules, soluble vascular cell adhesion molecules, and risk of coronary heart disease. Obesity, 14(11), 2099–2106. https://doi.org/10.1038/oby.2006.245

Shimizu, H., Hagio, M., Iwaya, H., Tsuneki, I., Lee, J. Y., Fukiya, S., Yokota, A., Miyazaki, H., Hara, H., & Ishizuka, S. (2014). Deoxycholic acid is involved in the proliferation and migration of vascular smooth muscle cells. Journal of Nutritional Science and Vitaminology, 60(6), 450–454. https://doi.org/10.3177/jnsv.60.450

Suhre, K., Meisinger, C., Döring, A., Altmaier, E., Belcredi, P., Gieger, C., Chang, D., Milburn, M. V., Gall, W. E., Weinberger, K. M., Mewes, H. W., Angelis, M. H., Wichmann, H. E., Kronenberg, F., Adamski, J., & Illig, T. (2010). Metabolic footprint of diabetes: A multiplatform metabolomics study in an epidemiological setting. PLoS ONE, 5(11). https://doi.org/10.1371/journal.pone.0013953

Tarifeño-Saldivia, E., Aguilar, A., Contreras, D., Mercado, L., Morales-Lange, B., Márquez, K., Henríquez, A., Riquelme-Vidal, C., & Boltana, S. (2018). Iron overload is associated with oxidative stress and nutritional immunity during viral infection in fish. Frontiers in Immunology, 9(JUN). https://doi.org/10.3389/fimmu.2018.01296

Wang, T. J., Ngo, D., Psychogios, N., Dejam, A., Larson, M. G., Vasan, R. S., Ghorbani, A., O'Sullivan, J., Cheng, S., Rhee, E. P., Sinha, S., McCabe, E., Fox, C. S., O'Donnell, C. J., Ho, J. E., Florez, J. C., Magnusson, M., Pierce, K. A., Souza, A. L., Yu, Y., Carter, C., Light, P.E., Melander, E., Clish, C.B., & Gerszten, R. E. (2013). 2-Aminoadipic acid is a biomarker for

diabetes risk. Journal of Clinical Investigation, 123(10), 4309–4317. https://doi.org/10.1172/JCI64801

Yoshimoto, S., Loo, T. M., Atarashi, K., Kanda, H., Sato, S., Oyadomari, S., Iwakura, Y., Oshima, K., Morita, H., Hattori, M., Honda, K., Ishikawa, Y., Hara, E., & Ohtani, N. (2013). Obesity-induced gut microbial metabolite promotes liver cancer through senescence secretome. Nature, 499(7456), 97–101. https://doi.org/10.1038/nature12347

Zunino, S. J., Parelman, M. A., Freytag, T. L., Stephensen, C. B., Kelley, D. S., MacKey, B. E., Woodhouse, L. R., & Bonnel, E. L. (2012). Effects of dietary strawberry powder on blood lipids and inflammatory markers in obese human subjects. British Journal of Nutrition, 108(5), 900–909. https://doi.org/10.1017/S0007114511006027

4.3 Cambios en el metaboloma de tejido cardiaco de raton son asociados al consume de calafate y reducción de riesgo cardiovascular

Con el objetivo de complementar los análisis realizados en plasma de ratón y de evaluar el posible efecto benéfico del fruto de calafate frente a la patología cardiovascular, se realizó la extracción y el procesamiento de muestras de corazón obtenidas para el mismo modelo murino de dieta alta en grasas. Artículo en redacción

Article

Changes in the metabolome of heart tissue of mice associated to calafate intake and reduction of cardiovascular risk.

Lia OLIVARES-CARO[a,b], Daniela NOVA[a], Danilo ESCOBAR[c] , Claudia RADOJKOVIC[b], Daniel DURAN[b], Luis BUSTAMANTE[a], Andy PEREZ[a], Claudia MARDONES [a,c*]

[a] Departamento de Análisis Instrumental, Facultad de Farmacia, Universidad de Concepción, Concepción, Chile

[b] Departamento de Bioquímica Clínica e Inmunología, Facultad de Farmacia, Universidad de Concepción, Concepción, Chile

[c] Unidad de Desarrollo Tecnológico, Universidad de Concepción, Coronel, Chile

*Corresponding author. Tel.: +56 983616340. E-mail address cmardone@udec.cl (C. Mardones).

Abstract

Cardiovascular disease (CVD) is the first cause of death in the world. Heart is a vital organ and is the most affected organ in CVD. Risk factor of this pathology are chronic kidney disease, hypertension, diabetes and obesity, which caused an increase in reactive oxygen species (ROS) that can cause an electrophysiological change, contractile response, mitochondrial dysfunction and subsequent apoptosis in cardiomyocytes. Polyphenols are natural antioxidants than reduce oxidation processes and inhibit the production of free radicals. Calafate, an endemic shrub from Chilean-Argentine Patagonia, contains high concentrations of polyphenols and high antioxidant capacity in its fruit. The aim of this research was to evaluate by HPLC-QTOF-MS based metabolomics analyses the changes in the cardiac tissue of mice exposed to a high fat diet after consuming calafate extract, in order to establish their protective effect against CVD. The extract modified the cardiac tissue metabolome, decreasing metabolites associated with risk factors. Finally, we proposed that calafate could influence the insulin signaling pathway, through purine metabolism and inositol metabolism in cardiac tissue.

Keywords: *Berberis microphylla*, calafate, Polyphenols, cardiovascular disease risk, metabolomic

4.3.1 Introduction

Cardiovascular disease (CVD) is the first cause of death in the world, (https://www.who.int/es/news-room/fact-sheets/detail/the-top-10-causes-of-death) and ischemic heart disease produced 16% of deaths, as reported by the World Health Organization (WHO). In Chile, despite the fact that the frequency of deaths increased due to COVID-19, diseases associated to the circulatory system continued as the main cause of death between 2020 and 2021(https://www.minsal.cl/wp-content/uploads/2021/01/Informe-Semanal-del-ene-7-2021.pdf). Heart is a vital organ whose function is to propel oxygenated blood from the left ventricle to the blood vessels and throughout the body, thus allowing the body's cells to obtain oxygen, nutrients and other substances necessary for their functioning (López Farré & Macaya Miguel, 2009). The heart is the most affected organ in a cardiovascular pathology.

Chronic exposure of endothelial cells to LDL (low density lipoprotein) can result in the increase of ROS and consequently the oxidative stress, causing a state known as endothelial dysfunction (Campos et al., 2014). Levels of cellular adhesion molecules, such as vascular cell adhesion molecule-1 (VCAM-1), P- and E-selectin, are reflectives of endothelial activation (Weil & Neelamegham, 2019). These molecules favor the transmigration of

lymphocytes and in consequence coronary microvascular dysfunction and myocardial interstitial fibrosis (Patel et al., 2020). In the Multi-Ethnic Study of Atherosclerosis (MESA) serum levels of VCAM-1 has been directly associated with heart failure (Patel et al., 2020). Glycocalyx damage marker sSyndecan-1, sE-selectin, sVCAM-1 and thrombomodulin were higher in Out-of-hospital cardiac arrest compared to healthy controls (Chaban et al., 2021). Cardiovascular disease risk factor such as, chronic kidney disease, hypertension, diabetes and obesity, cause an increase in reactive oxygen species (ROS) can cause an electrophysiological change, contractile response, mitochondrial dysfunction and subsequent apoptosis in cardiomyocytes (Lubrano & Balzan, 2020). According with Wang et al, there is a positive association between heart rate and cardiovascular risk, with increase of 72% in the risk of suffering myocardial infarction for normotensive patients (Wang et al., 2021). The increase in heart rate is accompanied by a high work of the heart, increasing the activity of the sympathetic nervous system, which can trigger myocardial apoptosis and sudden death (Reil & Böhm, 2007). The produced hemodynamic stress induces endothelial dysfunction and subsequent atherosclerosis in the aorta and iliac vessels (Reil & Böhm, 2007).

Polyphenols are natural antioxidants than reduce oxidation processes and inhibit the production of free radicals (Lobo et al., 2010). Calafate (*Berberis microphylla)*, an endemic shrub from Chilean-Argentine Patagonia, contains high concentrations of polyphenols and high antioxidant capacity in its fruit (Ruiz et al., 2013;Ruiz et al., 2013;Schmeda-Hirschmann et al., 2019). Our research group has reported that calafate extract (2 mg fresh fruit/mL) reduced oxidative stress in HUVEC cells (human umbilical vein endothelial cells) by around 51% and completely inhibited human LDL oxidation, demonstrating its potential on lipid peroxidation (Olivares-Caro et al., 2020). Recently, we demonstrated that the calafate intake produced a change in plasma proteins and in the metabolome of mice fed with a high fat diet (HFD), both related to a reduction in CVD risk factors associated with the HFD. However, there are not studies about the protective effect of the intake of its fruit directly on heart, which is important to enhance the knowledge about cardiovascular protective effects of calafate. This research evaluated the changes in the metabolites of heart tissue after a high fat diet, with and without calafate intake

Metabolomics is a comprehensive analytical tool that allows to detect, identify, and quantify many metabolites in biological samples.

Non-targeted metabolomics can discriminated metabolites associated with a genotype, pharmacological treatment, clinical population, or other comparative group, usually by contrast with their control group (McGarrah et al., 2018). The wide coverage of metabolomics provides the potential to identify new metabolic pathways or new biomarkers (McGarrah et al., 2018). The aim of this research was to evaluate by HPLC-QTOF-MS based metabolomics analyses the changes in the cardiac tissue of mice exposed to a HFD after consuming a calafate extract, to establish a protective effect against cardiovascular pathology of this fruit. This is the first study including the effect of calafate metabolites in heart tissue, as an holistic view of its cardiovascular beneficial effects.

4.3.2. Materials and Methods

4.3.2.1. Reagents and vegetable material

Formic acid (LiChropur®) for LC–MS (98-100%), acetonitrile (hyper grade), methanol (hyper grade), ethanol, water (HPLC–MS), and ammonium formate for mass spectrometry (>99.0%) were provided by Merck (Darmstadt, Germany).

Vegetable material: calafate berries (*Berberis microphylla*) were collected near Punta Arenas, Chile (53.1548309, -70.911293).

4.3.2.2. Instrumentation

A Heraeus-Fresco17 centrifuge from Thermo Fisher (Waltham, MA, USA), an analytical balance from Denver Instrument Company (NY, USA), Mixer mill RETCH MM400 (Haan, Alemania) and a refrigerated CentriVap concentrator from LABCONCO (Kansas City, MO, USA) were used for sample preparation.

The untargeted metabolomics was carried out with a UHPLC-DAD Bruker Elute LC system coupled in tandem with a Q-TOF spectrometer Compact, Bruker (Bremen, Germany). The control system used was Compass HyStar (Bruker), and the acquisition software was Bruker to control 4.1.402.322-7977-vc110 6.3.3.11. Data analysis was performed with Compass DataAnalysis 4.4.200 (Bruker) software, Compass QuantAnalysis 4.4 (Bruker Daltonics, Bremen, Germany), MetaboScape 3.0 (Bruker Daltonics, Bremen, Germany), and freely accessible software MetaboAnalyst (https://www.metaboanalyst.ca/).

Cytokine quantification was carried out in a MAGPIX instrument by Luminex XMAP Technology (Life Technologies, Grand Island, NY, USA), using a MILLIPLEX® MAP Mouse Adipokine Magnetic Bead Panel, MILLIPLEX® MAP Mouse Adipokine Magnetic Single Bead and

MILLIPLEX® MAP Mouse CVD Magnetic Bead Panel 1. Data analysis and data acquisition were carried out with Luminex xPONENT® version 4.3229.0 (Luminex Corporation, TX, USA). Plate shaking for wash and incubation time was carried out in Thermomixer® C serial number 5382KG639268 (Eppendorf, Hamburg, Germany).

4.3.2.3.1 Calafate extract

The fruit extraction was carried out as previously described by (Ruiz, et al., 2013)[a], using ethanol/formic acid (97:3) as solvent extraction (raw extract), which was subsequently characterized. Hydroxycinnamic acid (HCA) and flavonol determination required an additional purification step using solid-phase extraction with cation exchange columns (Oasis MCX Water, USA), as previously described by Ruiz et al. (called purified extract) (Ruiz, et al., 2013)[b]. The raw extract was evaporated, lyophilized and suspended in ultrapure water for the *in vivo* study in C57BL/67 mice (5 mg dry extract/mL). The calafate extract was characterized by HPLC-DAD-MS (Bustamante et al., 2018). The sugar and ascorbic acid content of the calafate extract was determined according to (Morlock & Vega-Herrera, 2007).

4.3.2.3.2 *In vivo* assay

Ten- to twelve-week-old outbred C57BL/6J mice (n= 24) purchased from the Instituto de Salud Pública (ISP, Santiago, Chile) were housed in a conventional animal facility maintained at 25±1 °C under a 12 h light:12 h dark photoperiod, in accordance with the Guidelines for the Care and Use of Laboratory Animals (https://grants.nih.gov/grants/olaw/Guide-for-the-Care-and-use-of-laboratory-animals.pdf) (Morton & Griffiths, 1985). After the acclimation period, mice were randomized and were fed *ad libitum* with a D12450H low-fat diet (10% fat; Open Source Diets - Research Diets, Inc, New Brunswick, NJ, EEUU), which is named a normal diet (N), or with a D12451 high-fat isocaloric diet (45% fat; Open Source Diets - Research Diets, Inc, New Brunswick, NJ, EEUU), which was named a high-fat diet (H) (n=12 and 6 mice per group). After three months, H group was randomized into another subgroups (n=6 mice per group) that received either water (H group) or calafate extract in water, freshly prepared every 2 days, as the only source of liquid (called the Hcal subgroups). Both calafate extract and water had similar pH values and sugar contents (pH 3 and 1.8 mg/mL of sugar) (Bustamante et al., 2018). Pellet and liquid consumption were quantified daily, and animal weight was assessed weekly. At the end of the study, animals were fasted for 12 h at the beginning of the dark cycle, then

were anesthetized with isoflurane and sacrificed through exsanguination at the fourth month after calafate extract supplementation. The heart of each mouse was dissected and immediately immersed in liquid nitrogen and subsequently stored at -80°C.

4.3.2.3.3 Tissue sample treatment

The organ samples were lyophilized for one week and after were crushed at 30 cicles/s x 180 s using mixer mill RETCH 400 to be stored in cryotubes at -80°C.

A methanolic extraction was performed for each sample following the protocol described by (Wells et al., 2018) with modifications. Briefly, 430 µL of hypergrade methanol (at -80°C) was added to 1.5 mg of the lyophilized tissue, it was stirred in vortex for 1 minute and then incubated at -80°C for 15 minutes. Then, it was stirred again in a vortex for 5 seconds and finally it was centrifuged for 5 minutes at 13,200 rpm at 4°C. 350 µL of the supernatant was transferred to a vial and evaporated on a CentriVap at 4°C. The extracts were reconstituted in 250 µL of hypergrade methanol (-80°C) and 20 µL of each sample was analyzed by LC-MS. Other 40 µL of each extract were mixed to form the control quality mix (QCs) for the metabolomics analysis.

4.3.2.3.4 UHPLC-DAD-ESI-QTOF-MS/MS analyses

The analyses of tissue extracts were carried out by UHPLC-DAD-ESI-QTOF-MS/MS based on the method previously described by (Laursen et al., 2017) (Method 1) and (Patterson et al., 2015) (Method 2) for compounds with medium polarity and non-polar, respectively. A Phenomenex column Kinetex® C18 100 x 4.6 mm 2.6 μm (Torrance, CA, USA), oven temperature 50 °C, autosampler temperature 4 °C, and partial loop injection mode were used for both methods. The chromatographic separation conditions were as follows:

Method 1: mobile phase A was composed of 0.1% formic acid in water, and mobile phase B was composed of 0.1% formic acid in acetonitrile, with a flow rate of 0.5 mL/min and an injection volume of 20 μL. The acetonitrile gradient ranged from 0% for 2 min, from 0% to 5% for 4 min, from 5% to 60% for 0.5 min, from 60% to 88% for 6.5 min, from 88% to 100% for 0.5 min, from 100% for 1 min and from 100 to 0% for 1 min with a stabilization period of 7.5 min.

Method 2: mobile phase A: 60:40 acetonitrile:water, 0.1% formic acid , and 10 mM ammonium formate; and mobile phase B: 90:10

isopropanol:acetonitrile, 0.1% formic acid, 10 mM ammonium formate, a flow rate of 0.2 mL/min and an injection volume of 20 µL. The mobile phase B gradient ranged from 32 to 43% for 2 min, 43% for 2 min, from 43% to 75% for 6 min, 75% for 2 min, 75% to 100% for 2 min, 100% for 1 min and from 100 to 32% for 1 min with a stabilization period of 5 min.

The tissue extract analysis by normal phase chromatography UHPLC-DAD-ESI-QTOF-MS/MS was based on the method described by (Armirotti et al., 2014) for polar metabolites (Method 3). A HILIC BEH Amide 100 x 2.1 mm y de 1.7 µm (Waters, Milford, MA, EEUU), oven temperature 40 °C, autosampler temperature 4 °C, and partial loop injection mode were used. The chromatographic separation conditions were as follows: mobile phase A was composed of 10 mM ammonium formate in water, and mobile phase B was composed of 95:5 ammonium formate in acetonitrile:water. A flow rate of 0.4 mL/min and an injection volume of 20 µL were used. The gradient ranged from 100% B for 1 min, from 100% to 70% B for 16 min, 70% B for 1 min, and from 70 to 100% for 1 min with a stabilization period of 5 min.

The MS conditions in all the metabolomic studies were positive ionization ESI +4500 V and negative ionization ESI -3500 V, dry gas: 9 L/min,

nebulizer: 4 Bar, T°: 200 °C, end capillary 500 V, collision energy at 10-25 eV in stepping mode, auto MS/MS mode (2 precursor/cycle), 50-1500 m/z (scan 0.2 s centroid mode) and internal calibration using sodium formate (0.01 M) with a mass accuracy < 3 ppm.

All metabolomic sequences started with 2 blank injections (solvent only), followed by 3 technical blanks (considering extraction process) and 3 QC. Then, every 12 samples, a QC was injected (Alseekh et al., 2021).

4.3.2.3.5 Data Processing and Data Analysis

Bucket Table: UHPLC-ESI-QTOF-MS/MS was processed in MetaboScape 3.0 (T-ReX 3D algorithm) under the parameters shown in Table 4.3.1. This software transformed the raw data into a matrix with the features (m/z – retention time (t_R) pairs and normalized peak intensity) (file: .csv). The workflow included mass recalibration, t_R alignment, feature extraction (m/z – t_R pairs), adduct and neutral loss administration, import of MS/MS spectra, and generation of the bucket table.

Data Prefilter: the matrix was processed in MetaboAnalyst software, and the data were filtered considering RSDs > 20% compared to QC and normalized for weight. The purpose of data filtering is to identify and remove variables

that are unlikely to be of use when modeling the data. Principal component analysis (PCA) and volcano plot (fold change threshold: 1.5, and p value threshold: 0.05 FDR-adjusted) were used to select characteristic features of each group (comparisons between 2 group were: H-Hcal and N-H). Peak area integration was manually curated with Compass QuantAnalysis 4.4 software.

Filter and feature selection: the new bucket table was processed in MetaboAnalyst 5.0, and normalized, data filtering and Pareto scaling were performed again. All variables were Pareto scaled to reduce the relative importance of large values and keep the data structure partially intact (Curtasu et al., 2019). ANOVA ($p < 0.05$) was used to select the significant characteristic features of each group.

Metabolite annotation workflow: in DataAnalysis software, the molecular formula with the smallest mass error was selected. The spectra were sent to databases such as MetFrag (In silico fragmentation for computer-assisted identification of metabolite mass spectra) (https://msbi.ipb-halle.de/MetFrag/), HMDB (The human metabolome database) (https://hmdb.ca/), and METLIN

(https://metlin.scripps.edu/landing_page.php?pgcontent=mainPage) by comparing the accurate mass and fragments information obtained from UHPLC-QTOF/MS. Furthermore, the theoretical isotopic pattern was compared with the experimental isotopic pattern. Metabolite annotation was based on the guide for annotation, quantification and best reporting practices proposed by (Alseekh et al., 2021). Tolerance to the m/z value was set to 10 ppm.

Table 4.3.1: Parameters of Metaboscape software

Parámetros	**Método1 NEG**	**Método1 POS**	**Método2 NEG**	**Método2 POS**	**Método3 NEG**	**Método3 POS**
Intensity threshold [counts]	200.0	400.0	200.0	200.0	200.0	300
Minimum peak length [spectra]	5	3	21	13	6	16
Minimum peak length (recursive) [spectra]	4	2	20	12	5	15
Minimum # Features for Extraction	2	2	2	2	2	2
Presence of features in minimum # of analyses	2	2	2	2	2	2
Lock mass calibration	false	false	false	false	false	false
Mass calibration	true	true	true	true	true	true
Primary Ion	[M-H]-	[M+H]+	[M-H]-	[M+H]+	[M-H]-	[M+H]+
Seed Ions	[2M-H]-, [M+HCOO-H]-	[M+Na]+, [M]+, [2M+H]+, [M+HCOOH]+	[M-HCOO-H]-, [2M-H]-	[M+Na]+, [M]+, [2M+H]+, [M+HCOOH]+	[2M-H]-, [M+HCOO-H]-	[M+Na]+, [M]+, [2M+H]+, [M+HCOOH]+

Common Ions	[M-H-H_2O]-	[M-H_2O+H]+	[M-H-H_2O]-	[M-H_2O+H]+	[M-H-H_2O]-	[M-H_2O+H]+
EIC correlation	0.8	0.8	0.8	0.8	0.8	0.8
Mass range: Start [m/z]	50.0	50.0	50.0	50.0	50.0	50.0
Mass range: End [m/z]	1500.0	1500.0	1500.0	1500.0	1500.0	1500.0
Retention time range: Start [min]	0.5	0.5	0.5	0.5	0.5	0.5
Retention time range: End [min]	13.5	13.5	15.0	15.0	17	17
Perform MS/MS import	*true*	*true*	*true*	*true*	*true*	*true*
Group by collision energy	false	false	false	false	false	false
MS/MS import method	average	average	average	average	average	average

4.3.3 Results and discussion

The effect of chronic consumption of calafate fruit extract on the heart tissue metabolome and its possible relationship with cardiovascular protection was evaluated by a metabolomic study of heart tissue obtained from the 3 groups of mice fed with normal and high-fat diets supplemented or not with calafate extract for 4 months (N, H, Hcal). The base peak chromatograms (BPC) of the heart tissue extracts, obtained with the 3 chromatographic methods in order to detect the maximum number of compounds of different nature and polarity, are illustrated in Figures 4.3.1 and 4.3.2.

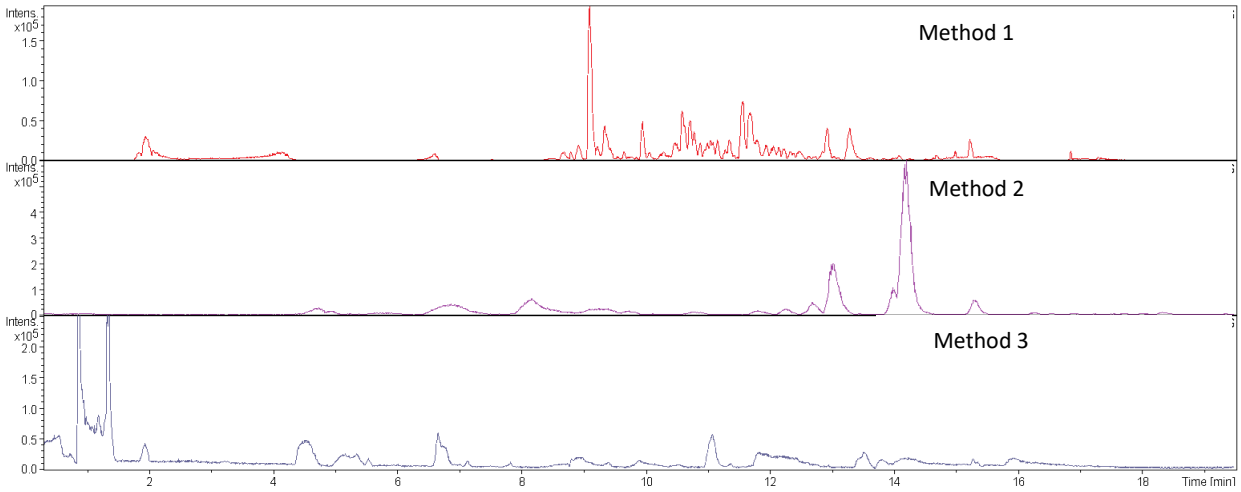

Figure 4.3.1: Base peak chromatogram (BPC) in negative polarity for different chromatographic method.

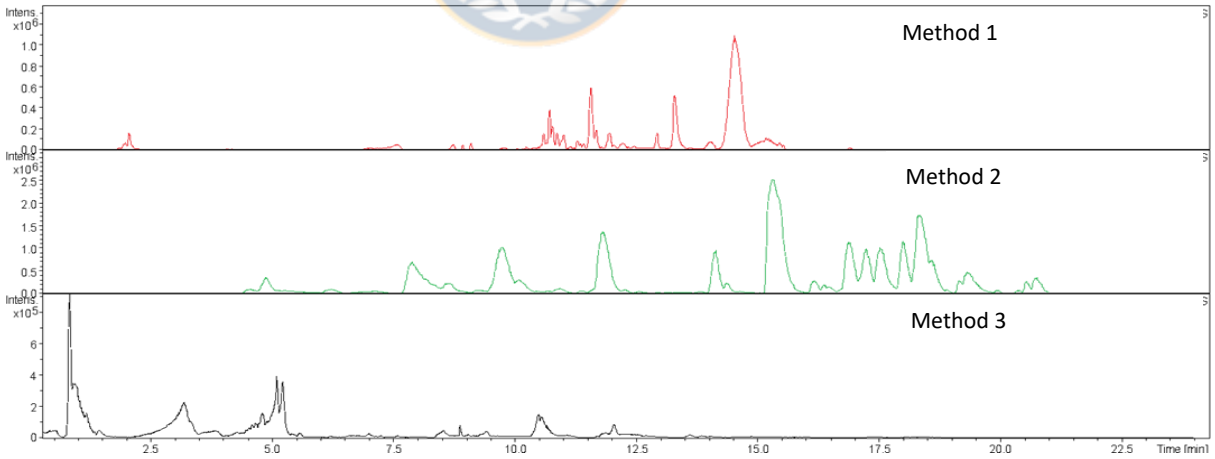

Figure 4.3.2: Base peak chromatogram (BPC) in positive polarity for different chromatographic method

4.3.3.1Multivariate analysis of the data

After applying the described workflow, the bucket table shows a total of 27,258, 5,830, 44,026 features obtained in negative mode, and 44,634, 37,465, 14,703 features in positive mode for methods 1, 2, and 3, respectively. After data filtering, a total of 22,648, 4,322, 34,578 features were eliminated in negative mode, and 33,358, 27,919, 9766 features in positive mode respectively.

PCA was performed as an exploratory analysis of the data, with the aim of observing separation between the groups. First, in the PCAs obtained with all the groups, the QCs were observed in the center of the model, which validates the data and is indicative of instrumental reproducibility of the procedure (Figure 4.3.3). A total separation of groups is observed for N with respect to H and Hcal (Figure 4.3.3b), which shows the change observed in the metabolome produced by the different diets. As relevant result is the clear separation between all groups observed in Figure 4.3.3 f which is produced by the calafate intake. These spontaneous separation between the groups indicates that calafate generates changes in heart tissue metabolome of mice fed with this fruit.

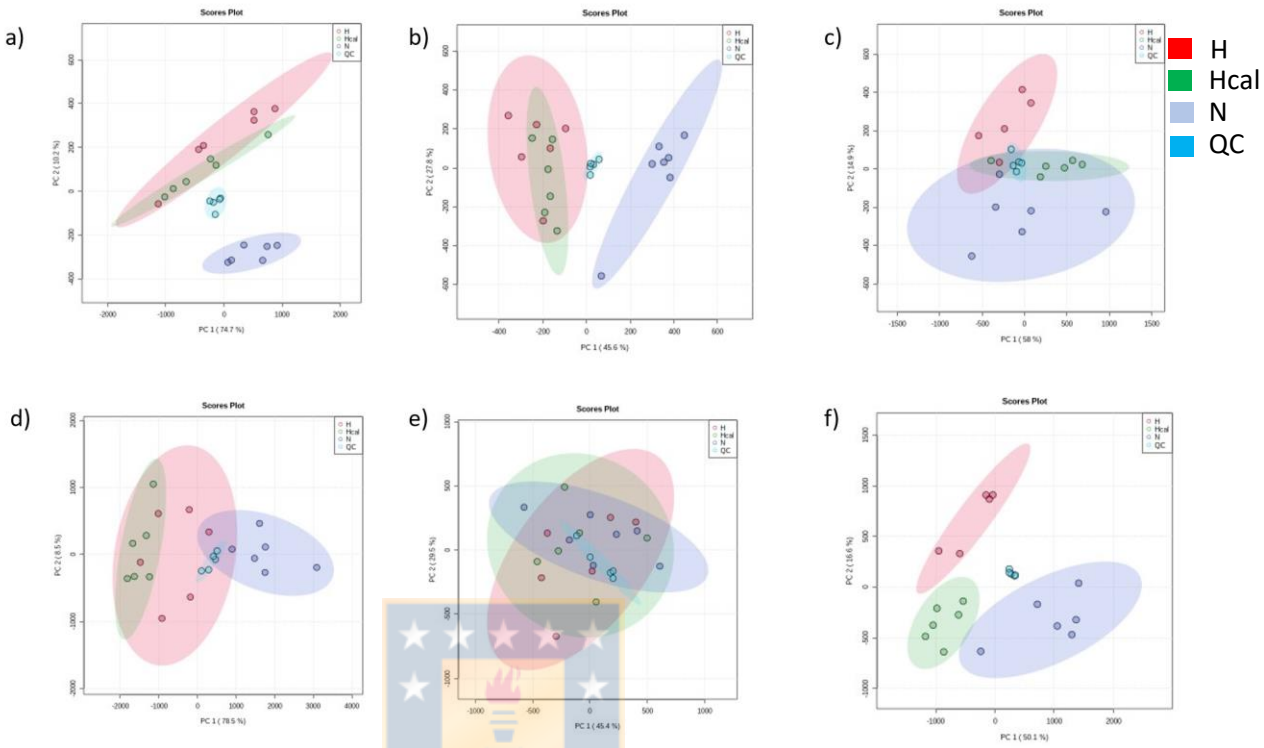

Figura 4.3.3: Principal component analysis (PCA). Score plot negative mode a) method 1, b) method 2 and c) method 3. Score plot positive mode d)method 1, e) method 2 and f) method 3. H:red, Hcal:green, N:Blue, QC:lightblue.

In the negative mode, the H-Hcal analysis showed that the main components 1 and 2 explained a variance of 92.8, 75.0 and 83.1%, for methods 1, 2 and 3 respectively (Figure 4.3.4). In positive mode, principal components 1 and 3 explained a variance of 68.2 and 58.3% for method 1 and 2, respectively (Figure 4.3. 4). In the case of the N-H analysis, the explained variances for

principal components 1 and 2 for the negative mode were 86.8, 75.7, 75.7% (Figure 4.3.5), and for the positive mode 86.5, 81.2, 71.6% (Figure 4.3.5), for the methods 1, 2 and 3, respectively.

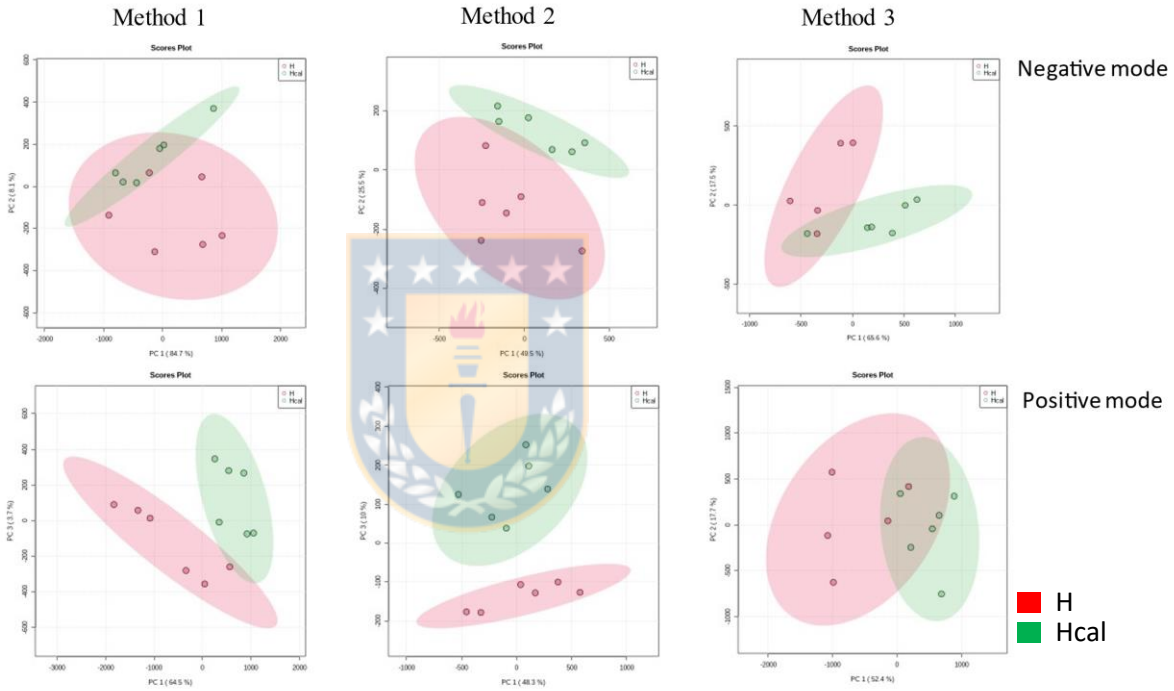

Figura 4.3.4 : Principal component analysis H vs Hcal. Score plot negative and positive a) method 1, b) method 2 y c) method 3 . H in red and Hcal in green

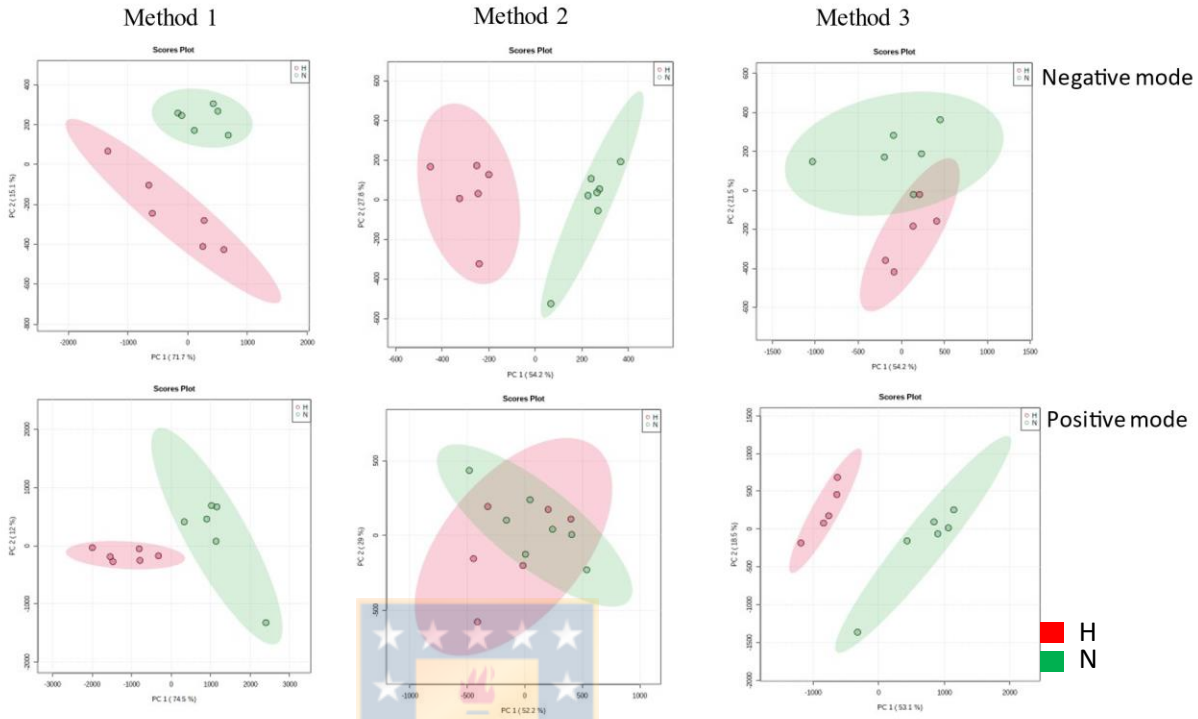

Figura 4.3.5: Principal component analysis H vs N. Score plot negative and positive a) method 1, b) method 2 y c) method 3. H in red and N in green

4.3.3.2 Significant features and biological interpretation

The analysis of main significant metabolites (obtained by ANOVA) using the data described previously for the different methods (positive and negative) showed a large number of significant features, which are related with different pathway. A detailed information of each identified metabolite are

showed in table 4.3.2, where only the metabolites associated to CVD are listed. The criteria of selection was ANOVA $p < 0.05$.

Tabla 4.3.2: Significant metabolites identified by UHPLC-DAD-QTOF related with CVD (positive and negative ionization modes).

Mass	Adduct	Fragment with intensity	Error (ppm)	Molecular Formula	Tentative ID	International identifier[2]	Identification level (A-D)[1]	Method[3]
103.0407	M-H		-10	$C_4H_8O_3$	2-Hydroxybutyric acid	HMDB0000008	D	2
179.0565	M-H		-2.2	$C_6H_{12}O_6$	Inositol isomer	HMDB0240208	D	3
259.0356	M-H	96.9698 676 124.0073 438 138.9792 94 185.9985 98	-0.6	$C_6H_{13}O_9P$	Inositolphosphate	C01177 HMDB0006814	B	1
267.0769	M-H	92.0216 108 108.0232 228 115.0034 560 116.0008 88 124.0083 218 130.0583 94 133.0128 1390 134.9371 82 135.0301 1430 153.0137 90 171.0137 86 204.0467 84 267.0768 296	4.3	$C_{10}H_{12}N_4O_5$	Inosine	C00294	B	1,2
295.2261	M-H	96.9566 16 137.0990 27 139.0730 26 139.1116 25 141.1248 14 141.1341 13 155.1422 51 181.1526 7 183.0157 8 195.1383 16 209.0290 13 251.2365 125 252.2402 57 252.2712 8 277.2161 13 278.2215 11 293.2169 7 294.1869 7 295.2255 1832 295.4004 12 295.5086 13 296.2291 403 297.2392 90 297.2618 18 298.2296 14 298.2616 26 207.0084 86 295.2235 800 297.2417 158	6	$C_{18}H_{32}O_3$	9(S)-HODE/ hydroxyoctadecadienoic acid	C14767	B	1

297.2422	M-H	152.1140 78 279.2327 230 293.1734 80 293.2108 454 295.2256 748 297.2412 1070	7.7	$C_{18}H_{34}O_3$	Epoxyoctadecanoic acid	C13791	B	1
321.2437	M-H		2.83	$C_{20}H_{34}O_3$	Eicosanoids_ 5-HETrE	CHEBI:72856	D	2
323.2570	M-H	183.0148 150 223.1707 112 277.1592 118 305.2466 128 306.2583 112 321.2385 88 323.2588 532 324.2612 150 325.1752 118	1.3	$C_{20}H_{36}O_3$	(Z)-15-Oxo-11-eicosenoic acid	HMDB29797;	B	1,2
335.0595	M-H+HCOONa	ND	0	$C_9H_{16}O_9$	galactose lactate	HMDB0252580	D	1
357.2624	M-H	124.0244 136 153.9982 94 157.0848 132 188.1436 82 197.1197 76 199.1450 88 214.1180 124 257.1733 102 311.2201 82 331.1183 92 336.6527 80 339.1181 92 355.2484 358 356.2477 106 357.2649 752	-0.7	$C_{20}H_{38}O_5$	13,14-Dihidro PGF-1a	HMDB05076	B	1
365.0493	M-H	ND	3	$C_{10}H_{15}N_4O_9P$	Phosphoribosylformamidocarboxamide	HMDB0001439	D	1
523.1564	2M-H	ND	7	$C_9H_{14}N_2O_7$	Glutamylaspartic acid	HMDB0028815	D	1
593.3617	M-H	ND	4	$C_{35}H_{50}N_2O_6$	Cholyltryptophan	HMDB0242374	D	1
538.3114	M+FA-H	154.0005 114 183.1374 146 236.0874 80 241.0124 78 253.2151 714 254.2242 78 255.2273 128 478.2867 386 538.3166 104	-8.5	$C_{24}H_{48}NO_7P$	LysoPC(16:1(9Z)/0:0)	HMDB0010383	B	1
269.0884	M+H	137.0469 818 119.0329 130 110.0350 334	-1.3	$C_{10}H_{12}N_4O_5$	inosine	HMDB0000195	B	3
137.0453	M+H		3.91	$C_5H_4N_4O$	hypoxanthine	HMDB0000157	D	3
398.3260	M+H	398.3240 394 382.2112 148 184.0700 134 144.0981 214 85.0288 406	1.04	$C_{23}H_{43}NO_4$	9-Hexadecenoylcarnitine	HMDB13207	B	3
400.3413	M+H	400.3439 234 341.2678 134 144.0996 42 95.0846 93 85.0288 690	-4.3	$C_{23}H_{45}NO_4$	Palmitoylcarnitine	HMDB0000222	B	3

[1]Identification level based in (Alseekh et al., 2021). [2]Data base used for identification. [3]Method of analysis.

The significant difference of metabolites between the groups H vs Hcal were obtained by ANOVA ($p < 0.05$) and are presented in the (Figure 4.3.6).

Figura 4.3.6: Significant metabolites found by ANOVA in negative and positive mode present in table 4.3.2. H red, Hcal green, N blue.

Among the metabolites identified, the feature 267.0769 m/z (4.3 ppm) was identified (level B) as inosine $C_{10}H_{12}N_4O_5$ (figure 4.3.6). Phosphoribosyl formamidocarboxamide $C_{10}H_{15}N_4O_9P$ 365.0493 m/z (3.0 ppm) showed the same profile than inosine. This metabolite came from purine metabolism in human, as inosine (KEEG pathway: hsa00230). Inosine decreased in the high-fat diet group consuming calafate ($p<0.05$) compared with H, reaching the same level of the N group. This metabolite has been related to cardiovascular pathology (Sikorski et al., 2021). Vlachogiannis et al.2021 demonstrated that a deaminase enzyme (ADAR1), which is responsible for converting adenosine into inosine, is related to cardiovascular atherosclerotic disease, because its activation increases the expression of NEAT1 lncRNA, a non-coding RNA, which causes an increased of the endothelial dysfunction markers VCAM-1 and ICAM-1. Furthermore, they found a strong linear association between NEAT1 and ADAR expression in peripheral blood mononuclear cells obtained from blood of patients with atherosclerotic cardiovascular disease (Vlachogiannis et al., 2021). The increase in ROS and apoptosis of endothelial cell has been related with endothelial dysfunction, key factor in atherosclerosis. The consumption of calafate would generated a positive effect by decreasing this marker. In a concordant previous result

obtained by our group, we have described that calafate reduced adhesion molecules in plasma (Olivares-Caro et al 2022), reducing the risk of endothelial dysfunction. In the same pathway we found the feature 137.0453 (3.91ppm) identified as hypoxanthine $C_5H_4N_4O$, which decreased in Hcal compared to H group ($p<0.05$). (Kim et al., 2017) demonstrated that hypoxanthine (1 mM) increased ROS production, BAD protein expression and reduced Bcl-2 in a HUVEC cell model, relating it to its apoptotic effect (Kim et al., 2017). In heart, Adenosine Triphosphate (ATP) is mainly produced by mitochondria, via aerobic oxidative phosphorylation. In ischemia/hypoxia ATP is rapidly depleted and catabolized to adenosine, inosine, hypoxanthine, xanthine, and uric acid (Farthing et al., 2015). Our results showed that calafate had similar metabolic changes, because the Hcal group showed a reduction of inosine and hypoxanthine in comparison with the H, reaching levels in the same magnitude than N group, which is in accordance with reduction or oxidative stress.

On the other hand, Hydroxybutyric acid 103.0407 m/z (-10.0 ppm) showed a tendency to decrease from H to N level ($p < 0.05$). In a metabolomic study was reported that 2-Hydroxybutyric acid is early biomarker for insulin resistance and impaired glucose regulation, distinguish Normal Glucose

Tolerance (NGT) -Insulin Sensible (IS) subjects from impaired glucose metabolism subjects, and hydroxybutyric acid serve as early indicators of Insulin Resistance (IR) by distinguishing NGT-IS from NGT-IR subjects in plasma (Gall et al., 2010). 2-Hydroxybutyric acid is synthesized due to a impaired oxidative phosphorylation, metabolism is then focused to the synthesis of acetoacetic acid and hydroxybutyric acid (Bruzzone et al., 2020). This is coherent with our previous findings in plasma, where changes in succinic acid and carnitines, showed an altered β-oxidation and an altered tricarboxylic cycle which was reversed by calafate intake (Olivares-Caro et al 2022).

Metabolite 5-hydroxy-6E,8Z,11Z-eicosatrienoic acid (5-HETrE) 321.2437 m/z (2.83 ppm) showed the same tendency of Hydroxybutyric acid. Calafate showed a reduction of 5HETrE level with respect to H, but without statistical significance (tendency), however, a difference was verified for H vs N ($p < 0.05$). 5- HETrE is an eicosanoid, which correspond to oxidized derivatives of 20-carbon polyunsaturated fatty acids (PUFAs), usually arachidonic acid. Eicosanoids are products of the endothelial cells that influence blood coagulation, inflammation, and vascular smooth muscle cells. In metabolic and cardiovascular disease its synthesis is altered contributing to the vascular

dysfunction, inflammation, and atherosclerosis (Imig, 2020). The tendency of reduction produced for calafate are in concordance with lipid peroxidation reduction.

The feature 295.2261 m/z (6 ppm) was identified as hydroxyoctadecadienoic acid $C_{18}H_{32}O_3$. This metabolite showed similar levels for H and N groups, due to the high data dispersion observed in H group. For Hcal group, we observed a reduction compared with N group ($p < 0.05$). Hydroxyoctadecadienoic (HODE) acid is an oxidation product of linoleic acid, a major constituent of low-density lipoproteins (LDLs), by the action of ROS. It has been shown that in obese patients, HODEs are increased by 59% in plasma LDL (Colas et al., 2011; Vangaveti et al., 2016). Besides, Epoxyoctadecanoic acid $C_{18}H_{34}O_3$ 297.2422 m/z (7.7 ppm) is other metabolite obtained from linoleic acid by epoxygenase isoenzymes, and we observed a similar behavior than hydroxyoctadecadienoic acid. (Bannehr et al., 2019) has shown that epoxyoctadecanoic acid decreases post-ischemic functional recovery of the left ventricle in murine hearts C57Bl6. Other metabolites found with similar behavior were 9-hexadecenoylcarnitine $C_{23}H_{43}NO_4$ 398.3260 m/z (1.0 ppm) and palmitoylcarnitine $C_{23}H_{45}NO_4$ 400.3413 m/z (-4.3 ppm), which decreased with calafate intake when it is

compared with H and N group ($p < 0.05$), however, differences between H and N group were not found. This finding is comparable with previous result obtained in plasma (Olivares-Caro, et al. 2022). An increase of acylcarnitines has been found in the plasma of obese volunteers and participants with type 2 diabetes mellitus, suggesting a defect in the use of succinyl-CoA in the tricarboxylic acid cycle and an increase in incomplete β-oxidation in skeletal muscle (Mihalik et al., 2010).

Feature 259.0356 m/z (-0.6 ppm) was identified as Inositolphosphate $C_6H_{13}O_9P$ which was found reduced in H group compared with N ($p < 0.05$). A tendency of increase from H group to Hcal group was observed. This metabolite is involucrate in glycerophospholipid metabolism and has been related with oxidative stress protection (Can Chen et al., 2019). Other study has been demonstrated that E10 cardiomyocytes exposed to Inositol 3-phosphate 10 μM produce spontaneous rate of calcium from sarcoplasmic reticulum, and increase the beating frequency in myocyte cultures by 27.3 ± 9.2% (Rapila et al., 2008). The same behavior was observed for inositol isomer $C_6H_{12}O_6$ 179.0565 m/z (-2.2ppm), which is product of Inositol 1-phosphate (KEEG pathway: map00562). Eight inositol structural stereoisomers naturally occurring, which are named scyllo-, muco-, epi-, neo-

, allo-, L-chiro-, D-chiro-, and myo-inositols (Monnard et al., 2020). (Croze & Soulage, 2013) has been reported that myo-inositol participate in glucose homeostasis, cell survival and growth, osteogenesis, metabolism and reproduction. Inositol isomers play insulin-mimetic activities, myoinositol administration in pregnancy reduced prevalence of gestational diabetes in 17.4% versus 54% in control group (D'Anna et al., 2011). An study has demonstrated that intragastrict administration of chiroinositol (10mg/Kg) in diabetics rats decreased 30- 40% the plasma glucose level (Ortmeyer et al., 1993). Thus, calafate have a positive effect increasing the level of some of these inositol derivatives.

15-Oxo-11-eicosenoic acid $C_{20}H_{36}O_3$ corresponds to feature 323.2570 m/z (1.3 ppm). It was observed an increased in this fatty acid from N to H group ($p < 0.05$) in heart tissue. A decreasing trend was observed in the Hcal group, which could be explained by the β-oxidation activated by calafate, which has been previously described by our research group in plasma (Olivares-Caro et al 2022).

Metabolite 357.2624 (-0.7 ppm) was identified as 13,14-Dihidro PGF-1a $C_{20}H_{38}O_5$. 13,14-Dihidro PGF-1a increased in H group compared to N group ($p < 0.05$), and a low tendency to decrease was observed in Hcal group. 13,14-

Dihydro PGF-1alpha is a prostanoid derived from C-20 polyunsaturated fatty acids through the action of cyclooxygenase (Masoodi & Nicolaou, 2007). Prostaglandins have been associated with inflammation, oxidative stress and lipid peroxidation (Van't Erve et al., 2016), and calafate intake showed a tendency of decreased it in heart tissue, which can be considered a beneficial effect on both oxidative stress and lipid peroxidation .

These findings are in agreement with our previous report (Olivares-Caro et al., 2020) in which calafate extract (2 mg fresh fruit/mL) reduced oxidative stress in HUVEC cells (human umbilical vein endothelial cells) by around 51% and completely inhibited human LDL oxidation (Olivares-Caro et al., 2020). Significant metabolites identified in the present research could be related to a protective effect of calafate at the heart tissue, as a complement of beneficial effects described in endothelium, ROS production and metabolome changes.

Other metabolites changed from N to H. Feature 538.3114 m/z (-8.5 ppm) was identified as LysoPC (16:1/0:0) $C_{24}H_{48}NO_7P$. This metabolite was decreased in H and Hcal mice compared to N mice ($p<0.05$). A negative association between LysoPC and coronary heart disease (CHD) has been found (Ganna et al., 2014). This metabolomic study profiling reported that

higher LysoPC levels were associated with high levels of high-density lipoprotein cholesterol (HDL- C), whose protective cardiovascular effects are well known; together, lysoPC levels are related to decreased low-density lipoprotein cholesterol (LDL-C) levels and lower body mass index (BMI), two cardiovascular risk factors in CHD patients (Ganna et al., 2014).

Cholyltryptophan $C_{35}H_{50}N_2O_6$ 593.3617 m/z (4 ppm) is a bile aminoacid-conjugated , which was increased in H group compared to N ($p < 0.05$). Bile acids play an important role in regulating various physiological systems, such as fat digestion (Guzior & Quinn, 2021), which explained Cholyltryptophan increase in H group.

523.1564 m/z (7 ppm) and 335.0595 m/z (0 ppm) were identified as glutamylaspartic $C_9H_{14}N_2O_7$ acid and galactoselactate $C_9H_{16}O_9$. These metabolites decreased in Hcal group compared with the H group ($p < 0.05$), reaching similar levels than the N group. Despite the statistical difference between groups, we don't found relation of these compound with the other findings.

Finally, it has been shown that obesity affects the insulin signaling pathway, which produces an inhibition of GLUT4 translocation and glucose uptake

(KEEG map04931 and map04910). Based on the above results, we propose that calafate could influence the insulin signaling pathway, through purine metabolism and inositol metabolism in cardiac tissue. Intake of calafate increased insulin mimetic metabolites, reduced metabolites derived from ATP catabolism, acylcarnitines and ketone bodies compared to group H. This suggests that calafate activates fatty acid oxidation and the TCA cycle, participates in the regulation of cardiac homeostasis. This effect is shown in Figure 4.3.7 (purple arrows).

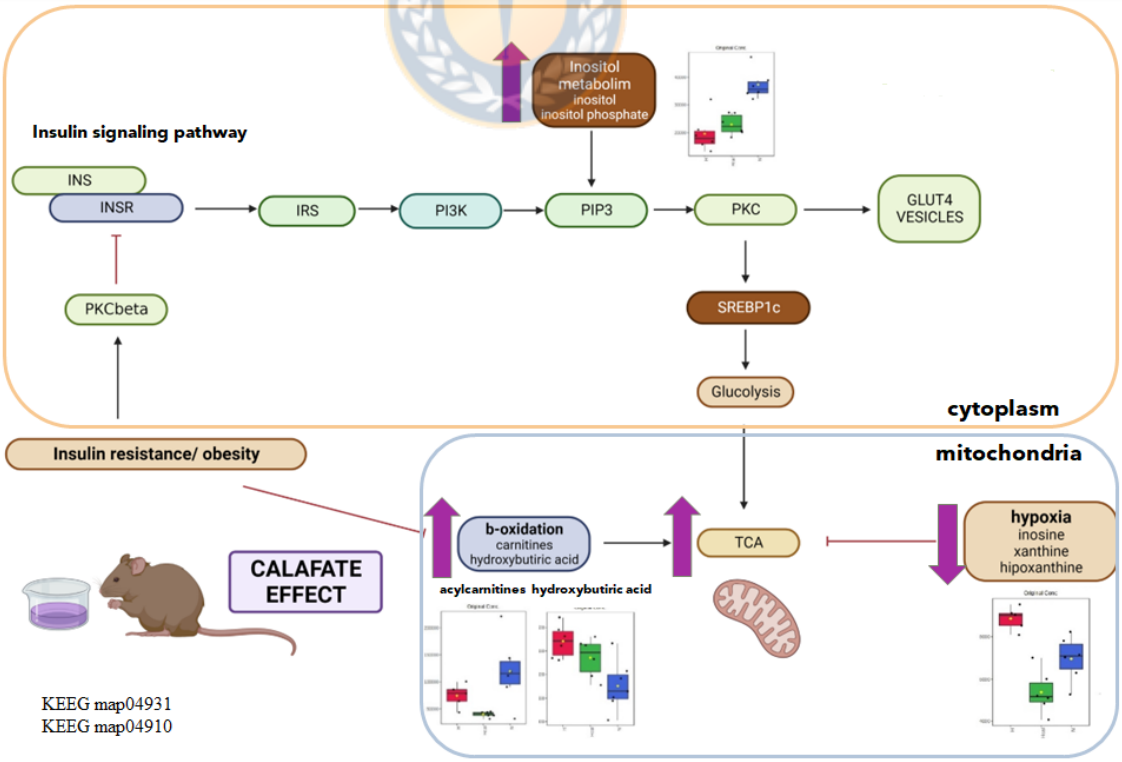

Figura 4.3.7: Biological effect of calafate on cardiac tissue (purple arrow).

4.3.4 Conclusion

Calafate extract modified the heart tissue metabolome of mice exposed to a high-fat diet. The increase of metabolites in H group, such as inosine, hypoxanthine, phosphoribosyl formamidocarboxamide and hydroxybutyric acid, are related to a purine metabolism altered and impaired oxidative phosphorylation. However, calafate intake reduced its levels, suggesting an effect on ROS, endothelial dysfunction, and oxidative phosphorylation in heart tissue, that could be related to a possible cardiovascular protective effect.

4.3.5. Acknowledgment

This work was supported by ANID Chile: Beca Doctorado Nacional [21170812]; FONDECYT [1191276]; and FONDEQUIP [170023], CENTROS BASALES ACE210012. Figure 4.3.7 was created with BioRender.com. We thank Mr. César Busolich from Secretos de la Patagonia, Punta Arenas, Chile, who provided calafate samples.

4.3.6. Conflict of interest

The authors declare they have no conflicts of interest.

4.3.7. CRediT author statement

Lia OLIVARES-CARO: Validation, Methodology, Formal analysis, Investigation, Data Curation, Writing - Original Draft, Funding acquisition. Daniela NOVA: Validation, Investigation, Data Curation. Danilo ESCOBAR: Data Curation. Claudia RADOJKOVIC: Writing - Review & Editing, Visualization. Daniel DURAN: Methodology, Investigation, Supervision. Luis BUSTAMANTE: Writing - Review & Editing, Visualization, Data Curation. Andy PEREZ: Methodology. Claudia MARDONES: Conceptualization, Data Curation, Resources, Writing - Original Draft, Writing - Review & Editing, Supervision, Project administration, Funding acquisition.

4.3.8 References

Alseekh, S., Aharoni, A., Brotman, Y., Contrepois, K., D'Auria, J., Ewald, J., C. Ewald, J., Fraser, P. D., Giavalisco, P., Hall, R. D., Heinemann, M., Link, H., Luo, J., Neumann, S., Nielsen, J., Perez de Souza, L., Saito, K., Sauer, U., Schroeder, F. C., … Fernie, A. R. (2021). Mass spectrometry-based metabolomics: a guide for annotation, quantification and best reporting practices. Nature Methods, 18(7), 747–756. https://doi.org/10.1038/s41592-021-01197-1

Armirotti, A., Basit, A., Realini, N., Caltagirone, C., Bossù, P., Spalletta, G., & Piomelli, D. (2014). Sample preparation and orthogonal chromatography for broad polarity range plasma metabolomics: Application to human

subjects with neurodegenerative dementia. Analytical Biochemistry, 455(1), 48–54. https://doi.org/10.1016/j.ab.2014.03.019

Bannehr, M., Löhr, L., Gelep, J., Haverkamp, W., Schunck, W. H., Gollasch, M., & Wutzler, A. (2019). Linoleic Acid Metabolite DiHOME Decreases Post-ischemic Cardiac Recovery in Murine Hearts. Cardiovascular Toxicology, 19(4), 365–371. https://doi.org/10.1007/s12012-019-09508-x

Bruzzone, C., Bizkarguenaga, M., Gil-Redondo, R., Diercks, T., Arana, E., García de Vicuña, A., Seco, M., Bosch, A., Palazón, A., San Juan, I., Laín, A., Gil-Martínez, J., Bernardo-Seisdedos, G., Fernández-Ramos, D., Lopitz-Otsoa, F., Embade, N., Lu, S., Mato, J. M., & Millet, O. (2020). SARS-CoV-2 Infection Dysregulates the Metabolomic and Lipidomic Profiles of Serum. IScience, 23(10). https://doi.org/10.1016/j.isci.2020.101645

Bustamante, L., Pastene, E., Duran-Sandoval, D., Vergara, C., Von Baer, D., & Mardones, C. (2018). Pharmacokinetics of low molecular weight phenolic compounds in gerbil plasma after the consumption of calafate berry (Berberis microphylla) extract. Food Chemistry, 268(February), 347–354. https://doi.org/10.1016/j.foodchem.2018.06.048

Campos, J., Schmeda-Hirschmann, G., Leiva, E., Guzmán, L., Orrego, R., Fernández, P., González, M., Radojkovic, C., Zuñiga, F. A., Lamperti, L., Pastene, E., & Aguayo, C. (2014). Lemon grass (Cymbopogon citratus (D.C) Stapf) polyphenols protect human umbilical vein endothelial cell (HUVECs) from oxidative damage induced by high glucose, hydrogen peroxide and oxidised low-density lipoprotein. Food Chemistry, 151, 175–181. https://doi.org/10.1016/j.foodchem.2013.11.018

Chaban, V., Nakstad, E. R., Stær-Jensen, H., Schjalm, C., Seljeflot, I., Vaage, J., Lundqvist, C., Benth, J. Š., Sunde, K., Mollnes, T. E., Andersen, G., & Pischke, S. E. (2021). Complement activation is associated with poor outcome after out-of-hospital cardiac arrest. Resuscitation, 166(May), 129–136. https://doi.org/10.1016/j.resuscitation.2021.05.038

Chen, C., Chen, K., Su, T., Zhang, B., Li, G., Pan, J., & Si, M. (2019). Myo-inositol-1-phosphate synthase (Ino-1) functions as a protection mechanism in

Corynebacterium glutamicum under oxidative stress. MicrobiologyOpen, 8(5), 1–12. https://doi.org/10.1002/mbo3.721

Colas, R., Sassolas, A., Guichardant, M., Cugnet-Anceau, C., Moret, M., Moulin, P., Lagarde, M., & Calzada, C. (2011). LDL from obese patients with the metabolic syndrome show increased lipid peroxidation and activate platelets. Diabetologia, 54(11), 2931–2940. https://doi.org/10.1007/s00125-011-2272-8

Croze, M. L., & Soulage, C. O. (2013). Potential role and therapeutic interests of myo-inositol in metabolic diseases. Biochimie, 95(10), 1811–1827. https://doi.org/10.1016/j.biochi.2013.05.011

Curtasu, M. V., Knudsen, K. E. B., Callesen, H., Purup, S., Stagsted, J., & Hedemann, M. S. (2019). Obesity Development in a Miniature Yucatan Pig Model: A Multi-compartmental Metabolomics Study on Cloned and Normal Pigs Fed Restricted or Ad Libitum High-Energy Diets. Journal of Proteome Research, 18(1), 30–47. https://doi.org/10.1021/acs.jproteome.8b00264

D'Anna, R., Benedetto, V., Rizzo, P., Raffone, E., Interdonato, M. L., Licata, G., Corrado, F., & Di Benedetto, A. (2011). O11. Myo-inositol may prevent metabolic and hypertensive disorders in PCOS pregnant women. Pregnancy Hypertension: An International Journal of Women's Cardiovascular Health, 1(3–4), 262. https://doi.org/10.1016/j.preghy.2011.08.043

Farthing, D. E., Farthing, C. A., & Xi, L. (2015). Inosine and hypoxanthine as novel biomarkers for cardiac ischemia: From bench to point-of-care. Experimental Biology and Medicine, 240(6), 821–831. https://doi.org/10.1177/1535370215584931

Gall, W. E., Beebe, K., Lawton, K. A., Adam, K. P., Mitchell, M. W., Nakhle, P. J., Ryals, J. A., Milburn, M. V., Nannipieri, M., Camastra, S., Natali, A., & Ferrannini, E. (2010). A-Hydroxybutyrate Is an Early Biomarker of Insulin Resistance and Glucose Intolerance in a Nondiabetic Population. PLoS ONE, 5(5). https://doi.org/10.1371/journal.pone.0010883

Ganna, A., Salihovic, S., Sundström, J., Broeckling, C. D., Hedman, Å. K., Magnusson, P. K. E., Pedersen, N. L., Larsson, A., Siegbahn, A., Zilmer, M., Prenni, J., Ärnlöv, J., Lind, L., Fall, T., & Ingelsson, E. (2014). Large-scale Metabolomic Profiling Identifies Novel Biomarkers for Incident Coronary Heart Disease. PLoS Genetics, 10(12). https://doi.org/10.1371/journal.pgen.1004801

Guzior, D. V., & Quinn, R. A. (2021). Review: microbial transformations of human bile acids. Microbiome, 9(1), 1–13. https://doi.org/10.1186/s40168-021-01101-1

Imig, J. D. (2020). Eicosanoid blood vessel regulation in physiological and pathological states. Clinical Science, 134(20), 2707–2727. https://doi.org/10.1042/CS20191209

Kim, Y. J., Ryu, H. M., Choi, J. Y., Cho, J. H., Kim, C. D., Park, S. H., & Kim, Y. L. (2017). Hypoxanthine causes endothelial dysfunction through oxidative stress-induced apoptosis. Biochemical and Biophysical Research Communications, 482(4), 821–827. https://doi.org/10.1016/j.bbrc.2016.11.119

Laursen, M. R., Hansen, J., Elkjær, C., Stavnager, N., Nielsen, C. B., Pryds, K., Johnsen, J., Nielsen, J. M., Bøtker, H. E., & Johannsen, M. (2017). Untargeted metabolomics reveals a mild impact of remote ischemic conditioning on the plasma metabolome and α-hydroxybutyrate as a possible cardioprotective factor and biomarker of tissue ischemia. Metabolomics, 13(67), 1–13. https://doi.org/10.1007/s11306-017-1202-2

Lobo, V., Patil, A., Phatak, A., & Chandra, N. (2010). Free radicals, antioxidants and functional foods: Impact on human health. Pharmacognosy Reviews, 4(8), 118–126. https://doi.org/10.4103/0973-7847.70902

López Farré, A., & Macaya Miguel, C. (2009). Libro de la salud cardiovascular del hospital clínico San Carlos y la fundación BBVAلبترول (Primera 20). https://www.fbbva.es/microsites/salud_cardio/mult/fbbva_libroCorazon.pdf

Lubrano, V., & Balzan, S. (2020). Role of oxidative stress-related biomarkers in heart failure: galectin 3, α1-antitrypsin and LOX-1: new therapeutic perspective? Molecular and Cellular Biochemistry, 464(1–2), 143–152. https://doi.org/10.1007/s11010-019-03656-y

Masoodi, M., & Nicolaou, A. (2007). Lipidomic Analysis of Twenty Seven Prostanoids and Isoprostanes by Electrospray Liquid Chromatography / Tandem Mass Spectrometry. Europe PMC Funders Group, 20(20), 3023–3029. https://doi.org/10.1002/rcm.2697.Lipidomic

McGarrah, R. W., Crown, S. B., Zhang, G., Shah, S. H., & Newgard, C. B. (2018). Cardiovascular Metabolomics. Circulation Reasearch, 122(9), 1238–1258. https://doi.org/10.1161/CIRCRESAHA.117.311002.Cardiovascular

Mihalik, S. J., Goodpaster, B. H., Kelley, D. E., Chace, D. H., Vockley, J., Toledo, F. G. S., & Delany, J. P. (2010). Increased levels of plasma acylcarnitines in obesity and type 2 diabetes and identification of a marker of glucolipotoxicity. Obesity, 18(9), 1695–1700. https://doi.org/10.1038/oby.2009.510

Monnard, I., Bénet, T., Jenni, R., Austin, S., Silva-Zolezzi, I., & Godin, J. P. (2020). Plasma and urinary inositol isomer profiles measured by UHPLC-MS/MS reveal differences in scyllo-inositol levels between non-pregnant and pregnant women. Analytical and Bioanalytical Chemistry, 412(28), 7871–7880. https://doi.org/10.1007/s00216-020-02919-8

Morlock, G. E., & Vega-Herrera, M. A. (2007). Two new derivatization reagents for planar chromatographic quantification of sucralose in dietetic products. Journal of Planar Chromatography - Modern TLC, 20(6), 411–417. https://doi.org/10.1556/JPC.20.2007.6.4

Morton, D. ., & Griffiths, P. H. . (1985). Guidelines in the recognition of pain, distress anddisconform in experimental animal and an hypothesis for assessment. Veterinary Record, 116, 431–436. https://doi.org/http://dx.doi.org/10.1136/vr.116.16.431

Olivares-Caro, L., Radojkovic, C., Chau, S. Y., Nova, D., Bustamante, L., Neira, J. Y., Perez, A. J., & Mardones, C. (2020). Berberis microphylla G. Forst (calafate) berry extract reduces oxidative stress and lipid peroxidation of human LDL. Antioxidants, 9(12), 1–20. https://doi.org/10.3390/antiox9121171

Olivares-Caro, L., Nova, D., Radojkovic, C., Duran, D., Mennickent, D., Bustamante, L., Melin, V., Contreras, D., Perez, A., & Mardones, C. Berberis microphylla G. Forst intake reduces the impact of a high-fat diet on plasma cardiovascular disease factors. "submitted"

Ortmeyer, H. K., Huang, L. C., Zhang, L., Hansen, B. C., & Larner, J. (1993). Chiroinositol deficiency and insulin resistance. II. Acute effects of D-chiroinositol administration in streptozotocin-diabetic rats, normal rats given a glucose load, and spontaneously insulin-resistant rhesus monkeys. Endocrinology, September. https://doi.org/10.1210/endo.132.2.8425484

Patel, R. B., Colangelo, L. A., Bielinski, S. J., Larson, N. B., Ding, J., Allen, N. B., Michos, E. D., Shah, S. J., & Lloyd-Jones, D. M. (2020). Circulating vascular cell adhesion molecule-1 and incident heart failure: The multi-ethnic study of atherosclerosis (MESA). Journal of the American Heart Association, 9(22). https://doi.org/10.1161/JAHA.120.019390

Patterson, R. E., Ducrocq, A. J., McDougall, D. J., Garrett, T. J., & Yost, R. A. (2015). Comparison of blood plasma sample preparation methods for combined LC-MS lipidomics and metabolomics. Journal of Cromatography B, Analytical Technologies in the Biomedical and Life Sciences, 1002, 260–266. https://doi.org/10.1016/j.jchromb. 2015.08.018

Rapila, R., Korhonen, T., & Tavi, P. (2008). Excitation-contraction coupling of the mouse embryonic cardiomyocyte. Journal of General Physiology, 132(4), 397–405. https://doi.org/10.1085/jgp.200809960

Reil, J. C., & Böhm, M. (2007). The role of heart rate in the development of cardiovascular disease. Clinical Research in Cardiology, 96(9), 585–592. https://doi.org/10.1007/s00392-007-0537-5

Ruiz, A., Hermosín-Gutiérrez, I., Vergara, C., von Baer, D., Zapata, M., Hitschfeld, A., Obando, L., & Mardones, C. (2013). Anthocyanin profiles in south Patagonian wild berries by HPLC-DAD-ESI-MS/MS. Food Research International, 51(2), 706–713. https://doi.org/10.1016/j.foodres.2013.01.043

Ruiz, A., Mardones, C., Vergara, C., Hermosín-gutiérrez, I., Baer, D. Von, Hinrichsen, P., Rodriguez, R., Arribillaga, D., & Dominguez, E. (2013). Analysis of hydroxycinnamic acids derivatives in calafate (Berberis microphylla G . Forst) berries by liquid chromatography with photodiode array and mass spectrometry detection. Journal of Chromatography A, 1281, 38–45. https://doi.org/10.1016/j.chroma.2013.01.059

Schmeda-Hirschmann, G., Jiménez-Aspee, F., Theoduloz, C., & Ladio, A. (2019). Patagonian berries as native food and medicine. Journal of Ethnopharmacology, 241, 111979. https://doi.org/10.1016/j.jep.2019.111979

Sikorski, V., Karjalainen, P., Blokhina, D., Oksaharju, K., Khan, J., Katayama, S., Rajala, H., Suihko, S., Tuohinen, S., Teittinen, K., Nummi, A., Nykänen, A., Eskin, A., Stark, C., Biancari, F., Kiss, J., Simpanen, J., Ropponen, J., Lemström, K., Savinainen, K., Lalowski, M., Kaarne, M., Jormalainen, M., Elomaa, O., Koivisto, P., Raivio, P., Bäckström, P., Dahlbacka, S., Syrjälä, S., Vainikka, T., Vähäsilta, T., Tuncbag, N., Karelson, M., Mervaala, E., Juvonen, T., Laine, M., Laurikka, J., Vento, A.,& Kankuri, E. (2021). Epitranscriptomics of ischemic heart disease-the IHD-EPITRAN study design and objectives. International Journal of Molecular Sciences, 22(12). https://doi.org/10.3390/ijms22126630

Van't Erve, T. J., Lih, F. B., Jelsema, C., Deterding, L. J., Eling, T. E., Mason, R. P., & Kadiiska, M. B. (2016). Reinterpreting the best biomarker of oxidative stress: The 8-iso-prostaglandin F2α/prostaglandin F2α ratio shows complex origins of lipid peroxidation biomarkers in animal models. Free Radical Biology and Medicine, 95, 65–73. https://doi.org/10.1016/j.freeradbiomed.2016.03.001

Vangaveti, V. N., Jansen, H., Kennedy, R. L., & Malabu, U. H. (2016). Hydroxyoctadecadienoic acids: Oxidised derivatives of linoleic acid and

their role in inflammation associated with metabolic syndrome and cancer. European Journal of Pharmacology, 785, 70–76. https://doi.org/10.1016/j.ejphar.2015.03.096

Vlachogiannis, N. I., Sachse, M., Georgiopoulos, G., Zormpas, E., Bampatsias, D., Delialis, D., Bonini, F., Galyfos, G., Sigala, F., Stamatelopoulos, K., Gatsiou, A., & Stellos, K. (2021). Adenosine-to-inosine Alu RNA editing controls the stability of the pro-inflammatory long noncoding RNA NEAT1 in atherosclerotic cardiovascular disease. Journal of Molecular and Cellular Cardiology, 160, 111–120. https://doi.org/10.1016/j.yjmcc.2021.07.005

Wang, Y., Yin, L., Hu, B., Tse, L. A., Liu, Y., Ma, H., & Li, W. (2021). Association of heart rate with cardiovascular events and mortality in hypertensive and normotensive population: a nationwide prospective cohort study. Annals of Translational Medicine, 9(11), 1–13. https://doi.org/10.21037/atm-21-706

Weil, B. R., & Neelamegham, S. (2019). Selectins and immune cells in aucte mycardial infarction and post-infarction ventricular remodelings: Pathophysiology and novel treatments. Frontiers in Immunology, 10(FEB), 1–15. https://doi.org/10.3389/fimmu.2019.00300

Wells, A., Barrington, W. T., Dearth, S., May, A., Threadgill, D. W., Campagna, S. R., & Voy, B. H. (2018). Tissue Level Diet and Sex-by-Diet Interactions Reveal Unique Metabolite and Clustering Profiles Using Untargeted Liquid Chromatography-Mass Spectrometry on Adipose, Skeletal Muscle, and Liver Tissue in C57BL6/J Mice. Journal of Proteome Research, 17(3), 1077–1090. https://doi.org/10.1021/acs.jproteome.7b00750

5. CONCLUSION GENERAL

El fruto de *Berberis microphylla*, calafate, posee un amplio perfil de compuestos bioactivos, dentro de los cuales es posible identificar compuestos fenólicos, ácidos grasos y metales. Su composición constituye un producto con propiedades nutracéuticas para el consumo humano.

El calafate tiene una alta capacidad antioxidante, lo que fue demostrado mediante ensayos *in-vitro*, utilizando modelos químicos y biológicos. Los extractos metanólico y etanólico de este fruto, disminuyeron la producción de ROS en un modelo de células HUVEC y la lipoxidación de LDL humana, procesos involucrados durante el estrés oxidativo y el desarrollo de enfermedad cardiovascular.

El consumo de un extracto de calafate provocó un cambio en proteínas y el metaboloma del plasma de ratones expuestos a una dieta alta en grasas, disminuyendo el efecto de la dieta en marcadores de riesgo cardiovascular. El consumo de calafate indujo una disminución en plasma de proteínas asociadas a disfunción endotelial, un desbloqueo de la β-oxidación mitocondrial y un aumento en la actividad del ciclo de Krebs.

Además, se observó un cambio en el metaboloma del corazón de estos ratones, un órgano protagonista en la patología cardiovascular y en los eventos agudos de la ECV. Posterior al consumo de calafate, se observó una disminución en un metabolito como inosina, que ha sido asociado a la patología aterosclerótica.

El conjunto de estos resultados sugiere que el consumo del calafate podría generar una reducción en el riesgo de sufrir enfermedad cardiovascular, debido a efectos protectores a nivel endotelial, plasmático y cardíaco.

Finalmente, respondiendo a la hipótesis de esta tesis doctoral, es posible destacar que:

1) Un extracto de calafate disminuye marcadores asociados con estrés oxidativo, disfunción endotelial y peroxidación lipídica relacionados con factores de riesgo de la patología cardiovascular en modelos biológicos *in vitro e in vivo*,
2) La implementación secuencial de estudios *in vitro* e *in vivo* permiten constituir una plataforma bioanalítica para el estudio integral del efecto del consumo de calafate.

3) La herramienta analítica metabolómica basada en UHPLC-QTOF-MS/MS constituye una poderosa herramienta analítica para detectar biomarcadores en el contexto de alimentos funcionales.

PRODUCTIVIDAD

1. Publicaciones científicas

- BERBERIS MICROPHYLLA G. FORST (CALAFATE) BERRY EXTRACT REDUCES OXIDATIVE STRESS AND LIPID PEROXIDATION OF HUMAN LDL

Olivares-Caro. L, Radojkovic. C, Chau. SY, Nova. D, Bustamante. L, Neira. JY, Perez. AJ and Mardones. C.

Paper publicado en *Antioxidants* año 2020 https://doi.org/10.3390/antiox9121171

- BERBERIS MICROPHYLLA G. FORST INTAKE REDUCES THE IMPACT OF A HIGH-FAT DIET ON PLASMA CARDIOVASCULAR DISEASE FACTORS

Lia OLIVARES-CARO, Daniela NOVA, Claudia RADOJKOVIC, Daniel DURAN, Daniela MENNICKENT, Luis BUSTAMANTE, Victoria MELIN, David CONTRERAS, Andy PEREZ, Claudia MARDONES*

Paper enviado a Food Chemistry FOODCHEM-D-22-05672 año 2022

- CHANGES IN THE METABOLOME OF HEART TISSUE OF MICE ASSOCIATED TO CALAFATE INTAKE AND REDUCTION OF CARDIOVASCULAR RISK.

Lia OLIVARES-CARO, Daniela NOVA, Danilo ESCOBAR, Claudia RADOJKOVIC, Daniel DURAN, Luis BUSTAMANTE, Andy PEREZ, Claudia MARDONES *

Paper en redacción, año 2022.

2. Participación en otras publicaciones

- METABOLIC PROFILE AND ANTIOXIDANT CAPACITY OF FIVE BERBERIS LEAVES SPECIES: A COMPREHENSIVE STUDY TO DETERMINE THEIR POTENTIAL AS NATURAL FOOD OR INGREDIENT

Daniela NOVA-BAZA, Lía OLIVARES-CARO, Luis BUSTAMANTE, Andy J. PEREZ, Carola VERGARA, Jorge FUENTEALBA , Claudia MARDONES*

Paper publicado en *Food Research International journal* año 2022 https://doi.org/10.1016/j.foodres.2022.111642

3. Participación en congresos

- EVALUACIÓN DEL EFECTO BENÉFICO DE BERBERIS MICROPHYLLA G. FORST (CALAFATE) UTILIZANDO UN MODELO MURINO DE DIETA ALTA GRASAS Y UNA ESTRATEGIA ANALÍTICA METABOLÓMICA BASADA EN UHPLC-QTOF.

Olivares-Caro, L., Mennickent, D., Nova, D., Radojkovic, C., Bustamante, L., Mardones, C.

Presentación oral

34° Congreso Latinoamericano de Química CLAQ 2020, el XVIII COLACRO, el X COCOCRO, el II SPAE y el IV C2B2.

11 al 15 de octubre de 2021, Cartagena, Colombia.

- CAMBIOS OBSERVADOS EN EL PERFIL DE COMPUESTOS BIOACTIVOS DURANTE EL PROCESO DE ONTOGENIA EN HOJAS DE BERBERIS MICROPHYLLA G.FORST.

Olivares. L, Nova. D, Bustamante. L, Mardones. C.

Poster.

XXXIII Jornadas chilenas de química.

Puerto Varas Chile 2020.

- COMPARACIÓN DE MÉTODOS DE EXTRACCIÓN PARA ANÁLISIS METABOLÓMICO NO DIRIGIDO EN PLASMA POR UHPLC-ESI-QTOF-MS

Mennickent, D., Olivares, L., Bustamante, L., Pérez, A., Mardones, C.

Poster.

XXXIII Jornadas chilenas de química 2020.

Puerto Varas Chile 2020.

- HPLC-DAD-QTOF PROFILES OF HYDROXYCINNAMIC ACIDS IN CALAFATE BERRIES AND LEAVES AND THEIR BIOLOGIC ACTIVITIES

Nova, D, Olivares, L, Véjar,C, von Baer, D, Radojkovic, C, Mardones

Poster y presentación oral.

Latin american symposium on chromatography and related techniques. national symposium on chromatography workshop in recent advances in sample preparation.

Aracaju Brasil 2019.

- EXTRACTS OF BERBERIS MICROPHYLLA (CALAFATE) REDUCE THE PRODUCTION OF ROS IN HUVEC.

Olivares, L., Vejar, C, Radojkovic, C, Mardones, C

Poster

III Meeting on research and innovation in vascular health. V Meeting on hipertension in pregnancy.

Chillán Chile 2019.

- CALAFATE (*Berberis microphylla*): A CHILEAN PATAGONIA FRUIT WITH HIGH ANTIOXIDANT CAPACITY

Olivares, L. Bustamante, L., Radojkovic, C., Mardones, C

Poster

IV Workshop anual INSA-UB “Ciència i propietats del cava i el vi".

Barcelona España 2018.

- EVALUACIÓN DE LA ACTIVIDAD ANTIMICROBIANA DE EXTRACTOS DE FRUTO DE CALAFATE (*Berberis microphylla*) G. FORST PREVIAMENTE CARACTERIZADOS POR HPLC-DAD Y SU CAPACIDAD ANTIOXIDANTE

Véjar-Vivar, C., Parra, C., Olivares, L. García, A., Mardones, C.

Poster

XIII Simposio Latinoamericano de Química Analítica y Ambiental, y el XIV Encuentro de Química Analítica y Ambiental

Chile 2018

- EXTRACTOS DE Berberis microphylla (CALAFATE) REDUCEN LA PRODUCCIÓN DE ROS EN UN MODELO CELULAR

Olivares, L., Vejar, C., Radojkovic, C., Mardones, C.

Poster

XIII Simposio Latinoamericano de Química Analítica y Ambiental, y el XIV Encuentro de Química Analítica y Ambiental.

Chile 2018.

4. Participación en proyectos de investigación

- Profesional Bioquímico FONDEF IDeA ID20I10078

ZebraMarTox: Herramienta toxicológica basada en pez cebra para el screening de toxinas marinas en bioseguridad alimentaria"

Investigadora responsable Dra. Alejandra Llanos

Actividades: Transporte de muestras biológicas, almacenamiento y organización. Extracción de muestras de plasma, análisis UHPLC-DAD-QTOF, procesamiento multivariado de datos y análisis de resultados. Gestión en la compra insumos de laboratorio. Organización y planificación de actividades prácticas.

- Encargada analítica Proyecto COVID 0370 "Identificación de los principales metabolitos plasmáticos asociados a severidad de COVID-19, a través de una estrategia metabolómica basada en UHPLC-QTOF-MS/MS". Investigador responsable Dra. Claudia Mardones

Actividades: Transporte de muestras biológicas (plasma y suero), almacenamiento y organización. Extracción de muestras de plasma, análisis UHPLC-DAD-QTOF, procesamiento multivariado de datos y análisis de resultados. Procesamiento de muestras por MAGPIX: determinación de marcadores de inflamación. Gestión en la compra insumos de laboratorio. Organización y planificación de actividades prácticas.

- Participación en proyecto FONDECYT Regular1191276. "A combined analytical strategr based on metabolomics and targeted analysis using UHPLC-QTOF-MS, UHPLC-ESI-MSII\4S and GC-EI-MSIIVíS for the study of health beneficial effects of calafate consumption".

Investigador responsable Dra. Claudia Mardones.

Actividades: Extracción de muestras de plasma y órganos de ratón, análisis UHPLC-DAD-QTOF, procesamiento multivariado de datos y análisis de resultados. Gestión en la compra insumos de laboratorio**.**

- Proyecto: Research network on functional food between the Technological Development Unit and the Institut de Recerca en Nutrició i Seguretat Alimentària.

Estancia en “Institut de Recerca en Nutrició i Seguretat Alimentària”.

Universidad de Barcelona. España.

Periodo: 03-Octubre-2018 al 03-Diciembre-2018

Financiamiento: Proyecto REDES170051

5. Becas y distinciones

- Beca CONICYT Doctorado Nacional 2017 folio 21170812. Beca que me ha dado la posibilidad de continuar estudios de postgrado con beca de arancel, manutención mensual y gastos de operación. https://www.conicyt.cl/becasconicyt/2016/09/28/becas-de-doctorado-nacional-ano-academico-2017/#tab-05

- Gastos de operación, Beca CONICYT Doctorado Nacional 2017 folio 21170812, fondos concursable para desarrollar trabajo de laboratorio y compra de instrumentación menor. https://www.conicyt.cl/becasconicyt/files/2019/08/Listado_GOP_Aprobado_PUBLICAR.pdf

- Premio Universidad de Concepción (UNIVERSIDAD DE CONCEPCION, Chile, 2015). Mejor egresado de la promoción Bioquímica 2010, que me ha otorgado la posibilidad de estudiar un postgrado exenta del pago de arancel.

- Distinción Poster XXXIII Jornadas chilenas de química 2020 (PUERTO VARAS, Chile, 2020). Se otorgó reconocimiento al poster presentado "Cambios observados en el perfil de compuestos bioactivos durante el proceso de ontogenia en hojas de Berberis microphylla G.Forst" con una membresía en American Chemical Society. https://www.schq.cl/jchq2020/.

- Distinción presentación oral en Salud Publica, en las II Jornadas de Especialidades farmacéuticas y Bioquímicas 2022, al trabajo titulado “Cambios en el metaboloma plasmático de población Chilena de pacientes COVID-19 asociados con su grado de severidad, utilizando una herramienta analítica metabolómica”.

ANEXOS

1. **SUPPLEMENTARY MATERIAL:** *Berberis microphylla* (calafate) berry extract reduces oxidative stress and lipid peroxidation of human LDL in *in vitro* models

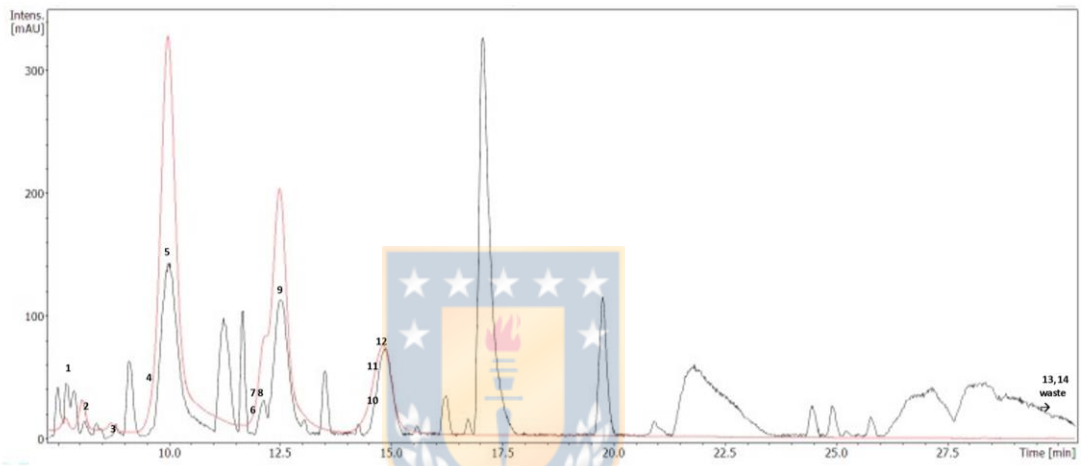

Figure S1: Base peak chromatogram ESI + crude extract calafate (black) and DAD chromatogram to 520 nm (red)

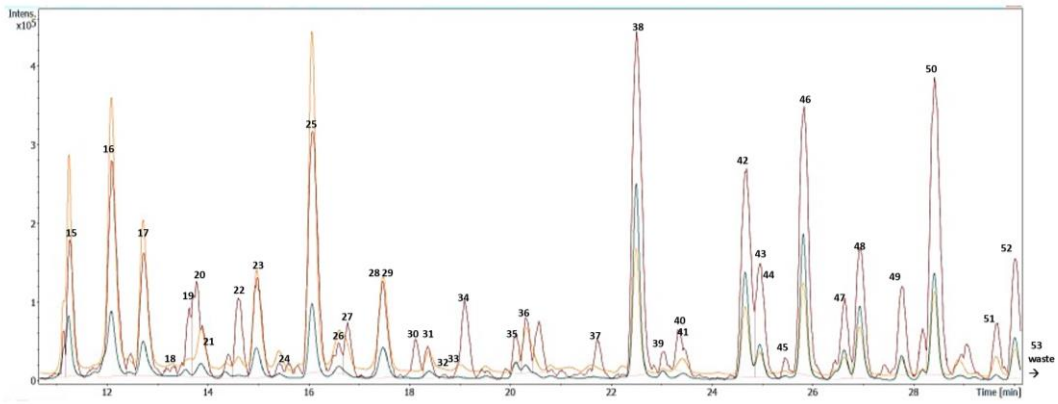

Figure S2: Base peak chromatogram ESI- extract previously purify with solid extraction for hydroxycinnamic acid derivatives (red), DAD chromatogram 320 nm (yellow) and DAD chromatogram 360 nm (green).

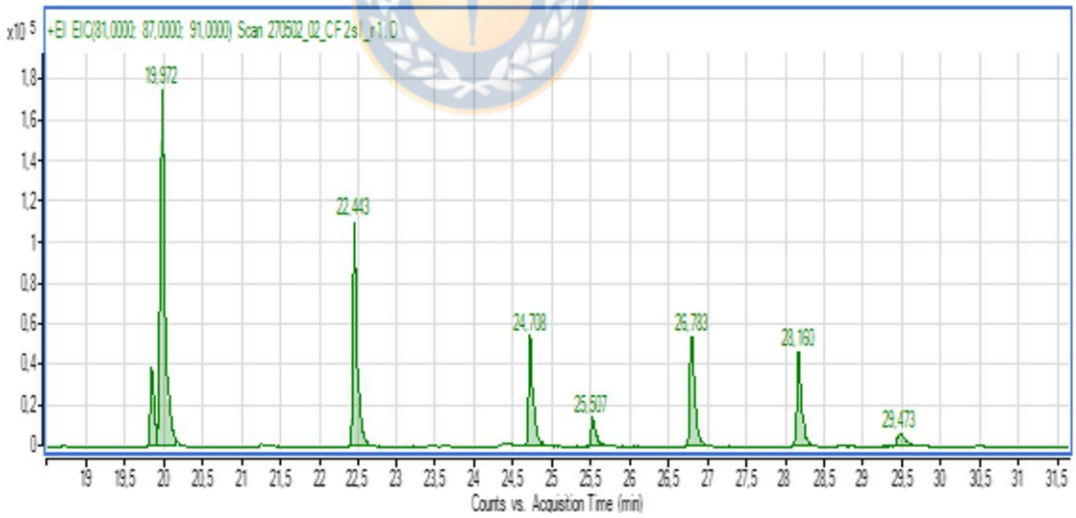

Figure S3: Extracted ion chromatogram (EIC) of fatty acids profile in calafate fruit (81 m/z; 87 m/z; 91 m/z).

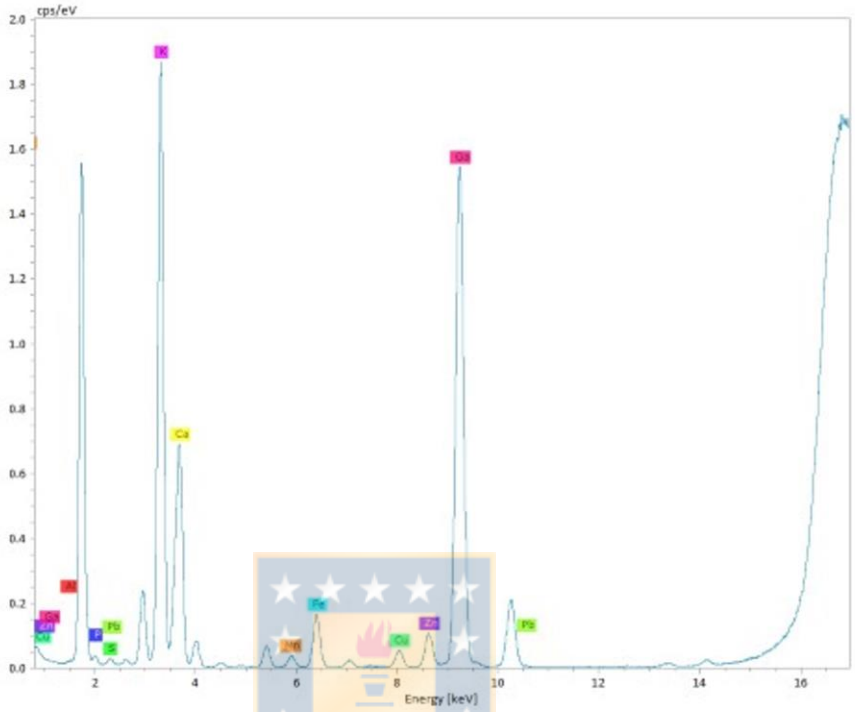

Figure S4: X-ray fluorescence spectra of calafate fruit. Internal standard Ga 0.5 mg/L. Scans 1,200 s.

Table S1: Comparative concentration of main polyphenolic compounds identified in calafate berry extracts

Polyphenolic compounds	**Methanolic extract** Concentration (µmol/ mL)	**Ethanolic extract** Concentration (µmol/ mL)
delphinidin-3,5-dihexoside	0.0974 ± 0.0084	0.0720 ± 0.0066
delphinidin 3-glucoside	0.958 ± 0.081	0.909 ± 0.029
petunidin 3-glucoside	0.508 ± 0.042	0.535 ± 0.015
petunidin-3-rutinoside	0.0531 ± 0.0056	0.0467 ± 0.0043
peonidin 3-glucoside	0.0269 ± 0.0023	0.0326 ± 0.0009
malvidin 3-glucoside	0.247 ± 0.013	0.262 ± 0.002
malvidin-3-rutinoside	0.0310 ± 0.0023	0.0300 ± 0.0009
O-caffeoylglucarate (15)	0.0791 ± 0.0016	0.0600 ± 0.0182
O-caffeoylglucarate (16)	0.122 ± 0.002	0.0822 ± 0.0184
O-caffeoylglucarate (17)	0.0283 ± 0.0011	0.0236 ± 0.0036
O-Caffeoylglucarate (20)	0.0267 ± 0.0015	0.0224 ± 0.0016
chlorogenic acid (25)	0.0456 ± 0.0130	0.0537 ± 0.0160
chlorogenic acid (34)	0.0538 ± 0.0058	0.0424 ± 0.0014

*$p<0.05$ vs methanolic extract. Data presented media ± standard error. Isomer number peak is present in parentheses

Table S2: Comparative concentration of FAME identified in calafate berry extracts

t_R (min)	Formula	Assigned identity	Concentration (mg/mL)	
			Methanol	Ethanol
19.972	$C_{15}H_{30}O_2$	Methyl tetradecanoate (Myristic acid methyl ester)	0.17 ± 0.02	0.21 ± 0.01
22.443	$C_{17}H_{34}O_2$	Hexadecanoic acid, methyl ester	0.043 ± 0.004	0.051 ± 0.003
24.708	$C_{19}H_{38}O_2$	Octadecanoic acid, methyl ester	0.051 ± 0.006	0.068 ± 0.003
26.783	$C_{19}H_{34}O_2$	9,12-octadecadienoic acid (Z,Z)-, methyl ester (Linoleic acid methyl ester ω6)	0.019 ± 0.002	0.023 ± 0.002
28.160	$C_{19}H_{32}O_2$	9,12,15-0ctadecatrienoic acid, methyl ester, (Z,Z,Z)- (Linolenic acid methyl ester ω3)	0.030 ± 0.002	0.036 ± 0.003
29.473	$C_{23}H_{44}O_2$	13-Docosenoic acid, methyl ester, (Z)- (Erucic acid methyl ester)	0.056 ± 0.005	0.12 ± 0.03

* $p<0.05$methanolic extract .Data presented media ± standard error.

Table S3: Figure of merit of the quantitative method

Polyphenol	Equation	SD slope (g FW/ µmol)	SD intercept	Linear range (µmol /g FW)	LOD (µmol /g FW)	LOQ (µmol /g FW)	S y/x	RSD (%)
Delphinidine-3-glucoside	y=1828382x-7283	9843	11297	0.06 – 2.14	0.02	0.06	12393	14.2
3-caffeoylquinic acid	y=2132698x-104532	46612	93993	0.41 – 7.05	0.12	0.41	87065	11.5
Totals Polyphenols	**Equation**	**SD slope (L/mg)**	**SD intercept**	**Linear range (mg/L)**	**LOD (mg/L)**	**LOQ (mg/L)**	**S y/x**	**RSD (%)**
Folin Ciocalteu	y=0.0125x+0.0191	0.0002	0.0176	21.19 – 150	0.48	21.19	0.026	12.3
Antioxidant capacity	**Equation**	**SD slope (L/µmol eq. Trolox)**	**SD intercept**	**Linear range (µmol eq. Trolox/L)**	**LOD (µmol eq. Trolox/L)**	**LOQ (µmol eq. Trolox/L)**	**S y/x**	**RSD (%)**
ABTS	y=0.0007x+0.057	0.0002	0.003	59.3- 84	16.6	59.3	0.0038	26.8
CUPRAC	y=0.0037x+0.0023	0.00022	0.0032	15.2- 300	4.5	15.2	0.0055	4.1
ORAC	y=34.347x+826.78	3.871	153.230	6.8- 70	2.0[a]	6.8[a]	224.5	4.5

[a]LOD-LOQ calculated by SD signal of 0 µmol eq. Trolox/L

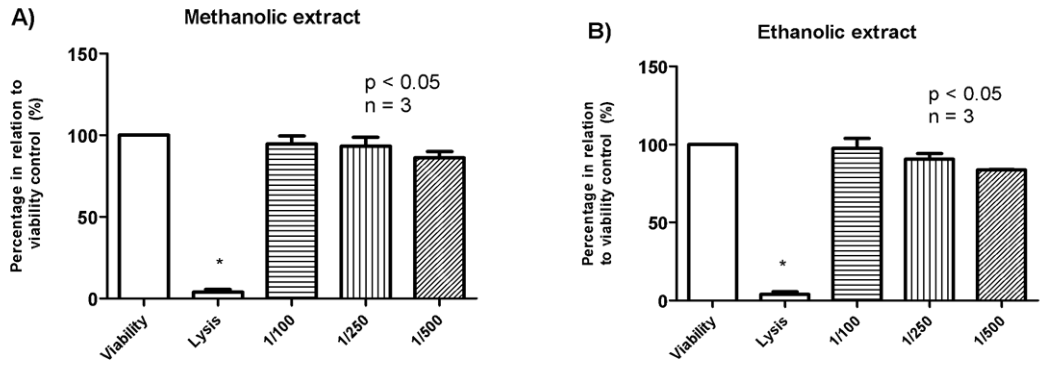

Figure S5: *In vitro* viability assay determined by MTT method. **A)** Methanolic extract (1/100, 1/250 and 1/500 dilutions) and **B)** Ethanolic extract (1/100, 1/250 and 1/500 dilutions). Data expressed as % to respect the viability control (mean ± standard error values, * $p < 0.05$ vs control). Lysis control: cells pretreated for 48 h with PBS 10 mM which was used as a positive control to induce cell death by serum deprivation.

Determination of Fe in calafate extract by atomic absorption spectroscopy (AAS)

Perkin Elmer Aanalyst 300 Atomic Absorption Spectrophotometer (Waltham, MA, USA) was used for the determination of Fe by atomic absorption with flame (air-acetylene). The adopted parameters for the operation of the equipment were those recommended by the manufacturer, wavelength of 248.3nm for Fe. A deuterium lamp was used as the background corrector for all measurements.

2. Evaluación de las diferencias existentes entre los extractos metánólico y etanólico, utilizando análisis multivariado.

Con el objetivo de evaluar que compuestos causaban las diferencias observadas en el efecto antioxidante de los extractos obtenido en los ensayos celulares, es que se decidió realizar un análisis de componentes principales (PCA) y un análisis de proyecciones ortogonales a estructuras latentes-análisis discriminante (OPLS-DA) entre ellos.

Para ello los extractos metanólico y etanólico del fruto de calafate fueron analizados por UHPLC-DAD-QTOF en modo negativo y posivo 10 veces cada uno utilizando un volumen de inyección 20 µL. El procesamiento de la data se llevó a cabo mediante el software MetaboScape de Bruker. Con el objeto de discriminar las variables significativas se llevó a cabo posterior al PCA un OPLS-DA. La identificación tentativa de los compuestos se realizó mediante bases de datos de libre acceso tales como las presentadas durante la estrategia analítica.

Resultados

En el PCA se observó una clara separación de los extractos indicando diferencias entre ellos. Entre el componente principal 1 y 2 se explicaron un 77.8% y 77.1% de la varianza para el modo negativo y positivo, respectivamente (Figura A 2.1). Para detectar las variables significativas se realizó un OPLS-DA para cada modo de ionización, seleccionando un total 14 variables significativas a partir del S-plot las cuales fueron numeradas en modo correlativo a cada lado, y diferenciadas por un asterisco. Los box-plot de las variables identificadas de manera tentativa se presentan en la figura A 2.2- 2.3

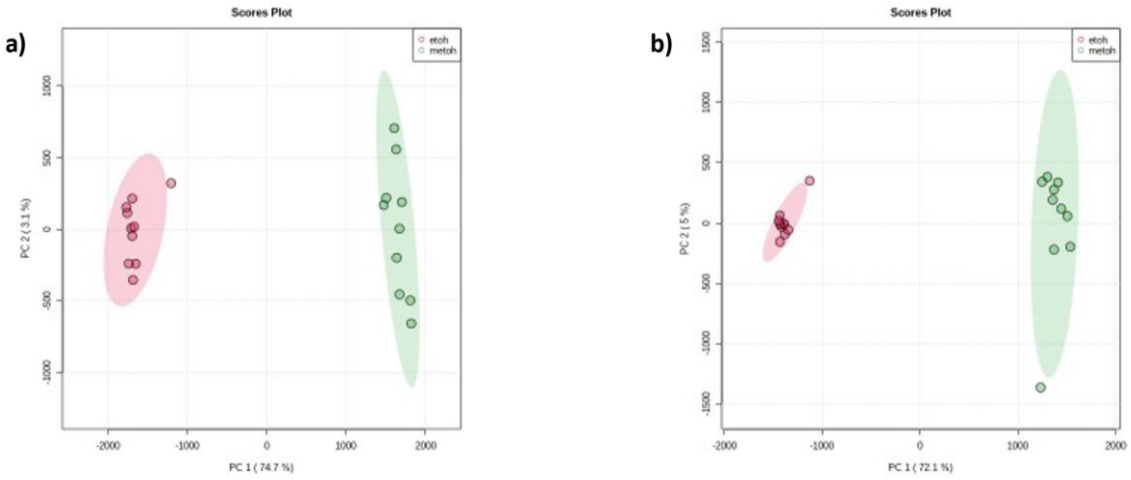

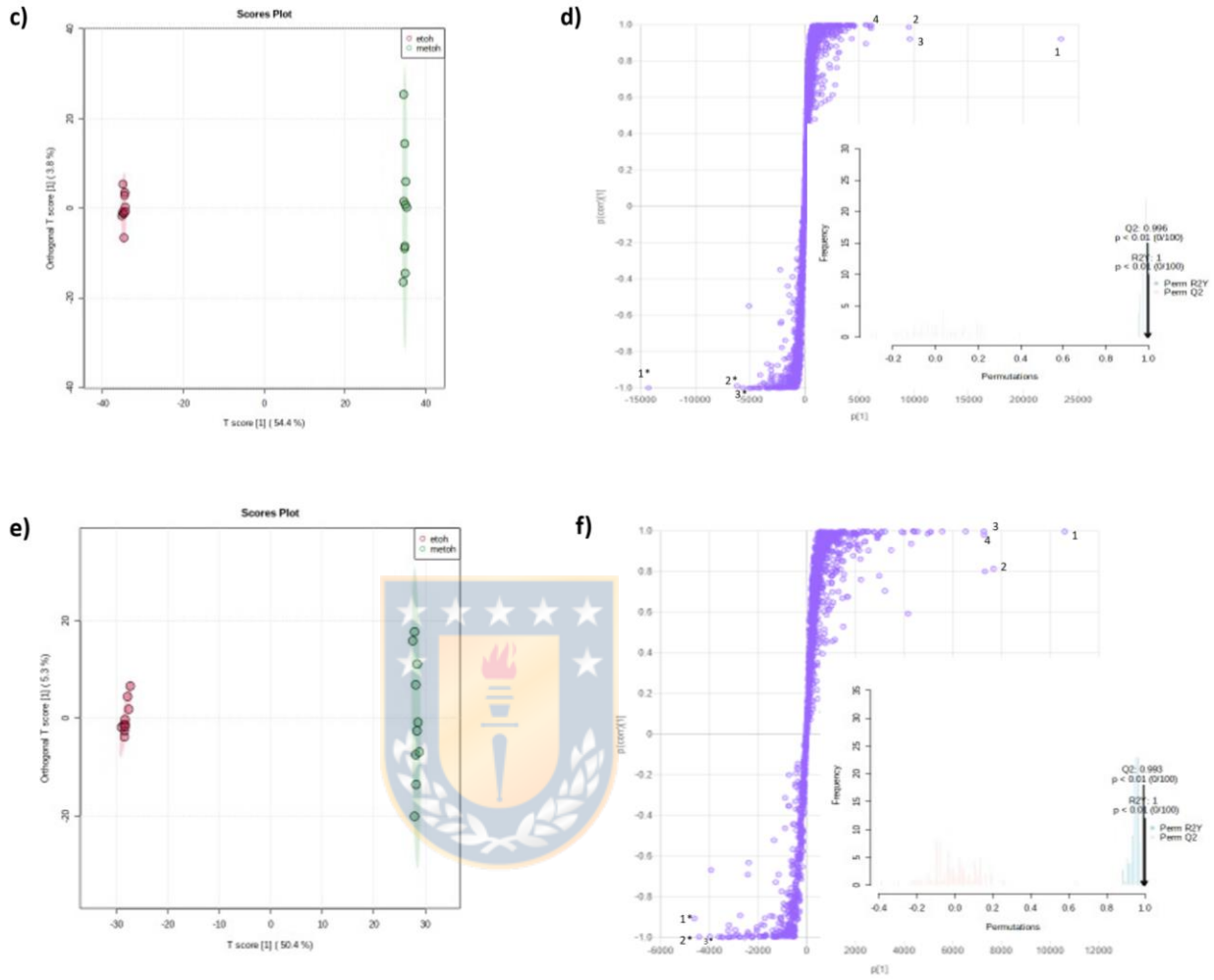

Figura A 2.1: Análisis multivariado de extractos metanólicos y etanólicos utilizados para evaluar el efecto biológico de calafate en modelos celulares. a y b) PCA producto del contraste del extracto metanólico y etanólico en modo negativo y positivo, respectivamente. c) Score plot OPLS-DA en modo negativo d) S-plot OPLS-DA en modo negativo e) Score plot OPLS-DA en

modo positivo d) S-plot OPLS-DA en modo positivo. Extracto metanólico en rojo y etanólico en verde.

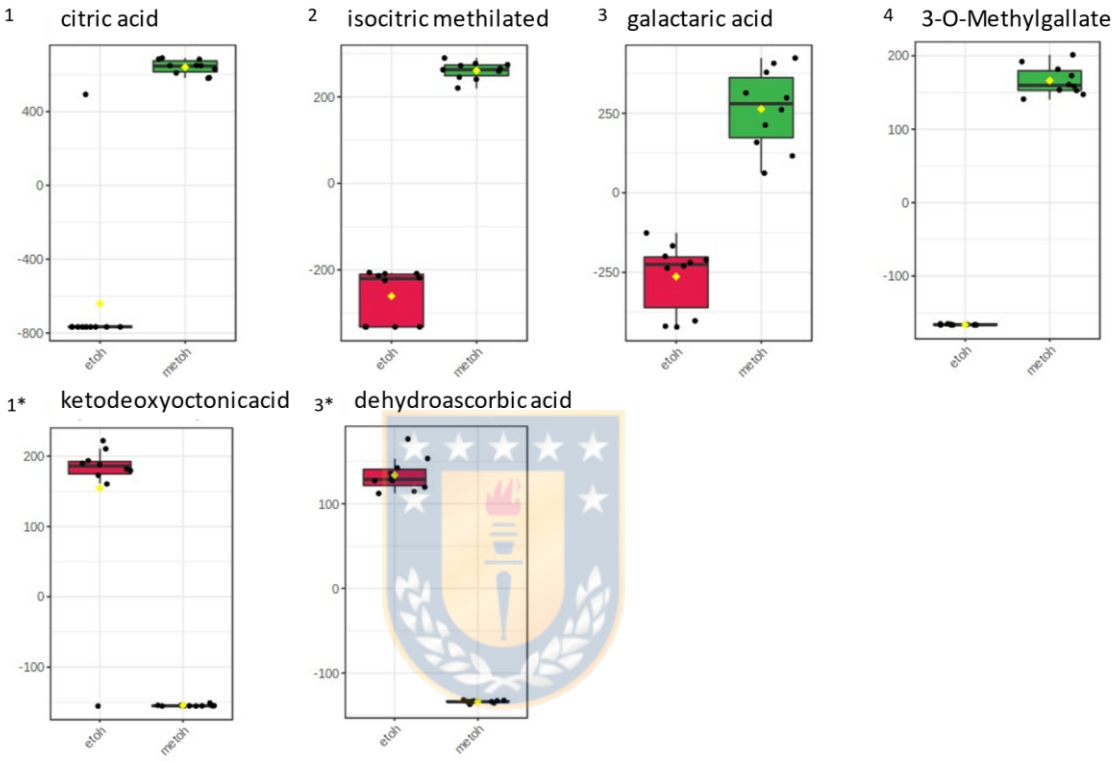

Figura A 2.2: Box-plot variables significativas identificadas en modo negativo. Extracto metanólico en verde y etanólico en rojo.

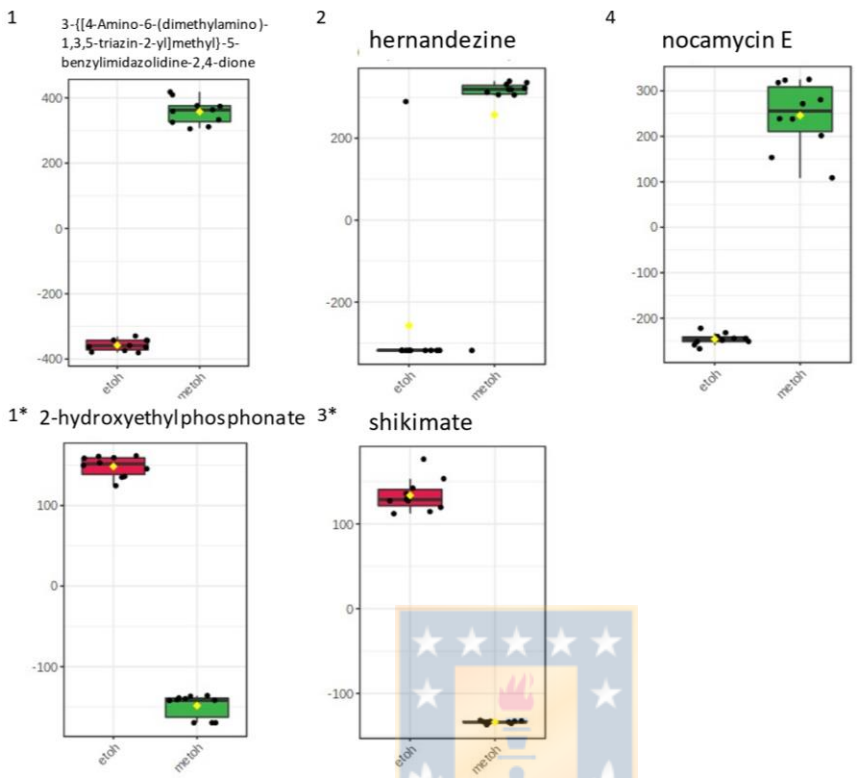

Figura A 2.3: Box-plot variables significativas identificadas en modo positivo. Extracto metanólico en verde y etanólico en rojo.

Conclusión

Se encontraron diferencias entre los extractos metanólicos y etanólicos, lo que se observó visualmente en el PCA.

Las variables tentativamente identificadas fueron principalmente ácidos orgánicos, por lo que se reafirman los hallazgos publicados que indican que no existen diferencia entre las concentraciones encontradas de polifenoles y

ácidos grasos entre ambos extractos. En consecuencia, se propone que la diferencia en su actividad antioxidante encontrada en modelos celulares se podría deber a las diferentes concentraciones de estos ácidos orgánicos.

3. SUPPLEMENTARY MATERIAL: *Berberis microphylla* G. Forst intake reduces the impact of high-fat diet on plasma cardiovascular disease factors.

Table S1: MetaboScape parameter

Columna1	Method1 NEG	Method1 POS	Method2 NEG	Method2 POS	Method3 NEG	Method3 POS
Intensity threshold [counts]	200.0	400.0	200.0	200.0	200.0	150.0
Minimum peak length [spectra]	4	5	30	5	12	8
Minimum peak length (recursive) [spectra]	3	4	29	4	11	7
Minimum # Features for Extraction	2	2	2	2	2	2
Presence of features in minimum # of analyses	2	2	2	2	2	2
Lock mass calibration	false	false	false	false	false	false
Mass calibration	true	true	true	true	true	true
Primary Ion	$[M-H]^-$	$[M+H]^+$	$[M-H]^-$	$[M+H]^+$	$[M-H]^-$	$[M+H]^+$
Seed Ions	$[2M-H]^-$, $[M+HCOO^-H]^-$	$[M+Na]^+$, $[M]^+$, $[2M+H]^+$, $[M+HCOOH]^+$	$[2M-H]^-$, $[M+HCOO^-H]^-$	$[M+Na]^+$, $[M]^+$, $[2M+H]^+$, $[M+HCOOH]^+$	$[2M-H]^-$, $[M+HCOO^-H]^-$	$[M+Na]^+$, $[M]^+$, $[2M+H]^+$, $[M+HCOOH]^+$
Common Ions	$[M-H-H2O]^-$	$[M-H2O+H]^+$	$[M-H-H2O]^-$	$[M-H2O+H]^+$	$[M-H-H2O]^-$	$[M-H2O+H]^+$
EIC correlation	0.8	0.8	0.8	0.8	0.8	0.8
Mass range: Start [m/z]	50.0	50.0	50.0	50.0	50.0	50.0
Mass range: End [m/z]	1500.0	1500.0	1500.0	1500.0	1500.0	1500.0
Retention time range: Start [min]	0.5	0.5	0.5	0.5	0.5	0.5
Retention time range: End [min]	13.5	13.5	14.0	14.0	17.0	17.0
Perform MS/MS import	true	true	true	true	true	true
Group by collision energy	false	false	false	false	false	false
MS/MS import method	average	average	average	average	average	average

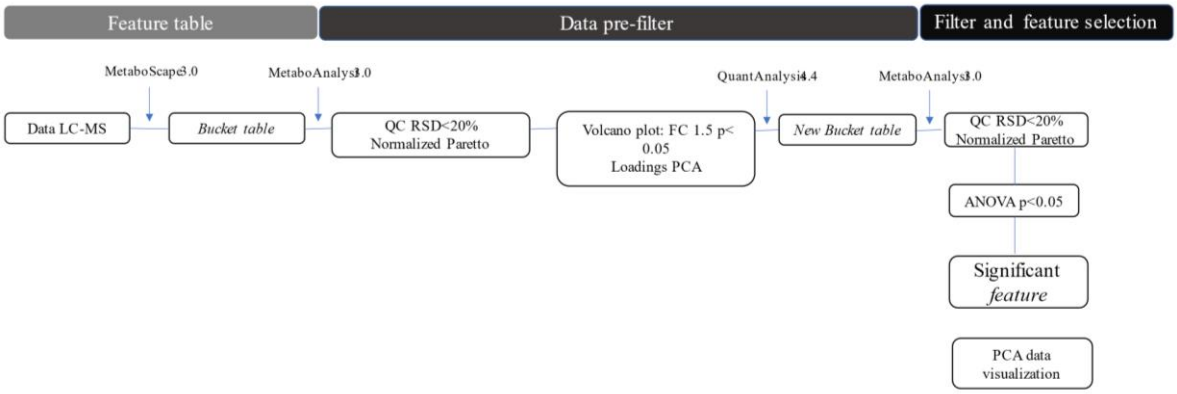

Figure S1: Flow data processing

Table S2: Weight of mice and clinical chemistry analysis for the different groups

	N	**Ncal**	**H**	**Hcal**
Weight (g)	23.0 ± 2.2	22.8 ± 0.8	23.7 ± 2.6	25.5 ± 2.8
Change in weight (g) (Final weight-Starting weight)	1.1 ± 0.9	-1.5 ± 4.3	1.4 ± 0.7[a]	1.2 ± 0.8[a]
Glycemia (mg/dL)	85.7 ± 21.8	85.0 ± 8.4	85.8 ± 10.9	88.2 ± 7.9
TRANSAMINASES				
GOT (UI/L)	102.6 ± 15.9	98.9 ± 37.8	104.8 ± 17.7	111.6 ± 59.0
GPT (UI/L)	46.4 ± 5.6	56.9 ± 7.2	47.4 ± 3.7	51.2 ± 10.7
LIPIDS				
TC (mg/dL)	60.7 ± 11.2	55.4 ± 7.3	91.9 ± 6.2[b]	85.4 ± 6.1
TG (mg/dL)	144.2 ± 60.9	92.1 ± 25.5	106.0 ± 26.7	126.2 ± 22.0

N: normal diet; Ncal: normal diet + calafate extract; H: high-fat diet; Hcal: high-fat diet + calafate extract; TC : total colesterol; TG: triglycerides; GOT:glutamic oxaloacetic transaminase; GPT: Glutamate Pyruvate Transaminase ; a: significant difference between final weight and starting weight $p < 0.05$;b: H vs N $p<0.05$

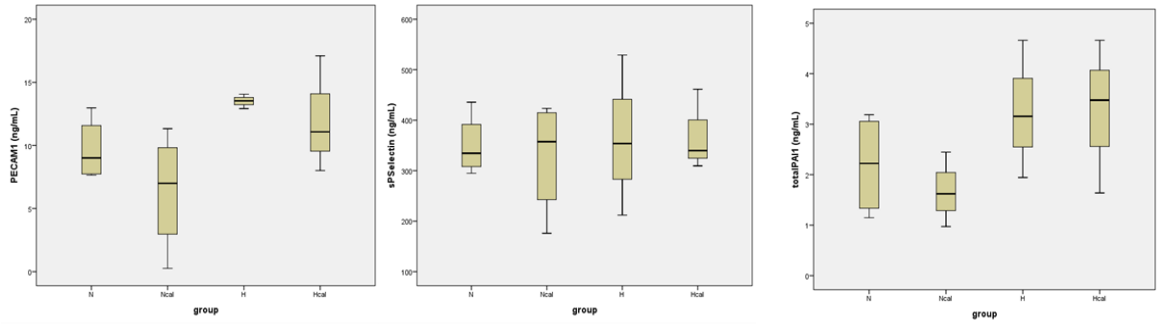

Figure S2: Cardiovascular panel cytokines quantified by MagPix intrument . Data expressed as concentration in plasma samples (ng/mL) in different groups (* $p < 0.05$).

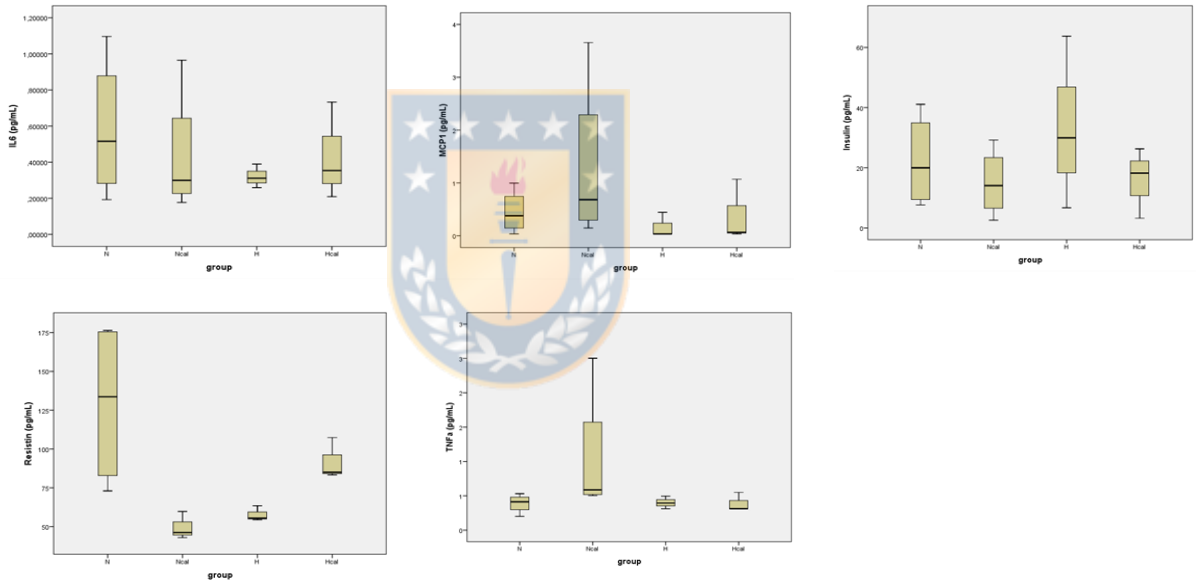

Figure S3: Mouse adipokine panel quantified by MagPix instrument . Data expressed as concentration in plasma samples (pg/mL) in different groups (* $p < 0.05$).

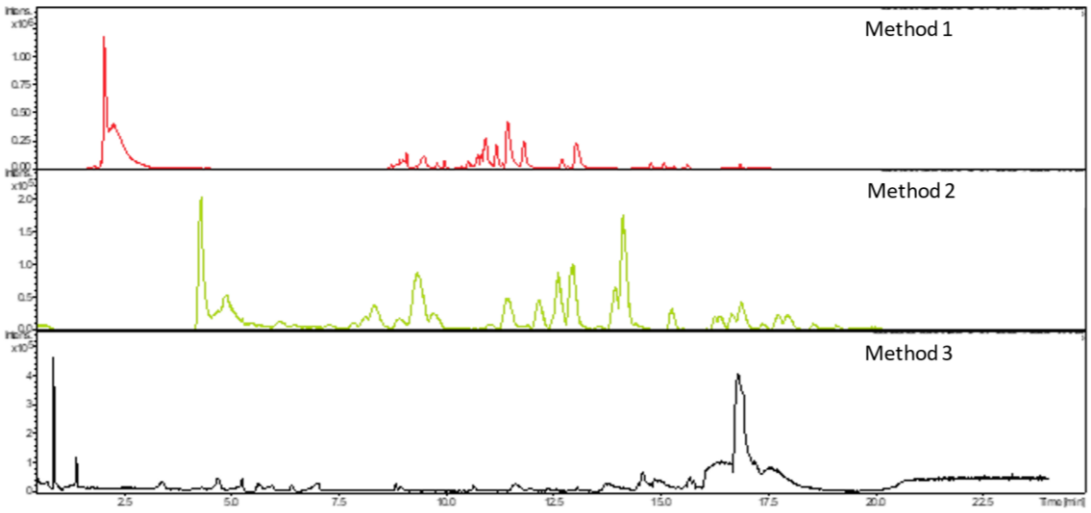

Figure S4: Base peak chromatogram (BPC) in negative polarity for different chromatographic method.

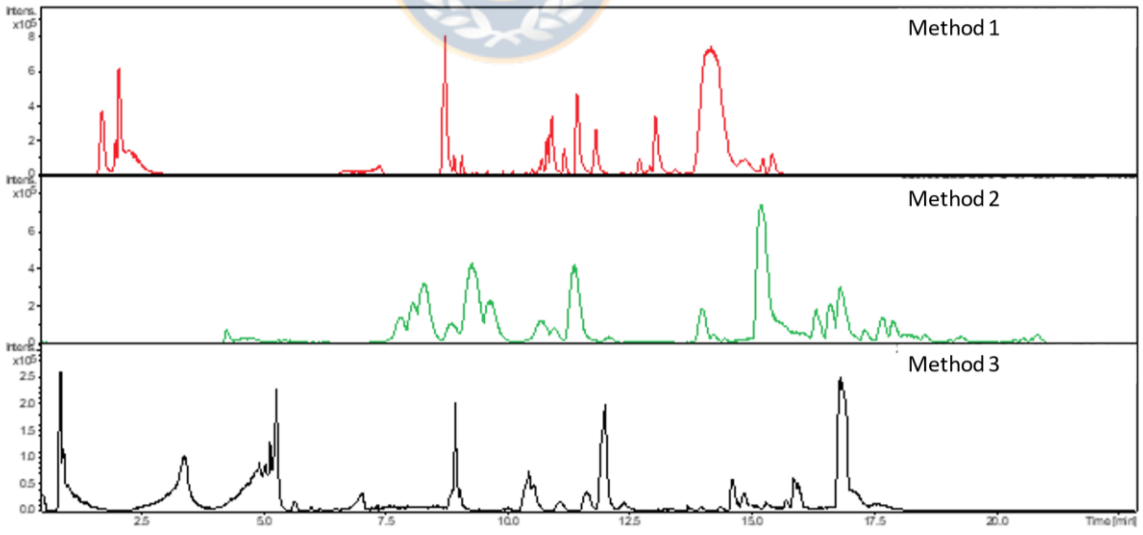

Figure S5: Base peak chromatogram (BPC) in positive polarity for different chromatographic method.

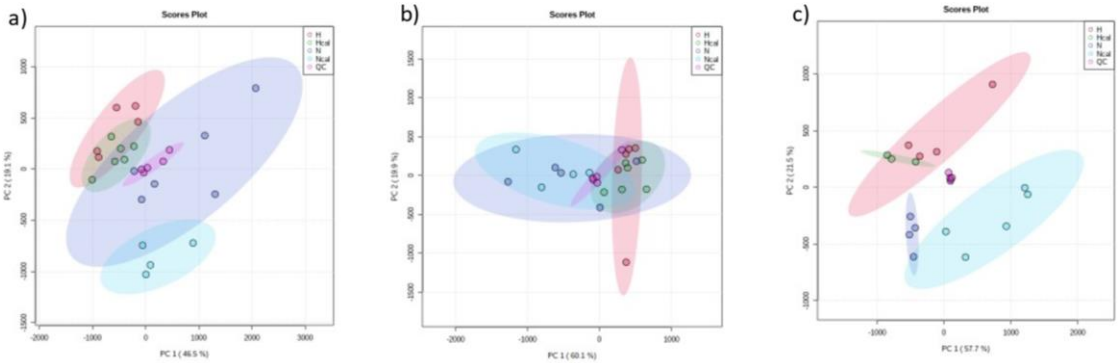

Figure S6: Principal component analysis (PCA). Score plot in negative mode a) method 1, b) method 2 and c) method 3, QC is a central cluster .

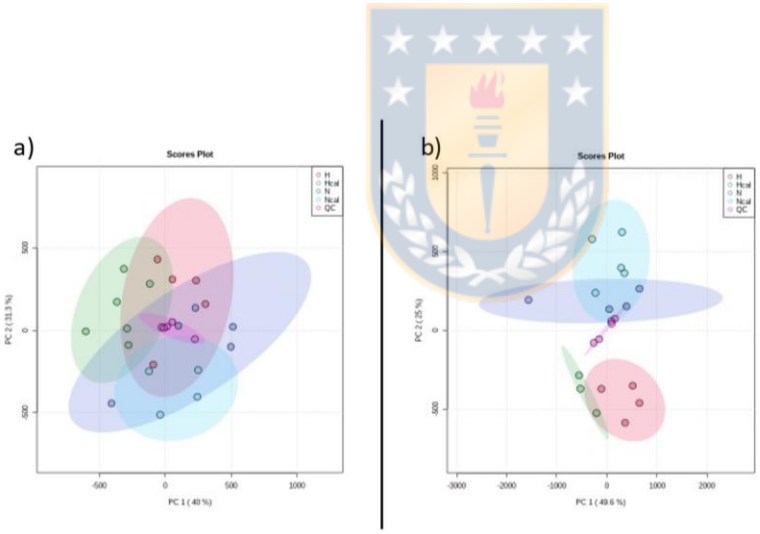

Figure S7: Principal component analysis (PCA). Score plot in positive mode a) method 2 and b) method 3, show QC is a central cluster.

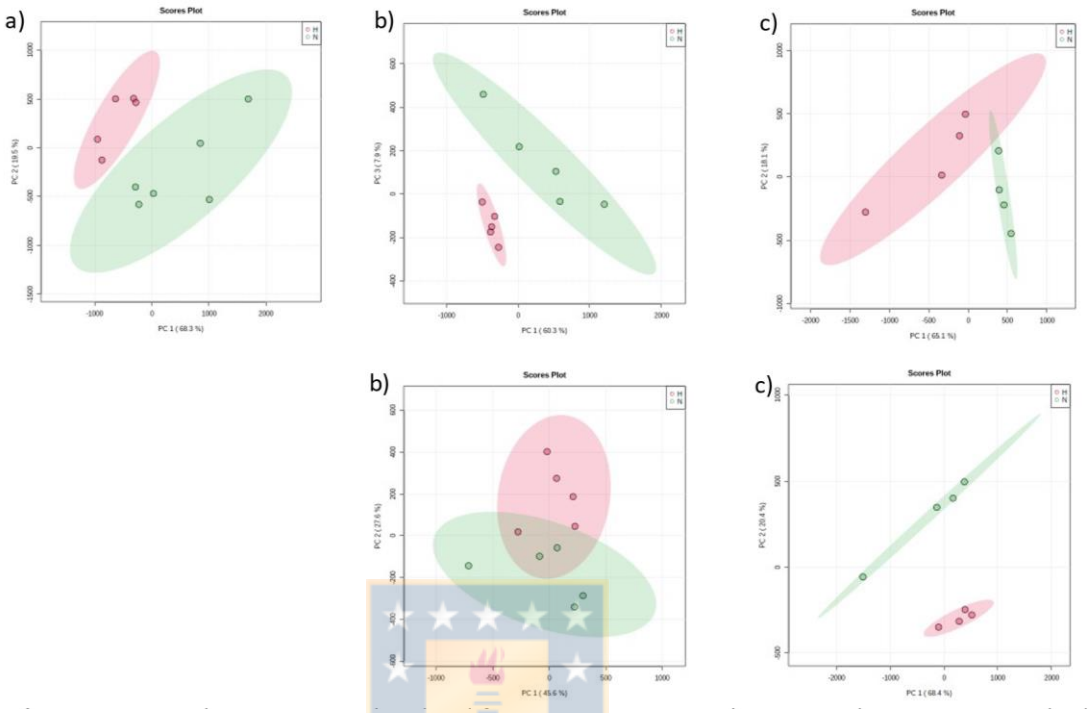

Figure S8: Principal component analysis (PCA) for N-H comparative analysis. Score plot in negative mode a) method 1, b) method 2 and c) method 3. Score plot in positive tive mode: d)method 2 and e) method 3. N: green H: red

Additional references to consider:

Achari, A. E., & Jain, S. K. (2017). Adiponectin, a therapeutic target for obesity, diabetes, and endothelial dysfunction. International Journal of Molecular Sciences, 18(6). https://doi.org/10.3390/ijms18061321

Andriantsitohaina, R., Auger, C., Chataigneau, T., Étienne-Selloum, N., Li, H., Martínez, M. C., Schini-Kerth, V. B., & Laher, I. (2012). Molecular mechanisms of the cardiovascular protective effects of polyphenols. British Journal of Nutrition, 108(9), 1532–1549. https://doi.org/10.1017/S0007114512003406

Bui, T. M., Wiesolek, H. L., & Sumagin, R. (2020). ICAM-1: A master regulator of cellular responses in inflammation, injury resolution, and tumorigenesis. Journal of Leukocyte Biology, 108(3), 787–799. https://doi.org/10.1002/JLB.2MR0220-549R

Bujak, R., García-Álvarez, A., Rupérez, F. J., Nuño-Ayala, M., García, A., Ruiz-Cabello, J., Fuster, V., Ibáñez, B., & Barbas, C. (2014). Metabolomics reveals metabolite changes in acute pulmonary embolism. Journal of Proteome Research, 13(2), 805–816. https://doi.org/10.1021/pr400872j

Chen, C. ye, Yi, L., Jin, X., Mi, M. tian, Zhang, T., Ling, W. hua, & Yu, B. (2010). Delphinidin attenuates stress injury induced by oxidized low-density lipoprotein in human umbilical vein endothelial cells. Chemico-Biological Interactions, 183(1), 105–112. https://doi.org/10.1016/j.cbi.2009.09.024

Delgado, G. E., Krämer, B. K., Siekmeier, R., Yazdani, B., März, W., Leipe, J., & Kleber, M. E. (2020). Influence of smoking and smoking cessation on biomarkers of endothelial function and their association with mortality. Atherosclerosis, 292(August 2019), 52–59. https://doi.org/10.1016/j.atherosclerosis.2019.11.017

Evans, A. M., O'Donovan, C., Playdon, M., Beecher, C., Beger, R. D., Bowden, J. A., Broadhurst, D., Clish, C. B., Dasari, S., Dunn, W. B., Griffin, J. L., Hartung, T., Hsu, P. C., Huan, T., Jans, J., Jones, C. M., Kachman, M., Kleensang, A., Lewis, M. R., Monge, M.E., Mosley, J., Taylor, E., Tayyari,

F., Theodoridis, G., Torta, F., Ubhi, B.K., & Vuckovic, D. (2020). Dissemination and analysis of the quality assurance (QA) and quality control (QC) practices of LC–MS based untargeted metabolomics practitioners. Metabolomics, 16(10), 1–16. https://doi.org/10.1007/s11306-020-01728-5

Gao, X., Guo, M., Li, Q., Peng, L., Liu, H., Zhang, L., Bai, X., Wang, Y., Li, J., & Cai, C. (2014). Plasma metabolomic profiling to reveal antipyretic mechanism of Shuang-Huang-Lian injection on yeast-induced pyrexia rats. PLoS ONE, 9(6), 1–10. https://doi.org/10.1371/journal.pone.0100017

He, J., Sun, C., Li, T., Luo, Z., Huang, L., Song, X., Li, X., & Abliz, Z. (2018). A Sensitive and Wide Coverage Ambient Mass Spectrometry Imaging Method for Functional Metabolites Based Molecular Histology. Advanced Science, 5(11). https://doi.org/10.1002/advs.201800250

Katja Dettmer, Aronov, P. A., & Hammock, B. D. (2007). MASS SPECTROMETRY-BASED METABOLOMICS Katja. Mass Spectrometry Reviews, 26(1), 51–78.

Keller, B. O., Sui, J., Young, A. B., & Whittal, R. M. (2008). Interferences and contaminants encountered in modern mass spectrometry. Analytica Chimica Acta, 627(1), 71–81. https://doi.org/10.1016/j.aca.2008.04.043

Kesherwani, V., Chavali, V., Hackfort, B. T., Tyagi, S. C., & Mishra, P. K. (2015). Exercise ameliorates high fat diet induced cardiac dysfunction by increasing interleukin 10. Frontiers in Physiology, 6(APR), 1–7. https://doi.org/10.3389/fphys.2015.00124

Li, Z. Z., & Dai, Q. Y. (2012). Pathogenesis of abdominal aortic aneurysms: Role of nicotine and nicotinic acetylcholine receptors. Mediators of Inflammation, 2012. https://doi.org/10.1155/2012/103120

Liu, J., Zhang, G., Chen, D., Chen, J., Yuan, Z. Bin, Zhang, E. L., Gao, Y. X., Xu, G., Sun, B. Da, Liao, W., & Gao, Y. Q. (2017). UPLC-QTOFMS-based metabolomic analysis of the serum of hypoxic preconditioning

mice. Molecular Medicine Reports, 16(5), 6828–6836. https://doi.org/10.3892/mmr.2017.7493

Otero, M., Lago, R., Lago, F., Casanueva, F. F., Dieguez, C., Gómez-Reino, J. J., & Gualillo, O. (2005). Leptin, from fat to inflammation: Old questions and new insights. FEBS Letters, 579(2), 295–301. https://doi.org/10.1016/j.febslet.2004.11.024

Ramirez, J. E., Zambrano, R., Sepúlveda, B., Kennelly, E. J., & Simirgiotis, M. J. (2015). Anthocyanins and antioxidant capacities of six Chilean berries by HPLC-HR-ESI-ToF-MS. Food Chemistry, 176, 106–114. https://doi.org/10.1016/j.foodchem.2014.12.039

Reyes-farias, M., Vasquez, K., Ovalle-marin, A., Fuentes, F., Parra, C., Quitral, V., Jimenez, P., & Garcia-diaz, D. F. (2015). Chilean Native Fruit Extracts Inhibit Inflammation Linked to the Pathogenic Interaction Between Adipocytes and Macrophages. JOURNAL OF MEDICINAL FOOD, 18(5), 601–608. https://doi.org/10.1089/jmf.2014.0031

Schmeda-Hirschmann, G., Jiménez-Aspee, F., Theoduloz, C., & Ladio, A. (2019). Patagonian berries as native food and medicine. Journal of Ethnopharmacology, 241, 111979. https://doi.org/10.1016/j.jep.2019.111979

Shih, D. M., Gu, L., Hama, S., Xia, Y. R., Navab, M., Fogelman, A. M., & Lusis, A. J. (1996). Genetic-dietary regulation of serum paraoxonase expression and its role in atherogenesis in a mouse model. Journal of Clinical Investigation, 97(7), 1630–1639. https://doi.org/10.1172/JCI118589

Soini, Y., Satta, J., & Ma, M. (2001). TIMP2 mRNA in valvular lesions of the heart. Journal of Pathology, The, 225–231.

Sumner, L. W., Amberg, A., Barrett, D., Beale, M. H., Beger, R., Daykin, C. A., Fan, T. W. M., Fiehn, O., Goodacre, R., Griffin, J. L., Hankemeier, T., Hardy, N., Harnly, J., Higashi, R., Kopka, J., Lane, A. N., Lindon, J. C., Marriott, P., Nicholls, A. W., … Viant, M. R. (2007). Proposed minimum

reporting standards for chemical analysis: Chemical Analysis Working Group (CAWG) Metabolomics Standards Initiative (MSI). Metabolomics, 3(3), 211–221. https://doi.org/10.1007/s11306-007-0082-2

Woznica, A., Cantley, A. M., Beemelmanns, C., Freinkman, E., Clardy, J., & King, N. (2016). Bacterial lipids activate, synergize, and inhibit a developmental switch in choanoflagellates. Proceedings of the National Academy of Sciences of the United States of America, 113(28), 7894–7899. https://doi.org/10.1073/pnas.1605015113

Xia, J., Psychogios, N., Young, N., & Wishart, D. S. (2009). MetaboAnalyst: A web server for metabolomic data analysis and interpretation. Nucleic Acids Research, 37(SUPPL. 2), 652–660. https://doi.org/10.1093/nar/gkp356

Zhou, C. X., Zhou, D. H., Elsheikha, H. M., Liu, G. X., Suo, X., & Zhu, X. Q. (2015). Global metabolomic profiling of mice brains following experimental infection with the cyst-forming Toxoplasma gondii. PLoS ONE, 10(10), 1–22. https://doi.org/10.1371/journal.pone.0139635

Pino Ramos, L. L., Jiménez-Aspee, F., Theoduloz, C., Burgos-Edwards, A., Domínguez-Perles, R., Oger, C., Durand, T., Gil-Izquierdo, Á., Bustamante, L., Mardones, C., Márquez, K., Contreras, D., & Schmeda-Hirschmann, G. (2019). Phenolic, oxylipin and fatty acid profiles of the Chilean hazelnut (Gevuina avellana): Antioxidant activity and inhibition of pro-inflammatory and metabolic syndrome-associated enzymes. Food Chemistry, 298. https://doi.org/10.1016/j.foodchem.2019.125026